NASA Technical Memorandum 87676

NASA-TM-87676 19860009817

LOADS AND AEROELASTICITY DIVISION RESEARCH AND TECHNOLOGY ACCOMPLISHMENTS FOR FY 1985 AND PLANS FOR FY 1986

J. E. GARDNER AND S. C. DIXON

JANUARY 1986

NASA
National Aeronautics and Space Administration
Langley Research Center
Hampton, Virginia 23665

LOADS AND AEROELASTICITY DIVISION
RESEARCH AND TECHNOLOGY ACCOMPLISHMENTS FOR FY 1985
AND PLANS FOR FY 1986

SUMMARY

The purpose of this paper is to present the Loads and Aeroelasticity Division's research accomplishments for FY 85 and research plans for FY 86. The work under each branch (technical area) will be described in terms of highlights of accomplishments during the past year and highlights of plans for the current year as they relate to five year plans and the objectives for each technical area. This information will be useful in program coordination with other government organizations and industry in areas of mutual interest.

ORGANIZATION

The Langley Research Center is organized by directorates as shown on figure 1. There were a number of changes of key personnel precipitated by the former Center Director, Dr. Donald P. Hearth leaving NASA to take a position with the University of Colorado. Mr. Richard H. Petersen, former Deputy Director of LaRC, was appointed to the position of Director, Mr. Paul F. Holloway, former Director for Space at LaRC, was appointed to the position of Deputy Director, and Mr. Robert E. Bower, former Director for Aeronautics at LaRC, was appointed to the position of Associate Director. Mr. Roy V. Harris, Jr., former Chief, High-Speed Aerodynamics Division at LaRC, was appointed Director for Aeronautics, and Mr. Robert R. Nunamaker, former Chief Engineer at NASA Ames Research Center, was appointed Director for Space. A new Directorate, Flight Systems, was formed and Dr. Jeremiah F. Creedon, former Chief, Flight Controls Systems Division at LaRC, was appointed Director. The former Projects Directorate was abolished and its functions and staff were reassigned to the Electronics Directorate.

The Loads and Aeroelasticity Division consists of five branches as shown on figure 2. This figure lists the key people in the division which consists of 65 NASA civil servants, eight members of the Army Aerostructures Directorate, USAARTA, Army Aviation Systems Command located at Langley Research Center, and one member of the Air Force. Each branch represents a technical area and disciplines under the technical areas are shown on the figure. All of the Army personnel work on the Rotorcraft Aeroelasticity and Rotorcraft Structural Dynamics disciplines.

The division conducts analytical and experimental research in the five technical areas to meet technology requirements for advanced aerospace vehicles. The research focuses on the long range thrusts shown in figure 3. The Configuration Aeroelasticity Branch (CAB), Unsteady Aerodynamics Branch (UAB), and Aeroservoelasticity Branch (ASEB) all work in the area of Prediction and Control of Aeroelastic Stability and Response for Aircraft and Rotorcraft. The Aerothermal Loads Branch (ALB) and the Thermal Structures Branch (TSB) work the areas of Aerothermal Structures and Materials for High Speed Vehicles (Aeronautics) and Aerothermal Structures and Materials for Space Transportation Systems (Space).

RESEARCH PHILOSOPHY

The basic philosophy and motivation of the Loads and Aeroelasticity Division research program can be captured in selected quotes from some leaders in Aerospace Research and Development. In his 13th Von Karman lecture on Aeroelasticity (ref. 1), I. E. Garrick related the following: "Von Karman's sense of humor, which was remarkably appropriate to a given occasion, has become legendary. Recognizing that the poor structures engineer was usually held accountable for structural integrity, he quipped, 'The aerodynamicist assumes everything but the responsibility.'"

"It has been gratifying to me to observe that in major aerospace industry the aeroelastician is no longer the stepchild he once was. From an almost parochial isolated specialist, he is now the generalist who tends to pull together the separate efforts in structures, aerodynamics, stability and control, and propulsion, even in early design stages. Yet, there are still human problems such as one-way communications and barriers between departments as well as physical problems that are often so recondite and difficult that aeroelastic problems may slip through the cracks."

In his Wright Brothers Lectureship in Aeronautics on Optimization (ref. 2), Holt Ashley observed: "Further mention will be made in what follows of the keen disappointment felt by many specialists because their theories have received so little practical application. This phenomenon is frequently attributed to a reluctance by developmental engineers to adopt unfamiliar and untried methods of analysis."

In an appraisal of a study of hypersonic airframe structures, (ref. 3), Rene Miller stated: "The cost effectiveness of .... (Thermal) Structural Concepts is greatly dependent on solutions to the detailed design problems. In fact, it is likely that these detailed design problems as demonstrated in the X-15 program will prove to be the pacing item in the development of Hypersonic Aircraft."

The Loads and Aeroelasticity Division program is aimed at producing the data and analysis methods required by those who are accountable for the structural integrity of aerospace vehicles; to provide the detailed design data and methods for the pacing item of development of hypersonic vehicles - cost effective thermal structures; to continue to pull together those separate efforts that ought to (or must) be considered as a single task; to preclude aeroelastic problems from slipping through the cracks; and to alleviate the reluctance by developmental engineers to adopt unfamiliar and untried methods by making them both familiar and proven.

FACILITIES

The Loads and Aeroelasticity Division has two major facilities available to support its research as shown in figure 4.

The Transonic Dynamics Tunnel (TDT) is a Mach 0.2 to 1.2 continuous flow, variable-pressure wind tunnel with a 16 ft. square test section which uses a Freon-12 test medium primarily for dynamic aeroelastic testing. This unique facility is used primarily by the Configuration Aeroelasticity Branch.

Semi-span, side-wall mounted models and full-span cable-mounted models are used for aeroelastic studies of fixed wing aircraft. The ARES (Aeroelastic Rotor Experimental System) test stand is used in the tunnel to study the aeroelastic effects on rotors. A General Rotor Aeroelastic Laboratory, located nearby, is used to setup the ARES test stand in preparation for entry into the TDT. A modernization of the TDT Data Acquisition System is underway. A major CofF activity for density increase has recently been completed. The upgraded facility can now operate at dynamic pressures up to 600 psf. The maximum Reynolds number is about 10 x 10^6/ft. The replacement cost for this facility is $63M.

The Aerothermal Loads Complex consists of five facilities which are operated by the Aerothermal Loads Branch to carry out their research. The 8-Foot High Temperature Tunnel (8' HTT) is a unique hypersonic Mach 7 blowdown wind tunnel with an 8' diameter test section (uniform temperature test core of 4') that uses products of combustion (methane and air under pressure) as the test medium. The tunnel operates at dynamic pressures of 250 to 1800 psf, temperatures of 2400 to 3600°R and Reynolds numbers of 0.3 to 2.2 x 10^6/ft. The tunnel is used to test flat and curved surface type models to determine aerothermal effects and to evaluate new high temperature structural concepts. A major CofF item is underway to provide alternate Mach number capability and provide O_2 enrichment for the test medium. This is being done primarily to allow the tunnel to test models that have hypersonic air breathing propulsion applications. The replacement cost for the tunnel is $45M.

The 7-Inch High Temperature Tunnel (7" HTT) is a 1/12 scale of the 8' HTT with basically the same capabilities as the larger tunnel. It is used primarily as an aid in the design of larger models for the 8' HTT and for aerothermal loads test on subscale models. The 7" HTT is currently being used to evaluate various new systems for the 8' HTT. The replacement cost for the tunnel is $0.8M.

The three Aerothermal Arc Tunnels (20 MW, 5 MW and 1 MW) are used to test models in an environment that simulates the flight reentry envelope for high speed vehicles such as the Space Shuttle. The amount of usable energy to the test medium in these facilities is 9 MW, 2 MW, and 1/2 MW. The 5 MW is a three phase AC arc heater while the 20 MW and 1 MW are DC arc heaters. Test conditions such as temperature, flow rate, and enthalpy vary greatly since a variety of nozzles and throats are available and since model sizes are different (3" diameter to 1' x 2' panels). The replacement cost for these arc tunnels are $24M.

FY 85 ACCOMPLISHMENTS

Configuration Aeroelasticity Branch

The Configuration Aeroelasticity Branch conducts research (figure 5) to produce, apply, and validate through experiments a set of analytical methods for predicting steady and unsteady aerodynamic loads and aeroelastic characteristics of rotorcraft; to determine, analytically and experimentally, effective means for predicting and reducing helicopter vibrations and to evaluate the aeroelastic characteristics of new rotor systems; to develop the aeroelastic understanding and prediction capabilities needed to apply new aerodynamic

and structural concepts to future flight vehicles and to determine and solve the aeroelastic problems of current designs. This work is more clearly identified in figure 6 which shows the five year plan of the three disciplines and their expected results.

The Configuration Aeroelasticity FY 85 accomplishments listed below are highlighted by figures 7 through 10.

Aircraft Aeroelasticity:
- NASA Propfan Testbed Aircraft Shown Safe From Flutter in TDT Test
- Modifications to Increase Test Medium Density in Langley Transonic Dynamics Tunnel Completed

Rotorcraft Aeroelasticity:
- Total Rotor Isolation System (TRIS) Very Effective in Reducing Helicopter Vibrations
- Second TDT Test Expands JVX Data Base to Include Design Updates

Each highlight is accompanied by descriptive material.

Unsteady Aerodynamics Branch

The Unsteady Aerodynamics Branch conducts research (figure 11) to produce, apply, and validate through experiments a set of analytical methods for predicting steady and unsteady aerodynamic loads and aeroelastic characteristics of flight vehicles--with continued emphasis on the transonic range and emerging emphasis on high angle-of-attack manuevering subsonic and supersonic conditions. This work is more clearly identified in figure 12 which shows the five year plan of the three disciplines and their expected results.

The Unsteady Aerodynamics FY 84 accomplishments listed below are highlighted by figures 13 through 18.

Theory Development:
- XTRAN3S Flutter Calculations Compared with RENOFT Model Results
- Wing-Fuselage Capability Developed for XTRAN3S
- XTRAN3S Extended to Include Oscillating Control Surface
- Computational Transonic Flutter Boundary Tracking
- Lifting Surface Theoretical Results Correlate Well with Experimental Data for Helicopter Rotor in Forward Flight
- Non-Isentropic Strong Shock Conditions Implemented in XTRAN3S

Each highlight is accompanied by descriptive material.

Aeroservoelasticity Branch

The Aeroservoelasticity Branch conducts research (figure 19) to develop methodologies for the analysis and synthesis of multifunctional

active control systems and conceives, recommends, and provides technical support for experiments to validate the methodologies; and generates mathematical models needed to support NASA projects and uses them to verify the theoretical developments and their computer implementations. This work is more clearly identified in figure 20 which shows the five-year plan of the three areas of concentration and their expected results.

The Aeroservoelasticity FY 85 accomplishments listed below are highlighted by figures 21 through 24.

Analysis and Design Methods:
- Comparison of Calculated and Experimental Bending Moment Due to Control Deflection
- Engineering Workstations Used in ASE Computation
- Integrated Structure/Control Design Methodology

Applications:
- X-Wing Aeroservoelastic Analyses

Each highlight is accompanied by descriptive material.

Aerothermal Loads Branch

The Aerothermal Loads Branch conducts research (figure 25) to develop and validate solution algorithms, modeling techniques, and integrated finite elements for flow-thermal-structural analysis and design; to identify and understand flow phenomena and flow/surface interaction parameters required to define detailed aerothermal loads for structural design via analysis and test; and to define methods for testing in high enthalpy flow environments including capability for testing of air breathing engines at hypersonic speeds. This work is more clearly identified in figure 26 which shows the five year plan of the three disciplines and their expected results.

The Aerothermal Loads FY 84 accomplishments listed below are highlighted by figures 27 through 32.

Thermal Loads:
- Aerothermal Test of Shuttle Split-Elevon Model in 8' HTT
- Quilted Tile Array Simulating Thermally Bowed Metallic TPS

Integrated Analysis:
- Inviscid Finite Element Flow Analysis Applied to Experimental Model
- Closed Form Evaluation of Taylor-Galerkin Finite Element Matrices Yields an Order of Magnitude Savings in Computational Resources for High Speed Flow
- Improvements in Spectral Collocation Through a Multiple Domain Technique

Facilities Operations and Development:
- 1x3 High Enthalpy Aerothermal Tunnel Combustor Liner Evaluation

Each highlight is accompanied by descriptive material.

Thermal Structures Branch

The Thermal Structures Branch conducts research (figure 33) to develop and validate concepts for aerospace structures whose design is significantly controlled by the thermal excursions of the operating environments of aerospace vehicles. Systems studies in concert with the Space Systems Division or High-Speed Aerodynamics Division help to identify structures and materials technology needs. Structural concepts are then developed, analyzed, fabricated, and tested to verify the required technology advances. This work is more clearly identified in figure 34 which shows the five year plan of the three major disciplines and their expected results. Thermal structures experimental needs are currently in the defining stage. Some static testing of small components is being done for structural concepts being developed and fabricated, with the support of contractors, ADFRF, and the Aerothermal Loads Branch.

The Thermal Structures FY 84 accomplishments listed below are highlighted by figures 35 through 39.

Structural Systems Studies:
- Ballute Shape Analysis Reveals Potential Instability

Concept Development:
- Reusable High-Temperature Cryogenic Foam Insulation System
- Curved Metallic TPS
- Carbon-Carbon Heat Shield for Aeroassisted Orbital Transfer Vehicle

Analytical Methods and Applications:
- Equations for Thermal Stress Around a Cylindrical Pin

Each highlight is accompanied by descriptive material.

PUBLICATIONS

The FY 85 accomplishments of the Loads and Aeroelasticity Division resulted in a number of publications. The publications are listed below and are identified by the categories of journal publications, formal NASA reports, conference presentations, contractor reports, and other.

Journal Publications

1. Mukhopadhyay, V. and Newsom, J. R.: A Multiloop System Stability Margin Study Using Matrix Singular Values. Journal of Guidance, Control, and Dynamics, Vol. 7, No. 5, pp. 582-587, September-October 1984.

2. Abel, I.; Doggett, R. V., Jr.; Newsom, J. R. and Sandford, M. C.: Dynamic Wind-Tunnel Testing of Active Controls by the NASA Langley Research Center. AGARDograph No. 262, Ground and Flight Testing for Aircraft Guidance and Control, pp. 3-1 - 3-23, December 1984.

3. Osher, S.; Hafez, M.; and Whitlow, W., Jr.: Entropy Condition Satisfying Approximations for the Full Potential Equation of Transonic Flow. Mathematics of Computations, Vol. 44, pp. 1-29, January 1985.

4. Wood, E. R.; Powers, R. W.; Cline, J. H.; and Hammond, C. E.: On Developing and Flight Testing a Higher Harmonic Control System. Journal of the American Helicopter Society, Volume 30, No. 1, pp. 3-20, January 1985.

5. Taylor, A. H.; Cerro, J. A.; Cruz, C. I.; Jackson, L. R.; Naftel, J. C.; and Wurster, K. E.: Orbit on Demand: Structural Analysis Finds Vertical Launches Weigh Less. Aerospace America, Vol. 23, No. 2, pp. 58-61, Feb. 1985.

6. Whitlow, W. and Seidel, D. A.: Nonreflecting Boundary Conditions for the Complete Unsteady Transonic Small-Disturbance Equation. AIAA Journal, Vol. 23, No. 2, pp. 315-317, February 1985.

7. McCain, W. F.: Measured and Calculated Airloads on a Transport Wing Model. Journal of Aircraft, Vol. 22, No. 4, pp. 336-342, April 1985.

8. Batina, J. T. and Yang, T. Y.: Transonic Time Responses of the MBB A-3 Supercritical Airfoil Including Active Controls. Journal of Aircraft, Vol. 22, No. 5, pp. 393-400, May 1985.

9. Newsom, J. R.; Pototzky, A. S.; and Abel, I.: Design of a Flutter Suppression System for an Experimental Drone Aircraft. Journal of Aircraft, Vol. 22, No. 5, pp. 380-386, May 1985.

10. Olsen, G. C. and Smith, R. E.: Analysis of Aerothermal Loads on Spherical Dome Protuberances. AIAA Journal, Volume 21, No. 5, pp. 650-656,May 1985.

11. Taylor, A. H.; Jackson, L. R.; Davis, R. C.; Cerro, J. A.; and Scotti, S. J.: Structural Concepts for Future Space Transportation System Orbiters. Journal of Spacecraft and Rockets, Vol. 22, pp. 333-339, May-June 1985.

12. Bhatia, K.; Nagaraja, K. S.; and Ruhlin, C. L.: Winglet Effects on the Flutter of Twin-Engine-Transport-Type Wing. Journal of Aircraft, vol. 22, pp. 587-594, July 1985.

13. Newsom, J. R.; and Mukhopadhyay, V.: A Multiloop Robust Controller Design Study Using Singular Value Gradients. Journal of Guidance and Control, Vol. 8, No. 4, pp. 514-519, July-August 1985.

14. Avery, D. E.; Kerr, P. A.; and Wieting, A. R.: Experimental Aerodynamic Heating to Simulated Shuttle Tiles. Journal of Spacecraft and Rockets, Vol. 22, No. 4, July-August 1985, pp. 417-424.

Formal NASA Reports

15. Nowak, R. J.; Albertson, C. W.; and Hunt, L. R.: Aerothermal Tests of a Large 12.5 Degree Cone at Mach 6.8 for Various Bluntness, Angles of Attack, and Reynolds Numbers. NASA TP-2345, January 1985.

16. Shore, C. P.: Reduction Method for Thermal Analysis of Complex Aerospace Structures. NASA TP-2373, January 1985.

17. Avery, D. E.: Experimental Aerodynamic Heating to Simulated Space Shuttle Tiles in Laminar and Turbulent Boundary Layers With Variable Flow Angles at a Nominal Mach Number of 7. NASA TP-2307, August 1985.

18. Davis, R. C.; Moses, P. L.; and Kanenko, R. S.: Joint Design for Improved Fatigue Life of Diffusion-Bonded-Stiffened Panels. NASA TP-2480, September 1985.

19. Singh, J. J.; Springkel, D. R.; and Puster, R. L.: New Method for Determining Heats of Combustion of Natural Gas Samples. NASA TP-2531, September 1985.

20. Cazier, F. W., Jr. and Kehoe, M. W.: Ground Vibration Test of F-16 Airplane with Initial Decoupler Pylon. NASA TM-86259, October 1984.

21. Whitlow, W., Jr.: Characteristics Boundary Conditions for Three-Dimensional Transonic Unsteady Aerodynamics. NASA TM-86292, October 1984.

22. Perry, B., III: Flight Test Technique for Evaluation of Gust Load Alleviation Analysis Methodology. NASA TM-86344, December 1984.

23. Howlett, J. T.: Efficient Self-Consistent Viscous-Inviscid Solutions for Unsteady Transonic Flow. NASA TM-86335, January 1985.

24. Gardner, J. E. and Dixon, S. C.: Loads and Aeroelasticity Division Research and Technology Accomplishments for FY 1984 and Plans for FY 1985. NASA TM-86356, January 1985.

25. Sawyer, J. W. and Moses, P. L.: Effects of Holes and Impact Damage on Tensile Strength of Two-Dimensional Carbon-Carbon Composites. NASA TM-86337, January 1985.

26. Williams, M. H.; Bland, S. R.; and Edwards, J. W.: Flow Instabilities in Transonic Small Disturbance Theory. NASA TM-86251, January 1985.

27. Batina, J. T.: Effects of Airfoil Shape, Thickness, Camber, and Angle of Attack on Calculated Transonic Unsteady Airloads. NASA TM-86320, Feb. 1985.

28. Batina, J. T.: Unsteady Transonic Flow Calculations for Two-Dimensional Canard-Wing Configurations with Aeroelastic Applications. NASA TM-86375, February 1985.

29. Berry, H. M.; Batina, J. T. and Yang, Y. T.: Viscous Effects on Transonic Airfoil Stability and Response, NASA TM-86374, February 1985.

30. Seidel, D. A.; Sandford, M. C.; and Eckstrom, C. V.: Measured Unsteady Transonic Aerodynamic Characteristics of an Elastic Supercritical Wing with an Oscillating Control Surface. NASA TM-86376, February 1985.

31. Turnock, D. L.: Two Degree-of-Freedom Flutter Solution for a Personal Computer. NASA TM-86381, February 1985.

32. Cole, S. R.: Exploratory Flutter Test in a Cryogenic Wind Tunnel. NASA TM-86380, February 1985.

33. Ricketts, R. H.: Selected Topics in Experimental Aeroelasticity at the NASA Langley Research Center. NASA TM-86436, April 1985.

34. Sandford, M. C.; Ricketts, R. H.; and Hess, R. W.: Recent Transonic Unsteady Pressure Measurements at the NASA Langley Research Center. NASA TM-86408, April 1985.

35. Batina, J. T.: Unsteady Transonic Flow Calculations for Interfering Lifting Surface Configurations. NASA TM-86432, May 1985.

36. Bennett, R. M.; Seidel, D. A.; and Sandford, M. C.: Transonic Calculations for a Flexible Supercritical Wing and Comparison with Experiment. NASA TM-86439, May 1985.

37. Dixon, S. C.: NASA R&T for Aerospace Plane Vehicles-Progress and Plans. NASA TM-86429, May 1985.

38. Bennett, R. M.; Wynne, E. C.; and Mabey, D. G.: Calculations of Transonic Steady and Oscillatory Pressures on a Low Aspect Ratio Model and Comparison with Experiment. NASA TM-86449, June 1985.

39. Mantay, W. R.; Yeager, W. T., Jr.; Hamouda, M-Nabil; Cramer, R. G., Jr. and Langston, C. W.: Aeroelastic Model Helicopter Rotor Testing in the Langley TDT. NASA TM-86440, June 1985. (

40. Bey, K. S.; Thornton, E. A.; and Dechaumphai, P.: A New Finite Element Approach for Prediction of Aerothermal Loads - Progress in Inviscid Flow Computations. NASA TM-86434, July 1985.

41. Macaraeg, M. G.: A Mixed Pseudospectral/Finite Difference Method for a Driven Fluid in a Nonuniform Gravitational Field. NASA TM-87581, July 1985.

42. Macaraeg, M. G.: The Effect of Power Law Forces on a Thermally-Driven Flow Between Concentric Rotating Spheres. NASA TM-87596, August 1985.

43. Murrow, H. N.: A Perspective on The Status of Measurement of Atmospheric Turbulence in the U.S. NASA TM-87610, September 1985.

44. Shideler, J. L.; Sawyer J. W.; Blosser, M. L.; and Webb, G. L.: Multiwall/RSI Concept for Local Application to Space Shuttle Body Flap. NASA TM-87589, September 1985.

45. Webb, G. L.; Clark, R. K.; and Sharpe, E. L.: Thermal Fatigue Tests of a Radiative Heat Shield Panel for a Hypersonic Transport. NASA TM-87583, September 1985.

Conference Presentations

46. Bennett, R. M.: Recent Developments in Unsteady Transonic Computational Aerodynamics. Presented at the Aeroservoelasticity Technical Specialists Meeting, Wright Patterson AFB, OH, October 1984. Published in the Proceedings of the Aeroservoelastic Specialists Meeting, AFWAL-TR-84-3105, Volume II, October 1984.

47. Edwards, J. W.: Experience with Transonic Unsteady Aerodynamic Calculations. Presented at the Aeroservoelasticity Technical Specialists Meeting, Wright Patterson AFB, OH, Oct. 1984. Published in the Proceedings of the Aeroservoelastic Specialists Mtg., AFWAL-TR-84-3105, Vol. II, Oct. 1984.

48. Dunn, H. J.: An Assessment of Unsteady Aerodynamics Approximations for Time Domain Analysis. Presented at the Aeroservoelasticity Technical Specialists Meeting, Wright Patterson AFB, OH, October 1984. Published in the Proceedings of the Aeroservoelastic Specialists Meeting, AFWAL-TR-84-3105, Volume II, October 1984.

49. Newsom, J. R.: An Overview of the NASA/LaRC Aeroservoelasticity Branch. Presented at the Aeroservoelasticity Technical Specialists Meeting, Wright Patterson AFB, OH, October 1984. Published in the Proceedings of the Aeroservoelastic Specialists Meeting, AFWAL-TR-84-3105, Volume II, Oct. 1984.

50. Perry, Boyd III: Flight Test Technique for Evaluation of Gust Load Alleviation Analysis Methodology. Presented at the Aeroservoelasticity Technical Specialists Meeting, Wright Patterson AFB, OH, October 1984. Published in the Proceedings of the Aeroservoelastic Specialists Meeting, AFWAL-TR-84-3105, Volume II, October 1984.

51. Wieseman, C. D.: A Method to Stabilize Linear Systems Using Eigenvalue Gradient Information. Presented at the Aeroservoelasticity Technical Specialists Meeting, Wright Patterson AFB, OH, October 1984. Published in the Proceedings of the Aeroservoelastic Specialists Meeting, AFWAL-TR-84-3105, Volume II, October 1984.

52. Sawyer, J.W.; Blosser, M. L.; and McWithey, R. R.: Derivation and Test of Elevated Temperature Thermal-Stress-Free Fastener Concept. Presented at Second Sym. on Welding, Bonding, and Fastening held at Langley Research Center, Oct. 23-25, 1984. NASA CP 2387, September 1985.

53. Hood, R. V.; Dollyhigh, S. M.; and Newsom, J. R.: Impact of Flight Systems Integration on Future Aircraft Design. Presented at the AIAA/AHS/ASEE Aircraft Design Systems and Operations Meeting, October 31 - November 2, 1984. AIAA Paper No. 84-2459.

54. Mantay, W. R.; Yeager, W. T., Jr.; Hamouda, M-Nabil; Cramer, R. G., Jr.; and Langston, C. W.: Aeroelastic Model Helicopter Rotor Testing in the Langley TDT. Presented at the AHS Specialists Meeting on Helicopter Test Methodology, October 29 - November 1, 1984, Williamsburg, VA.

55. Mantay, W. R. and Yeager, W. T., Jr.: Aeroelastic Considerations for Torsionally Soft Rotors. Presented at the AHS Specialists Meeting on Rotorcraft Dynamics, Ames Research Center, Moffett Field, CA, Nov. 7-9, 1984.

56. Tai, H. and Runyan, H. L.: Lifting Surface Theory for a Helicopter Rotor in Forward Flight. Presented at the AHS Specialists Meeting on Rotorcraft Dynamics, Ames Research Center, Moffett Field, CA, November 7-9, 1984.

57. Sawyer, J. W. and Moses, P. L.: Effects of Holes and Impact Damage on Tensile Strength of Two-Dimensional Carbon-Carbon Composites. Presented at the Sixth JANNAF Rocket Nozzle Technology Meeting, December 4-6, 1984, Huntsville, Alabama.

58. Sawyer, J. W. and Moses, P. L.: Effects of Holes and Impact Damage on Tensile Strength of Two-Dimensional Carbon-Carbon Composites. Presented at the Ninth Conference on Composite Materials, Cocoa Beach, FL, January 23-25, 1985. CP-2406, pp. 245-260.

59. Howlett, J. T.: Efficient Self-Consistent Viscous-Inviscid Solutions for Unsteady Transonic Flow. Presented at the AIAA 23rd Aerospace Sciences Meeting, Reno, NV, January 1985. AIAA Paper No. 85-0482.

60. Wood, G. M.; Lewis, B. W.; Nowak, R. J.; Puster, R. L.; Fishel, C.; and Paulin, R. A.: Determination of Inert Gas Mixing Ratios in Low Pressure, High Enthalpy Environments by Mass Spectrometry. Presented at New Orleans Convention Center, New Orleans, LA, February 25 - March 1, 1985.

61. Bennett, R. M. and Wynne, E. C.: Calculation of Transonic Steady and Oscillatory Pressures on a Low Aspect Ratio Model and Comparison with Experiment. Presented at the Second DGLR/DFVLR International Symposium on Aeroelasticity and Structural Dynamics, Technical University of Aachen, Germany, April 1-3, 1985. Paper No. 85-17.

62. Ricketts, R. H.: Selected Topics in Experimental Aeroelasticity at the NASA Langley Research Center. Presented at the Second DGLR/DFVLR International Symposium on Aeroelasticity and Structural Dynamics, Aachen, Germany, April 1-3, 1985. Paper No. 85-70.

63. Sandford, M. C.; Ricketts, R. H.; and Hess, R. W.: Recent Transonic Unsteady Pressure Measurements at the NASA Langley Research Center. Presented at the Second DGLR/DFVLR International Symposium on Aeroelasticity and Structural Dynamics, Aachen, Germany, April 1-3, 1985. Paper No. 85-23.

64. McWithey, R. R. and Jackson, L. R.: Structures for Mach 5, Reusable, JP Fueled Ramjet Engines. Presented at the 1985 JANNAF Propulsion Meeting, San Diego, CA, April 9-12, 1985. Paper is Confidential. CPIA-425-Vol. 1-6.

65. Batina, J. T.: Unsteady Transonic Flow Calculations for Two-Dimensional Canard-Wing Configurations with Aeroelastic Applications. Presented at the AIAA/ASME/ASCE/AHS 26th Structures, Structural Dynamics and Materials Conference, Orlando, FL, April 15-17, 1985. AIAA Paper No. 85-0585-CP.

66. Bennett, R. M.; Seidel, D. A.; and Sandford, M. C.: Transonic Calculations for a Flexible Supercritical Wing and Comparison With Experiment. Presented at the AIAA/ASME/ASCE/AHS 26th Structures, Structural Dynamics and Materials Conference, Orlando, FL, April 15-17, 1985. AIAA Paper No. 85-0665-CP.

67. Berry, H. M.; Batina, J. T.; and Yang, T. Y.: Viscous Effects on Transonic Airfoil Stability and Response. Presented at AIAA/ASME/ASCE/AHS 26th Structures, Structural Dynamics and Materials Conference, Orlando, FL, April 15-17, 1985. AIAA Paper No. 85-0586-CP.

68. Chipman, R.; Rauch, F.; Rimer, M.; Muniz, B.; and Ricketts, R. H.: Transonic Test of a Forward-Swept-Wing Configuration Exhibiting Body Freedom Flutter. Presented at the AIAA/ASME/ASCE/AHS 26th Structures, Structural Dynamics, and Materials Conference, Orlando, FL, April 15-17, 1985. AIAA Paper No. 85-0689-CP.

69. Cole, S. R.: Exploratory Flutter Test in a Cryogenic Wind Tunnel. Presented at the AIAA/ASME/ASCE/AHS 26th Structures, Structural Dynamics and Materials Conference, Orlando, FL, April 15-17, 1985. AIAA Paper No. 85-0736.

70. Fuglsang, D. F. and Williams, M. H.: Non-Isentropic Unsteady Transonic Small Disturbance Theory. Presented at the AIAA/ASME/ASCE/AHS 26th Structures, Structural Dynamics and Materials Conference, Orlando, FL, April 15-17, 1985. AIAA Paper No. 85-0600.

71. Pearson, R. M.; Giesing, J. P.; Nomura, J. K.; and Ruhlin, C. L.: Transonic Flutter Model Study of a Multi-jet Aircraft Wing with Winglets. Presented at the AIAA/ASME/ASCE/AHS 26th Structures, Structural Dynamics and Materials Conf., April 15-17, 1985, Orlando, FL. AIAA Paper No.85-0738-CP.

72. Piette, D. S.; Crooks, O. J.; McCreary, W. E.; and Cazier, F. W., Jr.: Experimental Transonic Steady State and Unsteady Pressure Measurements on a Supercritical Wing During Flutter and Forced Discrete Frequency Oscillations. Presented at the AIAA/ASME/ASCE/AHS 26th Structures, Structural Dynamics and Materials Conf., April 15-17, 1985, Orlando, FL. AIAA Paper No. 85-664-CP.

73. Pototzky, A. S. and Perry, Boyd III: Dynamic Loads Analysis of Flexible Airplanes - New and Existing Techniques. Presented at the AIAA/ASME/ASCE/AHS 26th Structures, Structural Dynamics and Materials Conference, Orlando, FL, April 15-17, 1985. Published in the AIAA Conference Proceedings. No. 852 (Part 2), April 1985.

74. Seidel, D. A.; Sandford, M. C.; and Eckstrom, C. V.: Measured Unsteady Transonic Aerodynamic Characteristics of an Elastic Supercritical Wing with an Oscillating Control Surface. Presented at the AIAA/ASME/ASCE/AHS 26th Structures, Structural Dynamics and Materials Conference, Orlando, FL, April 15-17, 1985. AIAA Paper No. 85-0548.

75. Shore, C. P.: Approximate Thermal Analysis of Complex Aerospace Structures Via A Reduction Method. Presented at the AIAA/ASME/ASCE/AHS 26th Structures, Structural Dynamics and Materials Conference, Orlando, FL, April 15-17, 1985. (Poster Session).

76. Dixon, S. C.: NASA R&T for Aerospace Plane Vehicles - Progress and Plans. Presented at the SAE Aerospace Vehicle Requirements Conference, Aerospace Plane Technology Session, Arlington, VA, May 20-23, 1985.

77. Spigel, B. S.; Sawyer, J. W.; and Prabhakaran, R.: An Investigation of the Iosipescu and Asymmetrical Four-Point Bend Tests for Composite Material. Presented at the SESA 1985 Spring Conference on Experimental Mechanics, Las Vegas, NV, June 9-13, 1985. Available in Proceedings.

78. Blosser, M. L.; Scotti, S. J.; Cerro, J. A.; Powell, R. W.; Jackson, L. R.; and Cruz, C. I.: Design Study of a Slant Nose-Cylinder Aeroassisted Orbital Transfer Vehicle. Presented at the AIAA 20th Thermophysics Conf., June 19-21, 1985, Williamsburg, VA. AIAA Paper No. 85-0548.

79. Batina, J. T.: Unsteady Transonic Flow Calculations for Interfering Lifting Surface Configurations. Presented at the AIAA 18th Fluid Dynamics, Plasma Dynamics and Lasers Conference, Cincinnati, OH, July 16-18, 1985. AIAA Paper No. 85-1711.

80. Bey, K. S.; Thornton, E. A.; Dechaumphai, P.; and Ramakrishnan, R.: A New Finite Element Approach for Prediction of Aerothermal Loads - Progress in Inviscid Flow Computations. Presented at the 7th AIAA Computational Fluid Dynamics Conference, Cincinnati, OH, July 15-17, 1985. AIAA Paper No. 85-1533.

81. Kandil, O. A. and Yates, E. C., Jr.: Computation of Transonic Vortex Flows Past Delta Wings - Integral Equation Approach. Presented at the AIAA 18th Fluid Dynamics, Plasmadynamics and Lasers Conference, July 16-18, 1985, Cincinnati, OH. AIAA Paper No. 85-1582.

82. Macaraeg, M. G. and Streett, C.: Improvements in Spectral Collocation Discretization Through a Multiple Domain Technique. Presented at the AIAA 17th Computational Fluid Dynamics Conference, July 15-17, Cincinnati, OH, 1985. AIAA Paper No. 85-1535.

83. Macaraeg, M. G.: A Mixed Pseudospectral/Finite Difference Method for a Thermally Driven Fluid in a Nonuniform Gravitational Field. Presented at the AIAA 18th Fluid Dynamics, Plasma Dynamics, and Laser Conference, Cincinnati, OH, July 16-18, 1985. AIAA Paper No. 85-1661.

84. Taylor, A.: Design Considerations for Reusable Flightweight Cryogenic Propellant Tanks. Presented at the JANNAF Conference, Aerospace Corporation, August 28, 1985. To be published in proceedings.

85. Sawyer, J. W. and Prabhakaran, R.: A Photoelastic Investigation of Asymmetric Four Point Bend Shear Test for Composite Materials. Presented at the Paisley College of Technology 3rd International Conference on Composite Structures, September 9-11, 1985, Paisley, Scotland. Proceedings pending.

86. Murrow, H. N: A Perspective on the Status of Measurement of Atmospheric Turbulence in the U.S. Presented at the 61st AGARD Structures and Materials Panel Meeting, Oberammergau, Federal Republic of Germany, Sept. 10-13, 1985.

87. Runyan, H. L. and Tai, H.: Application of a Lifting Surface Theory for a Helicopter in Forward Flight. Presented at the Eleventh European Rotorcraft Forum on September 10-13, 1985 in London, England. P-24-1-18.

88. Yates, E. C., Jr.: Preliminary on Candidates for AGARD Standard Aeroelastic Configurations. Presented at the 61st Meeting of the AGARD Structures and Materials Panel, Oberammergau, Federal Republic of Germany, September 9-13, 1985.

89. Blosser, M. L.: Carbon-Carbon Structural Concepts for AOTV. Presented at Interagency Planning Group on Carbon-Carbon Composites, Sept. 17-18, 1985, Falls Church, VA. To be published in Proceedings.

Contractor Reports

90. Clayton, J. D.; Haller, R. L.; and Hassler, J. M., Jr.: Design and Fabrication of the NASA Decoupler Pylon for the F-16 Aircraft. NASA CR-172354, January 1985.

91. Clayton J. D. and Haller, R. L.: Design and Fabrication of the NASA Decoupler Pylon for the F-16 Aircraft, Addendum I. NASA CR-172355, Jan. 1985.

92. Lakin, W. D.: Differentiating Matrices for Arbitrarily Spaced Grid Points. NASA CR-172556 (ICASE Report No. 85-5), January 1985.

93. Clayton, J. D.; Haller, R. L.; and Hassler, J. M., Jr.: Design and Fabrication of the NASA Decoupler Pylon for the F-16 Aircraft, Addendum II. NASA CR-172494, February 1985.

94. Freedman, M. I.; Sipcic, S.; and Tseng, K.: A First-Order Green's Function Approach to Supersonic Oscillatory Flow - A Mixed Analytic and Numerical Treatment. (NAG1-276 Boston Univ.) NASA CR-172207, Feb. 1985.

95. Rao, B. M. and Maskew, B.: Inviscid Analysis of Unsteady Blade Tip Flow Correlation Studies. NASA CR-172506, February 1985.

96. Freedman, M. I. and Tseng, K.: A First-Order Time-Domain Green's Function Approach to Supersonic Unsteady Flow. (NAG2-276 Boston University) NASA CR-172208, April 1985.

97. Maskew, B. and Rao, B. M.: Unsteady Analysis of Rotor Blade Tip Flow. NASA CR-3868, May 1985.

98. Shamroth, S. J.: User's Manual for Coordinate Generation Code "CRDSRA." (NAS1-15214 Scientific Research Associates, Inc.) NASA CR-172584, June 1985.

99. Shamroth, S. J.: User's Manual for Airfoil Flow Field Computer Code "SRAIR." (NAS1-15214 SRA, Inc.) NASA CR-172585, June 1985.

100. Levy, R. and Lin, S. J.: Tip Vortex Computer Code SRATIP - User's Guide. (NAS1-14904 SRA, Inc.) NASA CR-172603, July 1985.

101. Ho, T. and Allsup, H. C.: ACC Heat Shield Viability. (NAS1-17347 LTV Aerospace and Defense Company.) NASA R-177934, August 1985.

102. Lin, S-J; Levy, R.; Shamroth, S. J.; and Govindan, T. R.: A Three-Dimensional Viscous Flow Analysis for the Helicopter Tip Vortex Generation Problem. (NAS1-14904 Scientific Research Associates, Inc.) NASA CR-3906, August 1985.

103. Morino, L.: Scalar/Vector Potential Formulation for Compressible Viscous Unsteady Flows. (NAS1-17317 Institute for Computer Application Research and Utilization in Science, Inc.) NASA CR-3921, August 1985.

104. Shamroth, S. J.: Calculation of Steady and Unsteady Airfoil Flow Fields Via the Navier-Stokes Equations. (NAS1-15214 Scientific Research Associates, Inc.) NASA CR-3899, August 1985.

Tech Briefs

105. Taylor, A. H.: Carbon-Carbon Pistons for Internal Combustion Engines. NASA Tech Brief LAR-13150.

106. Puster, R. L.: A System for Controlling the Oxygen Content of a Gas Produced by Combustion. NASA Tech Brief LAR-13257-1.

107. Blosser, M. L.; McWithey, R. R.; and Karns, T. F.: Thermal-Stress-Free-Structural Fasteners for Orthotropic Materials. NASA Tech Brief LAR-13325.

108. Davis, R. C. (Langley Research Center) and Moses, P. L. (PRC Kentron, Inc.): Joint Design for Improved Fatigue Life of Diffusion Bonded Box Stiffened Panels. NASA Tech Brief LAR-13460.

Patents

109. Farmer, M. G.: Model Mount System for Testing Flutter. U. S. Patent 4,475,385. Issued October 9, 1984.

110. Jackson, R. L.; Davis, R. C.; and Taylor, A. H.: Daze Fasteners. U. S. Patent 4,512,699. Issued April 23, 1985.

FY 86 PLANS

The FY 86 plans for the Loads and Aeroelasticity Division are broken out by each of the branches (technical areas) and selected highlights of proposed FY 86 milestones are presented.

Configuration Aeroelasticity Branch

For FY 86 the Configuration Aeroelasticity Branch (CAB) will continue its broadly based research program on dynamic and aeroelastic phenomena of aircraft and rotorcraft as summarized in figure 40.

A large portion of this work is associated with tests in the Langley Transonic Dynamics Tunnel (TDT) with companion theoretical studies. Research studies are planned for both rotorcraft and airplanes. The rotorcraft studies will use the aeroelastic rotor experimental system (ARES). Rotorcraft work will focus on studies of aerodynamically and structurally advanced UH-60 blades and on new rotor concepts such as the hingeless rotor. Airplane focused studies include such items as active flutter suppression, aeroelastic tailoring, and shock induced oscillations. In addition to research studies, an aeroelastic verification test is planned for the JAS-39 airplane.

Work will continue in the area of prediction of helicopter vibration characteristics by using finite element modeling procedures. Studies involving the major airframe manufacturers will be continued.

Significant progress in the development of a new data acquisition, display, and control system for the TDT is expected. Major hardware components will be installed at the TDT site. The installation of the wiring to connect the system to the viscous stations to be served will be completed also.

Selected highlights of proposed FY 86 milestones are listed below and are shown by figures 41 through 44.

Aircraft Aeroelasticity:
- Aircraft Aeroelasticity
- Upgrading the Data Acquisition System for the Langley Transonic Dynamics Tunnel

Rotorcraft Aeroelasticity:
- Rotorcraft Dynamics and Aeroelasticity

Rotorcraft Structural Dynamics:
- A National Capability to Analyze Vibration as Part of Helicopter Structural Design

Each highlight is accompanied by descriptive material.

Unsteady Aerodynamics Branch

For FY 86 there will be a continuing level of activity in developing and applying computational finite-difference algorithms for the solution of the nonlinear unsteady fluid flow equations (Figure 45). To expedite this effort the Branch was collocated with three other Branches at Langley working in the area of CFD: Theoretical Aerodynamics Branch, Transonic Aerodynamics Division; Analytical Methods Branch, Low-Speed Aerodynamics Division; and the Computational Methods Branch, High-Speed Aerodynamics Division. It is anticipated that the synergism of many CFD researchers working in close proximity to each other will be beneficial to all and, for the Unsteady Aerodynamics Branch, offset the decreased interactions with the Configuration Aeroelasticity Branch which remains located at the TDT.

A cooperative effort between NASA - Langley, NASA - Ames, and AFWAL/FDL - FIB was begun this year to establish and maintain a common code for the XTRAN3S program on the Langley VPS 32 and the Ames and AFWAL CRAY Computers. Effort will continue on comparisons with extant data sets and on augmentation of the code moving towards the capability of providing results for a complete vehicle within the constraints of the transonic small disturbance theory on which it is based. New contractual efforts will be started to develop 3-D Unsteady Boundary Layer Code and a Full Potential Aeroelastic Code. In addition, a new grant effort will be started to study the effects of leading-edge vortices on aeroelastic stability. Work continues on the design and fabrication of a model for study of unsteady loads for a delta wing/canard configuration to be conducted in FY 87 and design will start of a simple rectangular benchmark aeroelastic model for testing in FY 88.

Aeroservoelasticity Branch

There are several efforts planned for FY 86 (Figure 46) in each of the three major areas of analysis methods, design methods, and applications and validations.

In the analysis methods area, a new area of research in static aeroservoelasticity will begin. Both linear and nonlinear methods will be investigated. There will be a continued development of optimal sensitivity analysis for both analysis and control law synthesis. This continued

development will provide the basis for integrated structure/control design methodology.

In the applications and validations area, a comparison of predicted and wind-tunnel data for ARW-2 will be undertaken. There is also a plan to apply the advanced control law optimization methods to integrated active controls for a supersonic-cruise fighter configuration. A wind-tunnel test will be conducted to explore the possibility of actively controlling a "shock-induced" instability observed on the ARW-2 wing.

Reporting will begin on results of the spanwise gradient measurements of atmospheric turbulence.

Selected highlights of proposed FY 86 milestones are listed below and are shown by figures 47 and 48.

Analysis and Design Methods:
- Active Control of "Shock-Induced" Instability

Applications:
- Comparison of ARW-2 Wind-Tunnel Data with LInear Steady and Unsteady Unsteady Aerodynamic Predictions

Each highlight is accompanied by descriptive material.

Aerothermal Loads Branch

For FY 86, there will be a continuing level of activity in all three disciplines as summarized in figure 49.

Thermal Loads - The major thrusts of the thermal loads research effort for FY 86 consist of four specific tasks: 1) test to determine the aerothermal loads on a blunt leading edge model with an impinging shock and the chine gap model will be performed in the 8' HTT; 2) numerical analyses of a gas-jet-nose-tip and a simulated space shuttle wing-elevon cove will be completed; 3) results of aerothermal loads tests on the spherical protuberances, split elevon, simulated thermally bowed metallic TPS and gas-jet-nose-tip will be documented; 4) high temperature instrumentation techniques for the 8' HHT will be evaluated.

Integrated Analysis - The major thrust for the ALB analytical effort in FY 86 consists of two specific tasks: 1) continued development of finite element methodology for the prediction of aerothermal loads to complement and supplement the experimental effort including implementation and evaluation of 3-D viscous analysis and adaptive refinement techniques; 2) continued development of the integrated fluid-thermal-structures analysis capability as a tool to design and evaluate structural concepts for super/hypersonic vehicles including implementation and evaluation of a single Taylor-Galerkin algorithm to simultaneously solve all three disciplines.

Facilities Operations and Development - The facilities effort involves the safe and efficient operation and the expansion of the test capabilities of the five active high energy facilities of the Aerothermal Loads Branch--the 8'

High Temperature Tunnel (8' HTT) the 7" High Temperature Tunnel (7" HTT), and the 1, 5, and 20 MW Aerothermal Arc Tunnels.

A major thrust will be the verification testing in the 7" HTT of techniques for providing alternate Mach numbers (4, 4.5, and 5) and oxygen enrichment of the methane air combustion products test stream. This effort is in support of the modification (FY 85 CofF) of the 8' HTT which will make it a unique national research facility for testing air-breathing propulsion systems for very high speed aircraft and missiles.

During FY 86 the Blunt Body Impinging Shock, CSTA Chine Gap Heating, Turbulent Boundary Layer Survey, Transpiration Cooled Radome, and 2-D Shock/Boundary Layer Interaction models will be tested in the 8' HTT.

Selected highlights of proposed FY 85 milestones are listed below and are shown by figures 50 through 53.

Thermal Loads:
- Numerical Analysis of a Gas-Jet-Nose-Tip
- Numerical Analysis of the Aerothermal Environment in a Simulated Space Shuttle Wing-Elevon Cove

Integrated Analysis:
- Integrated Flow-Thermal-Structural Finite Element Analysis

Facilities Operation and Development:
- Oxygen Enrichment and Alternate Mach Number Modification to the Langley 8' High Temperature Tunnel

Each highlight is accompanied by descriptive material.

Thermal Structures Branch

There are several major research activities for FY 86 which collectively represent a concerted thrust to advance the state of the art in thermal structures (figure 54).

Systems studies will continue to identify structural technology needs and to assess various concepts proposed to meet these needs. Emphasis will be on transatmospheric vehicles although efforts will continue in support of two proposed (but as yet not approved) NASA flight experiments, the Entry Research Vehicle (ERV) and the Aeroassisted Orbital Transfer Vehicle (AOTV). Work on airframe structure will transition from titanium concepts developed for a Mach 5 airplane to carbon-carbon structures for use as control surfaces of high speed vehicles.

Work on TPS will be focused on: Solving the gap flow problem for superalloy metallic concepts, with tests of the modified curved surface TPS model scheduled for late FY 86; completion of tests of the 1 ft. x 2 ft. ACC panel with analysis of results for the gap heating at panel edges; and a new effort looking at heat pipes and active cooling for stagnation heating regions such as leading edges and nose caps. The latter effort will consist of

analytical studies and preliminary designs in FY 86 followed by detailed design, fabrication, and test of selected hardware components in FY 87.

In the area of propulsion structure, work will continue of the scramjet fuel injector strut, with fabrication expected to be complete by mid CY 86 and tests starting in early CY 87. Work on COWL lip cooling will be initiated with an analytical study of the effects of variations of geometries and heating rates on concept designs. Low level-of-effort contractor studies will continue on a ramjet indirect cooling system for use on a Mach 5 class cruise airplane, and a missile/scramjet engine structure program.

Analytical efforts will continue to focus on enhanced thermal structural analysis, optimization methods for thermal structural concepts, and documentation of programs developed in-house for conceptual design studies.

CONCLUDING REMARKS

This publication documents the FY 1985 accomplishments, research and technology highlights, and FY 1986 plans for the Loads and Aeroelasticity Division.

REFERENCES

1. Garrick, I. E.: Aeroelasticity - Frontiers and Beyond. J. of Aircraft, Vol. 13, No. 9, September 1976. pp. 641-657.

2. Ashley, Holt: On Making Things The Best - Aeronautical Uses of Optimization. J. of Aircraft, Vol. 19, No. 1, January 1980. pp. 5-28.

3. Stone, J. E. and Koch, L. C.: Hypersonic Airframe Structures Technology Needs and Flight Test Requirements. NASA CR-3130. Appendix B, Page 124.

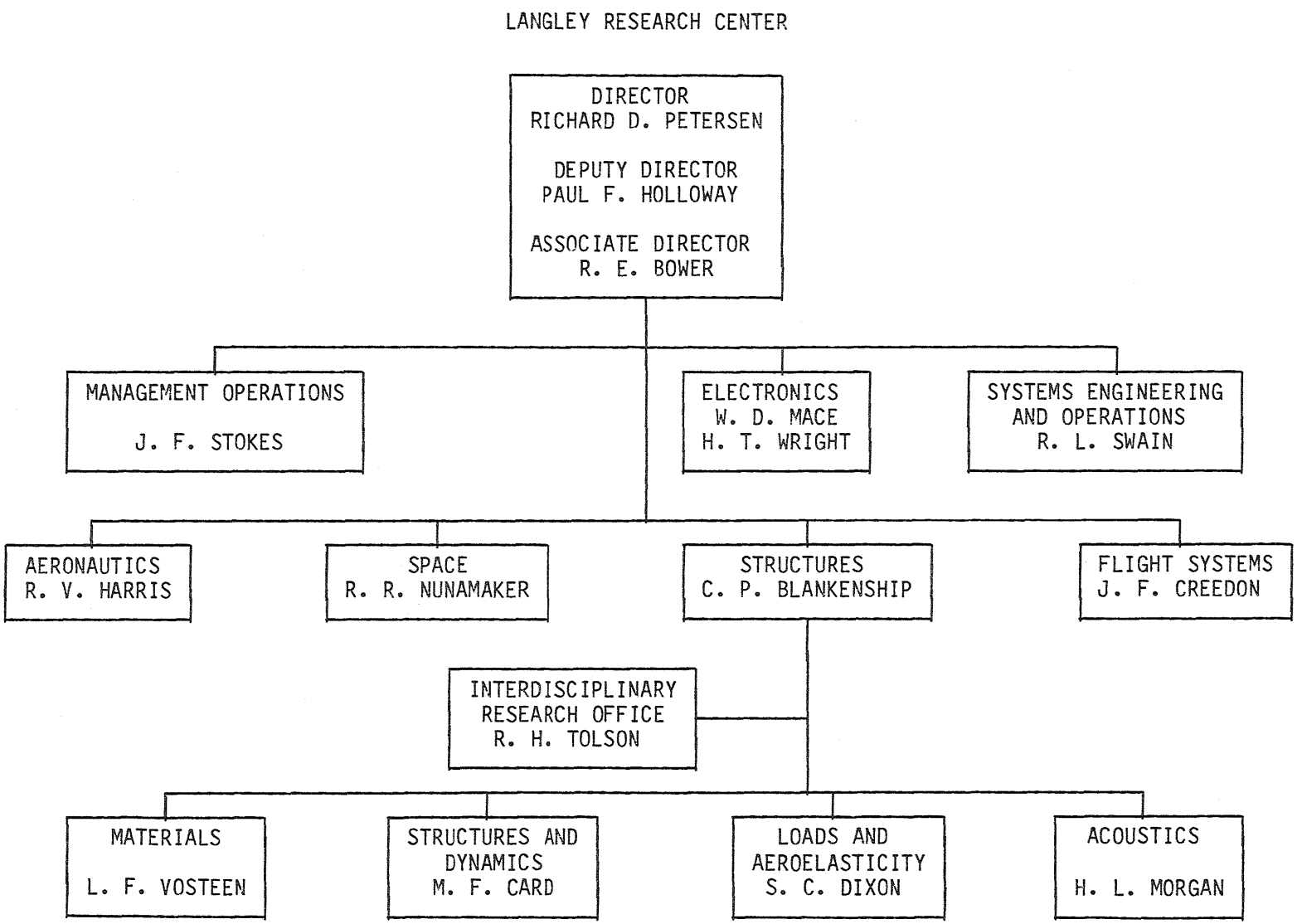
LANGLEY RESEARCH CENTER
DIRECTOR
RICHARD D. PETERSEN
DEPUTY DIRECTOR
PAUL F. HOLLOWAY
ASSOCIATE DIRECTOR
R. E. BOWER
MANAGEMENT OPERATIONS
J. F. STOKES
ELECTRONICS
W. D. MACE
H. T. WRIGHT
SYSTEMS ENGINEERING
AND OPERATIONS
R. L. SWAIN
AERONAUTICS
R. V. HARRIS
SPACE
R. R. NUNAMAKER
STRUCTURES
C. P. BLANKENSHIP
FLIGHT SYSTEMS
J. F. CREEDON
INTERDISCIPLINARY
RESEARCH OFFICE
R. H. TOLSON
MATERIALS
L. F. VOSTEEN
STRUCTURES AND
DYNAMICS
M. F. CARD
LOADS AND
AEROELASTICITY
S. C. DIXON
ACOUSTICS
H. L. MORGAN

Figure 1.

LOADS AND AEROELASTICITY DIVISION
5

CHIEF: SIDNEY C. DIXON
ASSISTANT CHIEF: IRVING ABEL
CHIEF SCIENTIST: E. CARSON YATES, JR.
TECHNICAL ASSISTANT: JAMES E. GARDNER

CONFIGURATION AEROELASTICITY BRANCH
12 + 9*

HEAD: ROBERT DOGGETT

- AIRCRAFT AEROELASTICITY
- ROTORCRAFT AEROELASTICITY
- ROTORCRAFT STRUCTURAL DYNAMICS

UNSTEADY AERODYNAMICS BRANCH
10

HEAD: JOHN EDWARDS

- THEORY DEVELOPMENT
- UNSTEADY PRESSURE EXPERIMENTS

AEROSERVOELASTICITY BRANCH
11

HEAD: JERRY NEWSOM

- ANALYSIS AND DESIGN METHODS
- APPLICATIONS

AEROTHERMAL LOADS BRANCH
15

HEAD: ALLAN WIETING

- THERMAL LOADS
- INTEGRATED THERMAL-FLUID ANALYSIS
- FACILITIES OPERATIONS AND DEVELOPMENT

THERMAL STRUCTURES BRANCH
12

HEAD: DONALD RUMMLER

- STRUCTURAL SYSTEMS STUDIES
- CONCEPT DEVELOPMENT
- ANALYICAL METHODS AND APPLICATIONS

TOTAL NASA - 65

* TOTAL ARMY - 8

* TOTAL AF - 1

Figure 2.

LOADS AND AEROELASTICITY DIVISION

LONG RANGE THRUSTS

AERONAUTICS

- PREDICTION AND CONTROL OF AEROELASTIC STABILITY AND RESPONSE FOR AIRCRAFT AND ROTORCRAFT
- AEROTHERMAL STRUCTURES AND MATERIALS FOR HIGH SPEED VEHICLES

SPACE

- AEROTHERMAL STRUCTURES AND MATERIALS FOR SPACE TRANSPORTATION SYSTEMS

Figure 3.

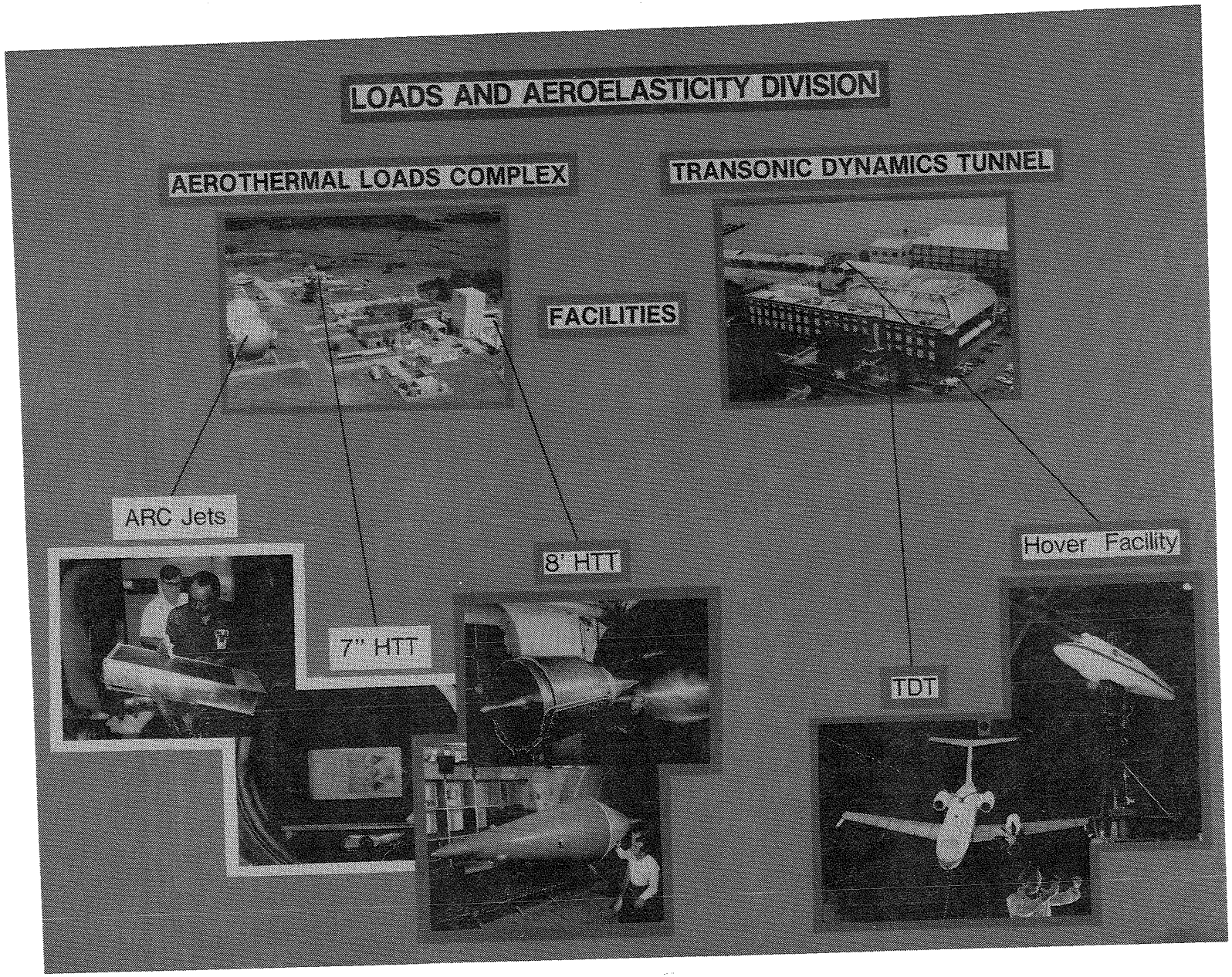
LOADS AND AEROELASTICITY DIVISION
AEROTHERMAL LOADS COMPLEX
TRANSONIC DYNAMICS TUNNEL
FACILITIES
ARC Jets
8' HTT
7" HTT
Hover Facility
TDT

Figure 4.

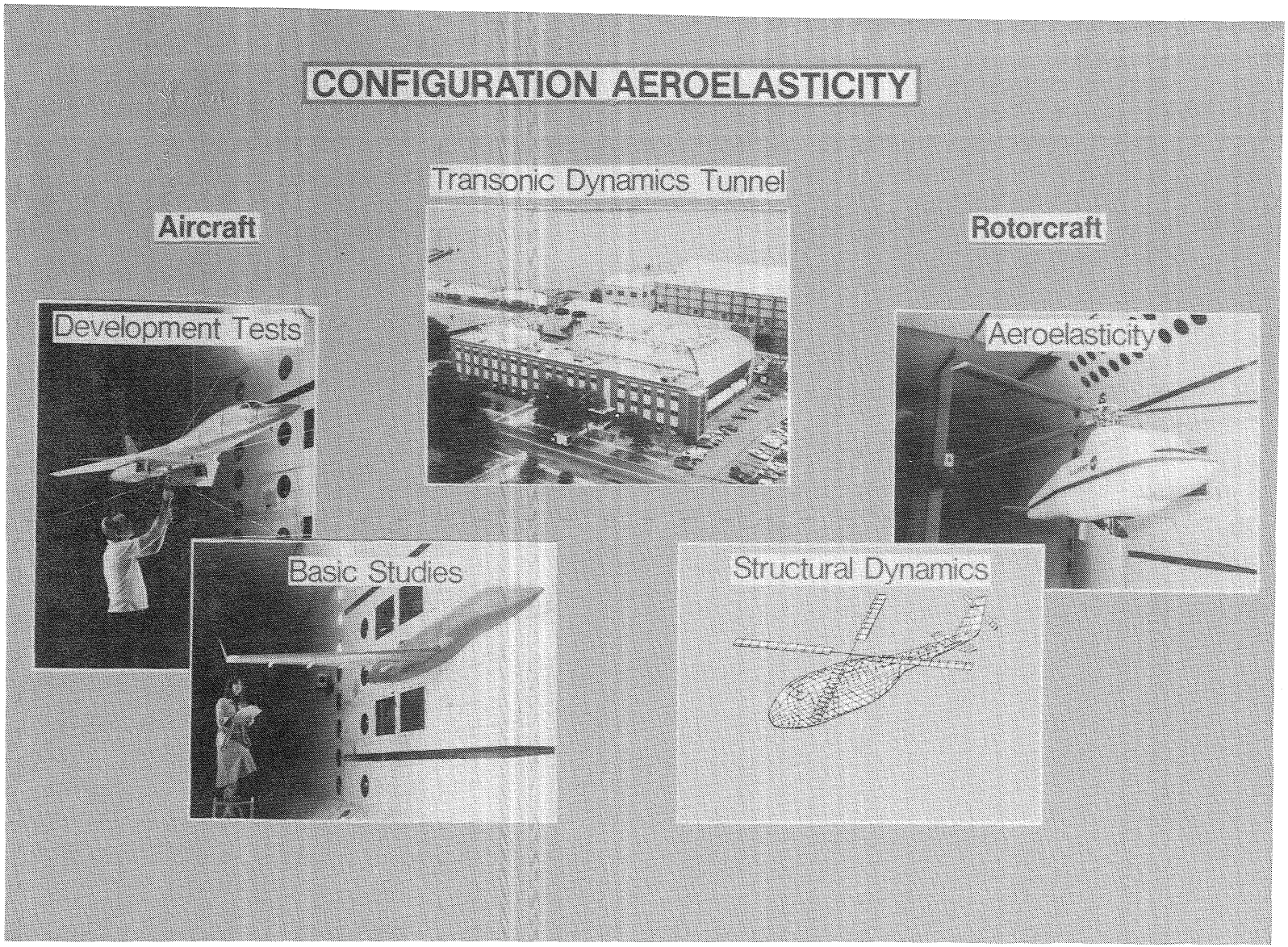
CONFIGURATION AEROELASTICITY
Transonic Dynamics Tunnel
Aircraft
Rotorcraft
Development Tests
Aeroelasticity
Basic Studies
Structural Dynamics

Figure 5.

CONFIGURATION AEROELASTICITY
FIVE YEAR PLAN

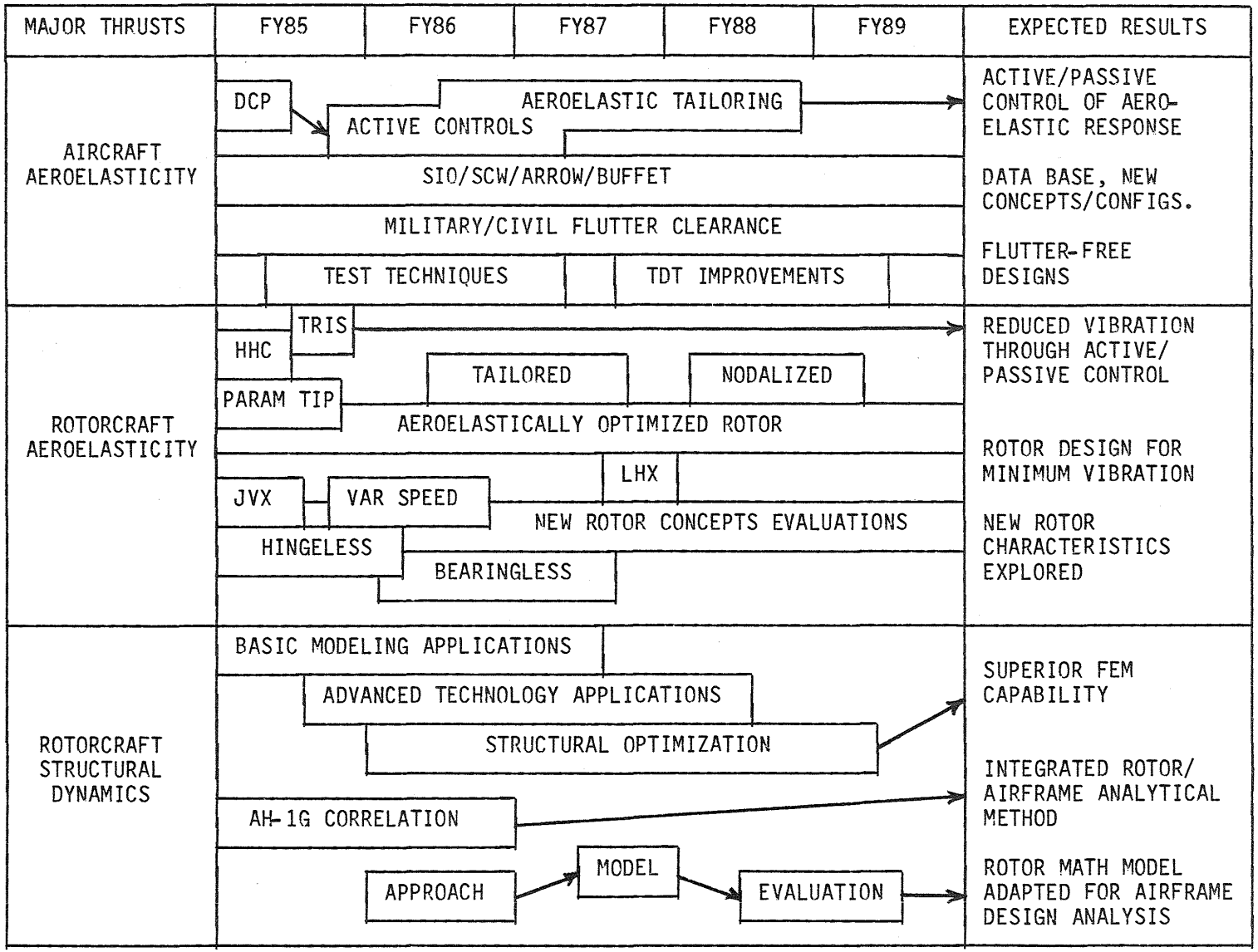

Figure 6.

NASA PROPFAN TESTBED AIRCRAFT SHOWN SAFE FROM FLUTTER IN TDT TEST

Charles L. Ruhlin
Configuration Aeroelasticity Branch
Ext. 2661

Michael H. Durham
PRC Kentron Inc.
Ext. 2661

RTOP 505-63-21

Research Objective - The NASA Propfan Test Assessment (PTA) program is underway to evaluate by flight tests the operational performance of a new propeller design (propfan). A propfan offers the advantage of high-speed flight at a 15-30 percent fuel savings over conventional jet engines. The Lewis Research Center has contracted with the Lockheed-Georgia Company (Gelac) to modify and fly a Gulfstream G-II airplane as a testbed with a propfan and powerplant on the left wing (Figure 7(b)). The flight test article consists of an eight-bladed propfan powered by a turbine engine through a gearbox. Airplane modifications include beefing-up of the left inboard wing box and adding a balance boom ($\approx$ 2500 lbm) on the right wing and a flutter boom ($\approx$ 300 lbm) on the left wing. To help ensure the flutter safety of this unusual asymmetric airplane, a 1/9-size flutter model was tested in the Langley Transonic Dynamics Tunnel (TDT). The test objectives were to demonstrate flutter safety margins for representative airplane configurations and to obtain flutter data for correlation with analysis.

Approach - The flutter model was furnished by Gelac. The TDT tests were conducted in Freon-12 at Mach numbers up to 0.9 and at up to 1.44 times scaled flight dynamic pressures. The model was supported on a two-cable mount system and tested in a trimmed level attitude by remote control of the all-movable horizontal tail, right wing flaperon, and rudder. The model components were elastically and dynamically scaled with these exceptions: the empennage and propfan blades were overstiff, and the fuselage mass properties were altered to eliminate a mount instability. Additional wing panels were built so that symmetric wing pairs could be simulated. Flight configurations tested were two fuel conditions (12 and 50 percent) for propfan blades off and on configurations. The propfan was unpowered but windmilling. To induce flutter, several configurations were investigated with different wingtip boom configurations.

Accomplishment Description - For the airplane represented by the scaled flutter model, the following results apply. The tests demonstrated that the propfan testbed airplane has the required flutter safety margin. Test results indicate that the flutter boom on the left wing may not be necessary. Some limited flutter data were obtained that show the effect of wing asymmetry to be slightly stabilizing and the effect of the windmilling propeller to be negligible. These experimental trends are generally consistent with those obtained analytically. Overall, the Gelac preliminary flutter analyses were conservative, i.e., the analyses predicted lower flutter speeds than experiments.

Future Plans: No further tests of this model are planned. Gelac will update the analytical structural representation to better match the model properties and conduct further flutter analyses to determine the effect of model-airplane differences. However, extensive analytical efforts are probably not warranted because of the ample flutter safety margins demonstrated in the model tests.

Figure 7(a).


NASA PROPFAN TESTBED AIRCRAFT
SHOWN SAFE FROM FLUTTER IN TDT TEST

Figure 7(b).

MODIFICATIONS TO INCREASE TEST MEDIUM DENSITY IN LANGLEY TRANSONIC DYNAMICS TUNNEL COMPLETED

Bryce M. Kepley
Configuration Aeroelasticity Branch
Ext. 2661

RTOP 505-63-21

Research Objective - As airplanes become lighter (more structurally efficient), as with the use of composite major structures, or as they incorporate the use of active controls (which means the models have to employ relatively heavy active control hydraulic systems internally), it became increasingly difficult to fabricate models which are light enough to match full-scale mass-density ratios with previous TDT density capability. To overcome this problem an increase in test medium density was proposed for the TDT.

Approach - This FY 83 CofF project provided for increasing the maximum test density by 50 percent at transonic speeds. The increased density capability was provided by rewinding the existing fan motor to increase the power rating from 20,000 hp to 30,000 hp. Additional tunnel cooling capacity was provided to accommodate the increased tunnel power limit. Other major modifications included changes to the electrical power distribution system and installation of a new speed control system. The design for the modifications provided for dividing the main aspects of work into a series of independent work packages to be performed by separate contractors.

Accomplishment description - Work for all seven of the work packages directly associated with the density increase, primarily, increasing the fan horsepower, installing new cooling system, and modifying the electrical distribution system, has been completed. (An eighth item, painting the tunnel exterior will be accomplished in spring-summer of 1986). An exhaustive checkout of all modifications has been completed and showed that all the work had been successfully accomplished. A comparison of the former and new operational boundary is shown in figure 8(b) as the variation of dynamic pressure with Mach number. A comparison of the two boundaries clearly shows that the intended increase in performance was obtained. For short periods of time, ten minutes or less, dynamic pressure greater than those shown in the figure are achievable, for example, 625 psf at a Mach number of 0.9.

Future Plans - The density increase work has been completed and research operations have been resumed.

Figure 8(a).

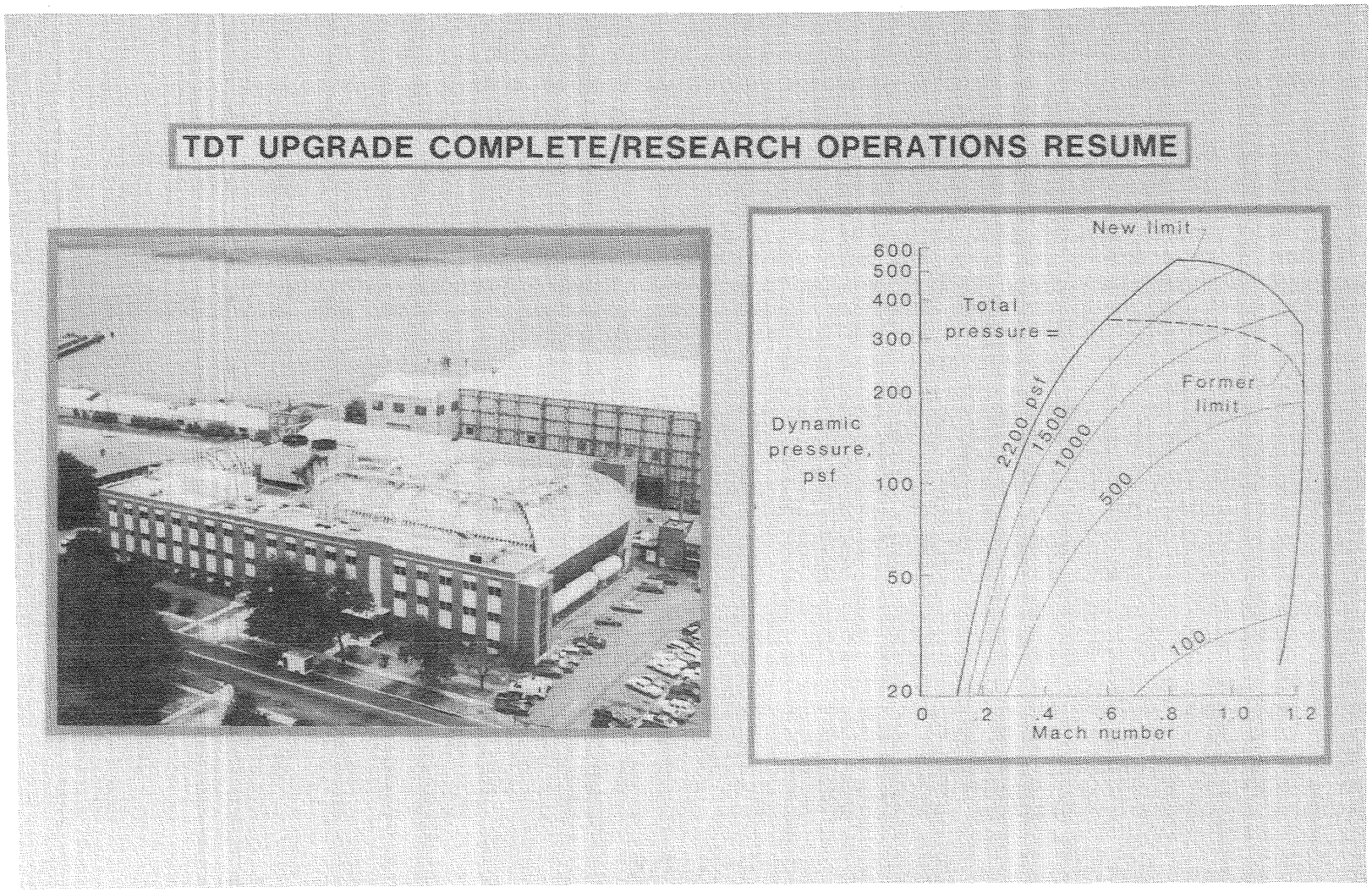
TDT UPGRADE COMPLETE/RESEARCH OPERATIONS RESUME
New limit
600
500
400
300
200
100
50
20
Total pressure =
Former limit
2200 psf
1500
1000
500
100
Dynamic pressure, psf
0
.2
.4
.6
.8
1.0
1.2
Mach number

Figure 8(b).

TOTAL ROTOR ISOLATION SYSTEM (TRIS) VERY EFFECTIVE IN REDUCING HELICOPTER VIBRATIONS

John H. Cline
Configuration Aeroelasticity Branch
Ext. 2661

RTOP 505-61-51

Research Objective - The development of methods for reducing helicopter vibrations has been an important research area for many years because vibrations can have a significant adverse effect on helicopter airframe fatigue life, electronic equipment failure rates, crew and passenger comfort and in some cases limit the forward speed of the aircraft. A number of methods, both passive and active, have been developed and utilized in flight with varying degrees of success. A promising new system, the Total Rotor Isolation System (TRIS), that employs Liquid Inertia Vibration Eliminator (LIVE) units has been developed for isolating all six degrees of freedom of aircraft fuselage dynamic response from the continuously changing airloads developed by the rotor. Each LIVE unit is a two cylinder, two reservoir, tuned port arrangement with liquid Mercury used as a "hydraulic fluid." The objective of this research was to evaluate the effectiveness of the TRIS system.

Approach - To determine the effectiveness of TRIS in reducing helicopter vibrations, a flight verification study was conducted at Bell Helicopter's Flight Research Center in Arlington, TX. The flight test program was performed under a NASA contract with funding by the U.S. Army Aerostructures Directorate. The objective was to demonstrate 90-percent (or greater) isolation of the helicopter fuselage from forces and moments input at the rotor hub at the blade passage frequency, four-per-revolution, for the TRIS-configured Bell 206LM helicopter used as a testbed. The test helicopter is shown on in figure 9(b).

Accomplishment Description - The illustrative data in the figure show the TRIS was very effective in reducing the four-per-revolution vibration levels at the pilots seat. For the case shown the goal of 0.05g's was reached over the range of forward speeds shown, including the transition from hover to forward flight condition with its traditionally high vibration levels. The flight test results generally indicate at least a 95-percent reduction in vibration levels from the rotor hub to the pilot's seat. In addition to substantial reductions in vibrations, the pilots commented that the flying qualities of the TRIS-equipped helicopter were significantly improved over those of the unmodified airplane. The reason for this unexpected improvement if not fully understood but appears to be attributable in part to TRIS and in part to the uncoupled control system used on the test helicopter. This matter is currently under study by Bell personnel.

Future Plans - Results will be documented in a contractor report.

Figure 9(a).

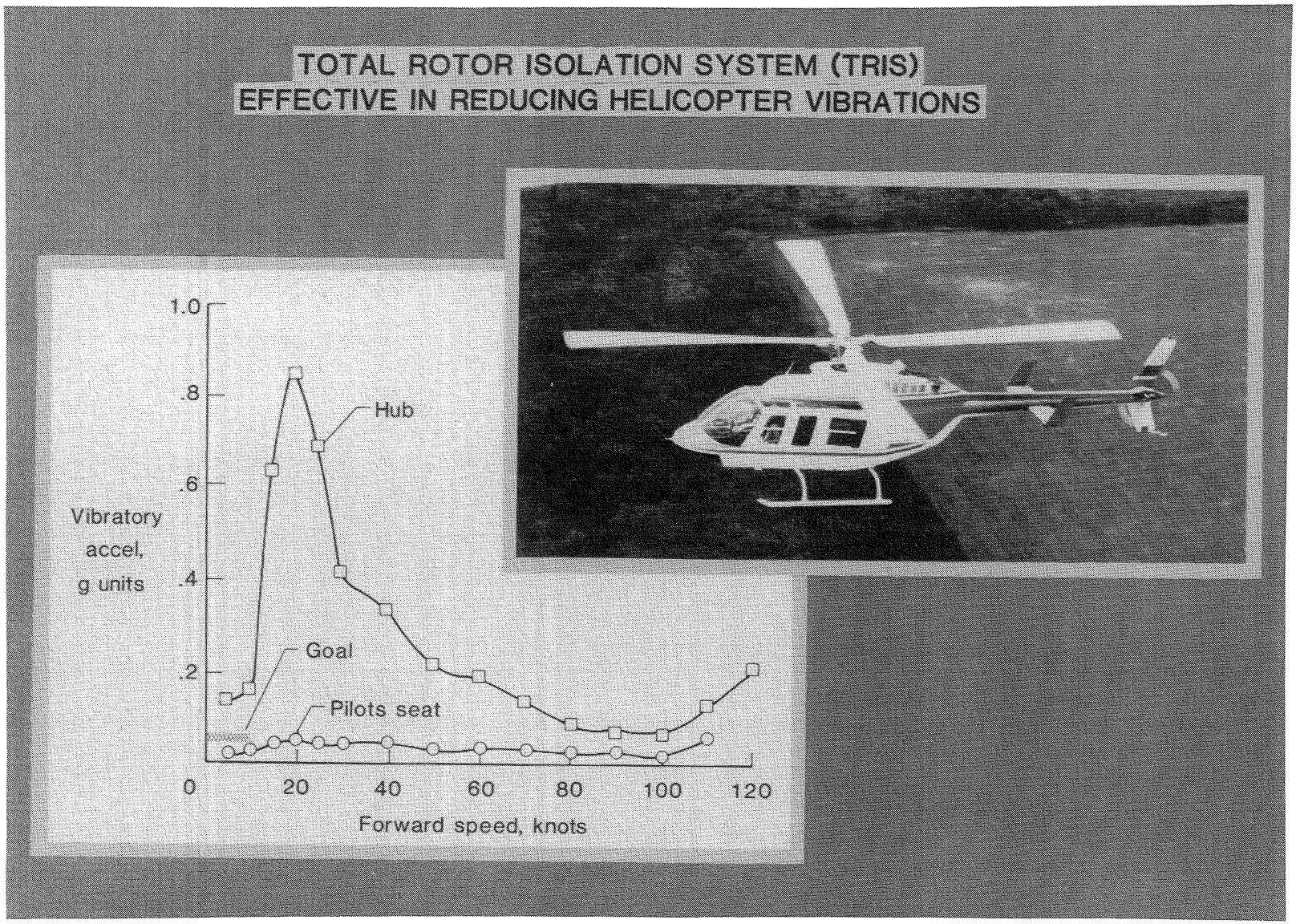
TOTAL ROTOR ISOLATION SYSTEM (TRIS)
EFFECTIVE IN REDUCING HELICOPTER VIBRATIONS
1.0
.8
.6
.4
.2
0
Vibratory
accel,
g units
Hub
Goal
Pilots seat
20
40
60
80
100
120
Forward speed, knots

Figure 9(b).

SECOND TDT TEST EXPANDS JVX DATA BASE TO INCLUDE DESIGN UPDATES

William T. Yeager, Jr., Charles L. Ruhlin, and Robert G. Cramer, Jr.
Configuration Aeroelasticity Branch
Extension 2661

RTOP 505-61-51

Research Objective - To provide an experimental data base needed for the JVX design development, a 0.2-size aeroelastically scaled, semi-span model of a JVX design was tested in the Langley Transonic Dynamics Tunnel (TDT). Test objectives were to determine wing/rotor stability in the airplane mode, to measure rotor and control system loads and vibration data primarily in the helicopter to airplane conversion mode, and to correlate these results with analysis. An initial test series (8 weeks, February-April 1984) was conducted to determine design parametric effects on an early baseline design. A second test series (6 weeks, June-July 1984) was conducted to determine the effects of the latest design updates. These updates included a new wing spar (increased chord and torsional stiffness, decreased bending stiffness), modified engine nacelle mass and c.g., stiffened rotor blades, and an updated rotor hub design having a coning hinge.

Approach - The test was conducted by a team of NASA-Army-Bell-Boeing/Vertol personnel. The model (see figure 10(b)) consisted of a scaled, cantilevered wing and pylon/rotor system that could be operated with the rotor either powered or windmilling. The model was tested in both air (low Mach number operation) and Freon (high Mach number operation) at densities corresponding to altitudes from sea level to 10,000 feet. Sub-critical damping data were obtained by exciting the model in the wing beam, chord, and torsion modes. Tested were three configurations: A) the new wing spar and modified engine nacelle with the initial hub and rotor blades, B) configuration A with the rotor blades stiffened, and C) configuration B with the new coning-hinge hub.

Accomplishment Description - Wing beam mode instabilities remained critical (lowest flutter speed) for the updated configurations tested, although at several test conditions the model was also close to a wing chord mode instability. The effects of the design updates on stability speed are shown in the attached figure for the model in air with windmilling rotors for either the engine nacelle locked (on downstop) or unlocked (off downstop) to the wing. The data were obtained at various percentages of the nominal rotor operating RPM and are normalized to a reference baseline instability speed from the initial test. It can be seen that the design updates generally increased the flutter speed, with the coning-hinge hub having the largest overall effect. Note that the design effects are considerably different for each downstop condition and are also different at the various RPM levels. Included in the figure are some preliminary analytical results calculated by Boeing Vertol using CAMRAD which show reasonable agreement with the experimental data.

Future Plans - No further JVX tests in the TDT are planned for the near future. A report on the TDT test results for the JVX model is under consideration as data reduction and analysis continues.

Figure 10(a).

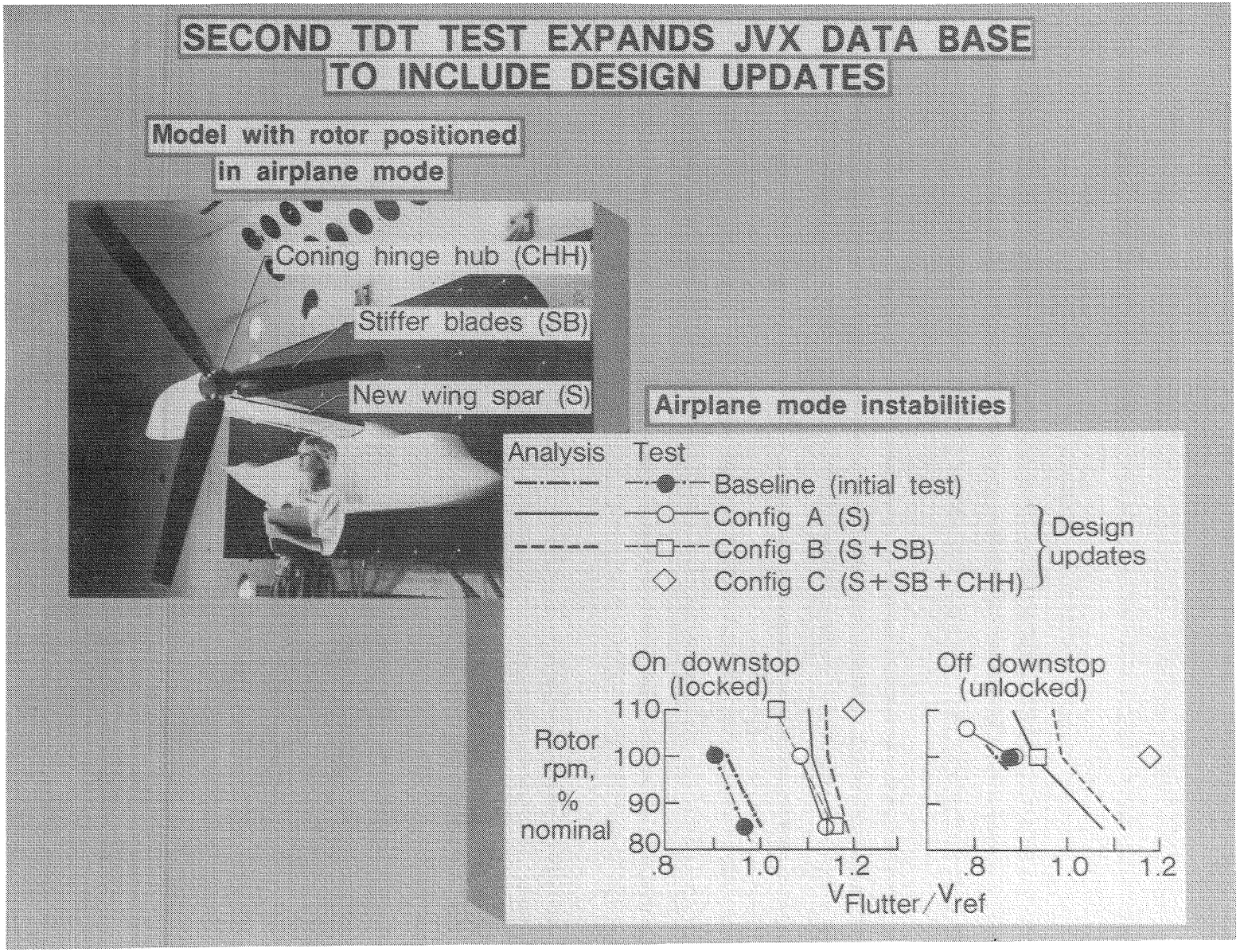
SECOND TDT TEST EXPANDS JVX DATA BASE TO INCLUDE DESIGN UPDATES
Model with rotor positioned in airplane mode
Coning hinge hub (CHH)
Stiffer blades (SB)
New wing spar (S)
Airplane mode instabilities
Analysis
Test
Baseline (initial test)
Config A (S)
Config B (S + SB)
Config C (S + SB + CHH)
Design updates
On downstop (locked)
Off downstop (unlocked)
Rotor rpm, % nominal
110
100
90
80
.8
1.0
1.2
$V_{Flutter}/V_{ref}$

Figure 10(b).

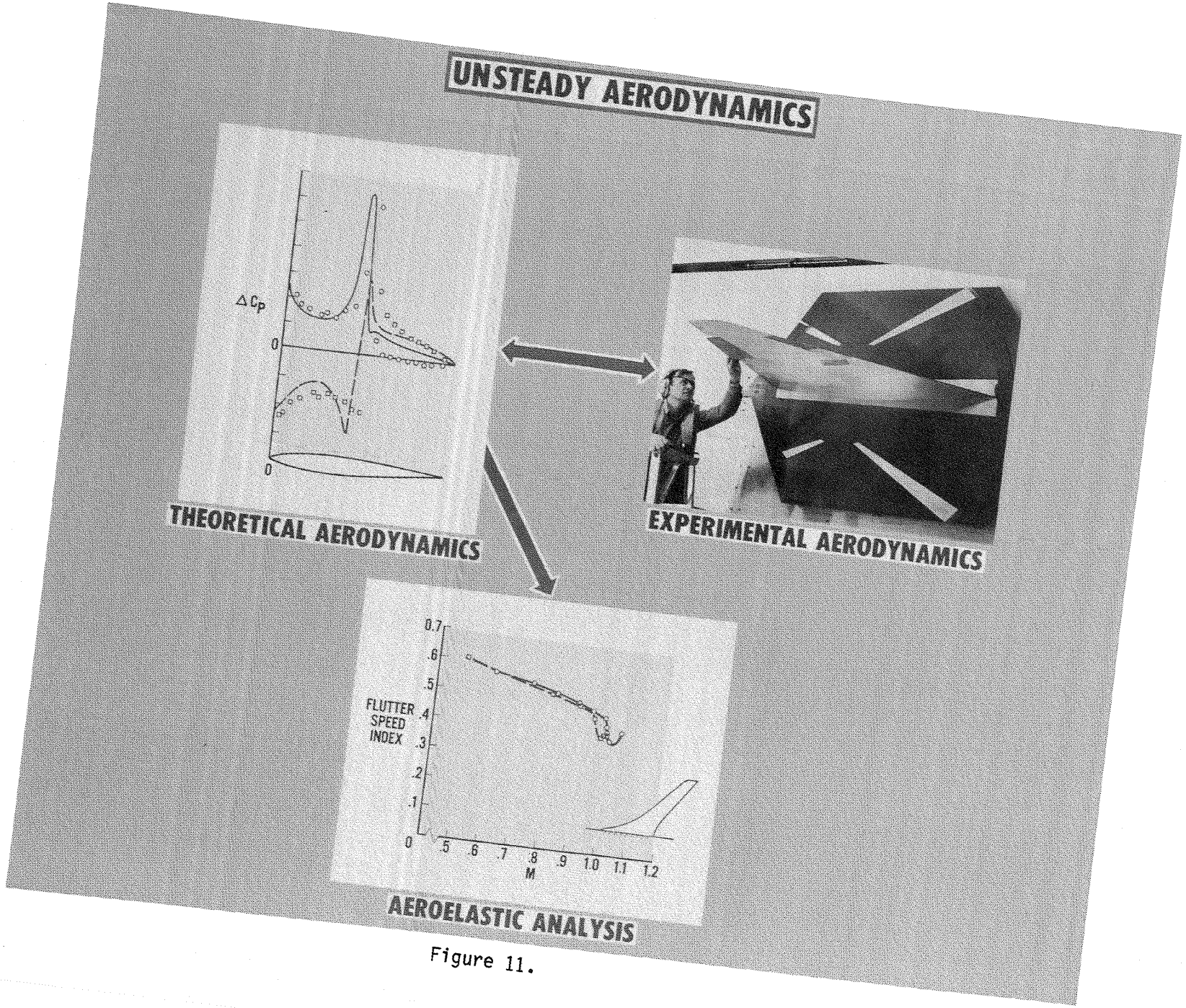
UNSTEADY AERODYNAMICS
ΔC_p
0
0
THEORETICAL AERODYNAMICS
EXPERIMENTAL AERODYNAMICS
FLUTTER SPEED INDEX
0.7
.6
.5
.4
.3
.2
.1
0
.5 .6 .7 .8 .9 1.0 1.1 1.2
M
AEROELASTIC ANALYSIS

Figure 11.

UNSTEADY AERODYNAMICS

FIVE YEAR PLAN

MAJOR THRUSTS	FY 85	FY 86	FY 87	FY 88	FY 89	EXPECTED RESULTS
THEORY DEVELOPMENT	ATTACHED FLOW AIRLOADS ON COMPLETE VEHICLE					ACCURATE PREDICTIONS OF AEROELASTIC RESPONSE FOR CONVENTIONAL AND NOVEL A/C
		SEPARATED AND VORTEX FLOW AIRLOADS				
DESIGN METHODS		EFFICIENT AEROELASTIC ANALYSIS				ACCURATE AND AFFORDABLE AEROELASTIC ANALYSIS TOOLS
			INTEGRATED DESIGN CAPABILITY			
EXPERIMENT	UNSTEADY PRESSURES OSCILLATING MODELS					VALIDATED ANALYSIS METHODS
		BENCHMARK FLUTTER MODEL TESTS				

Figure 12.

XTRAN3S FLUTTER CALCULATIONS COMPARED WITH RENOFT MODEL RESULTS

Herbert J. Cunningham
Unsteady Aerodynamics Branch
Ext. 4236

RTOP 505-63-21

Research Objective - The objective of this research was to evaluate XTRAN3S flutter boundary predictions by comparison with experimental results obtained in the 0.3M cryogenic wind tunnel at both subsonic and transonic Mach numbers.

Approach - The program XTRAN3S provides a finite-difference, time-marching solution to the nonlinear small disturbance potential equation for transonic flow over an aerodynamic body in three-dimensional space. After calculating a converged static solution, an initial structural disturbance is imposed and the transient response of the flutter model is calculated for a specified dynamic pressure. The dynamic pressure is varied in order to determine the flutter speed for which the resulting motion is neutrally stable, neither growing nor decaying.

Accomplishment Description - The semi-span model tested and analyzed has a rectangular planform, a full-span aspect ratio of 3.0, and an NACA 64A010 airfoil section. It was flexibly supported at its root and the three natural modes used in the analysis were an inelastic flapping (first bending) and pitching (first torsion), and elastic second bending. Figure 13(b) displays at the left steady upper-surface pressure distributions for M = 0.7 and 0.85 (negative pressure us up). For a specified dynamic pressure, the transient motion resulting from an initial disturbance is calculated by integrating the structural equations of motion simultaneously with the flowfield calculation. On the right hand side of the figure, the dynamic pressure at flutter, q_f, is compared to experimental results for a range of test temperatures. The open symbols of the test and the curves of linear theory are those of NASA TM 86380 by S. R. Cole and show that there is not a large effect of Reynolds number for this model. The solid symbols are the new XTRAN3S results for M = 0.7, 0.8, and 0.85. The solid unflagged symbols are from the complete nonlinear theory calculations while the flagged symbol was obtained by running the code for the linear case. For M of 0.7 and 0.8, the shock is nonexistent or very weak and the XTRAN3S calculations agree very well with both experiment and linear theory. In contrast, the nonlinear XTRAN3S result at M = 0.85 where there is a strong shock is 55 percent higher than experiment, while the linear code result remains in good agreement with experiment. This substantial difference is judged to indicate that the strong shock is not properly treated, and that an improved treatment is needed.

Future Plans - Potential equation codes do not properly account for entropy generated by shock waves. Modifications to the code are being made to account for these strong shocks conditions. It is anticipated that this will improve the agreement with the experimental results.

Figure 13(a).

XTRAN3S FLUTTER CALCULATIONS COMPARED WITH RENOFT MODEL RESULTS

- Calculated steady pressures

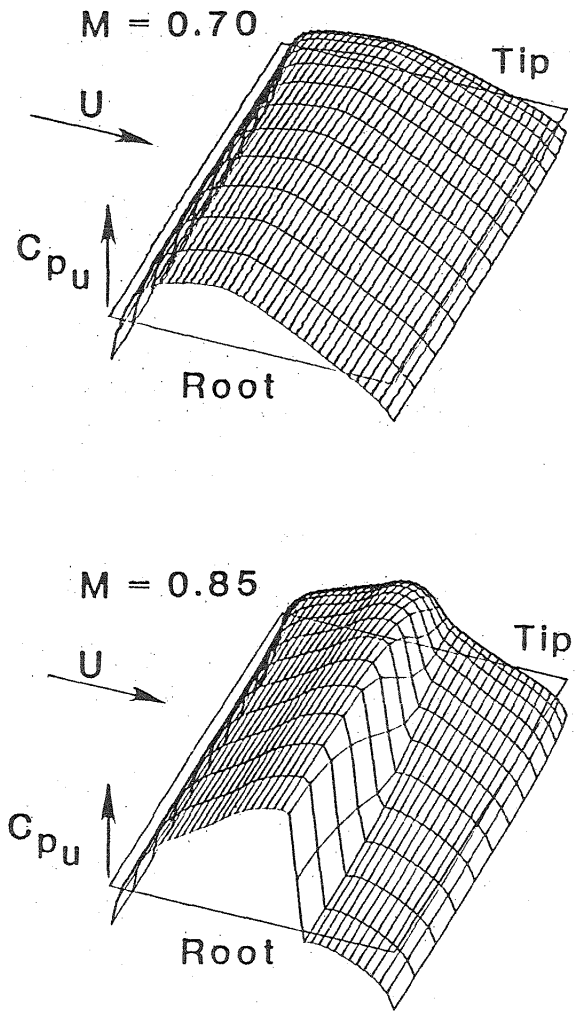

- Experimental and calculated flutter boundaries

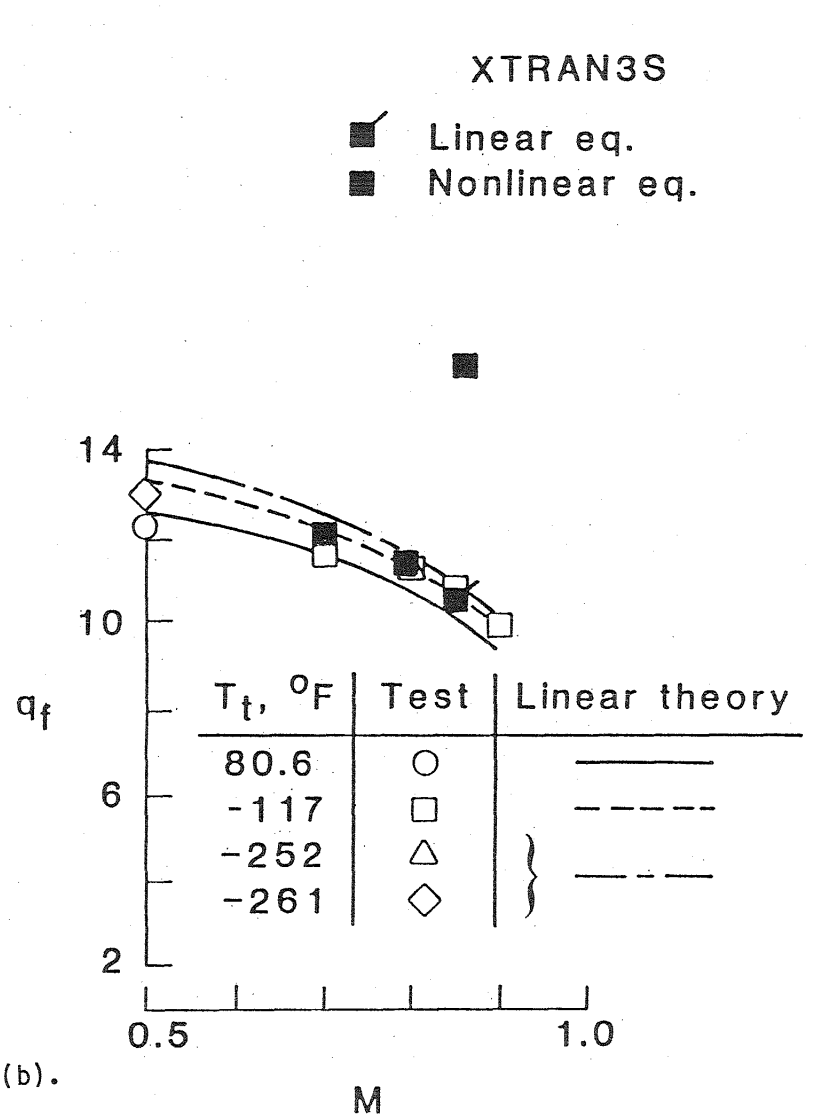

Figure 13(b).

WING-FUSELAGE CAPABILITY DEVELOPED FOR XTRAN3S

John T. Batina
Unsteady Aerodynamics Branch
Ext. 4236

RTOP 505-63-21

Research Objective - The objective of the research was to extend the XTRAN3S code to allow the treatment of wing-fuselage configurations.

Approach - The three-dimensional finite-difference code XTRAN3S provides a time-marching solution to the unsteady, transonic, small-disturbance equation. The solution procedure of XTRAN3S has been extended to allow the treatment of a fuselage by including a rectangular cross-section computational surface on which the fuselage boundary conditions are imposed. The program now is capable of computing unsteady transonic flowfields about relatively general wing-fuselage configurations.

Accomplishment Description - Linear aerodynamic results for a simple wing-fuselage configuration have been obtained at $M = 0.8$ for code validation purposes. This configuration is shown in the upper left of figure 14(b). The wing is a flat plate with no taper, a sweep of 45°, and an aspect ratio of four. The fuselage is a circular cylinder of infinite extent with radius equal to 20% wing semispan. Steady results shown in the lower left of the figure were obtained with the wing at an angle of attack of $\alpha = 1.0°$; unsteady results shown in the upper right of the figure were obtained for the wing pitching harmonically at a reduced frequency of $k = 1.0$. As shown in the upper left part of the figure, the steady lifting pressure coefficient ΔC_p is lowered when the fuselage is included in the calculation. The sectional lift coefficients c_ℓ, plotted in the lower left part of the figure, further show the interference effect of the fuselage on the wing loading. This effect is largest at the wing-fuselage junction and attenuates outboard towards the tip. The steady spanwise loading is in very good agreement with published doublet lattice results. The unsteady spanwise loading due to wing pitching shown in the upper right part of the figure are again in good agreement with the doublet lattice method. The XTRAN3S wing-fuselage capability is also being applied to transonic cases for further verification. Shown in the lower right part of the figure is an initial transonic application at $M = 0.93$ and $\alpha = 0°$. The upper surface steady pressure distribution shows a small embedded supersonic region located spanwise along the wing from the wing-fuselage junction outboard toward the tip.

Future Plans - The research was conducted as part of a continuing effort to upgrade and improve the XTRAN3S code, leading toward the capability to treat a complete aircraft configuration. The wing-fuselage capability will be exercised to calculate the effect of the fuselage interference upon unsteady airloads. Comparisons with measured transonic unsteady pressures will validate this extension to the code.

Figure 14(a).

WING-FUSELAGE CAPABILITY DEVELOPED FOR XTRAN3S

● Linear aero validation

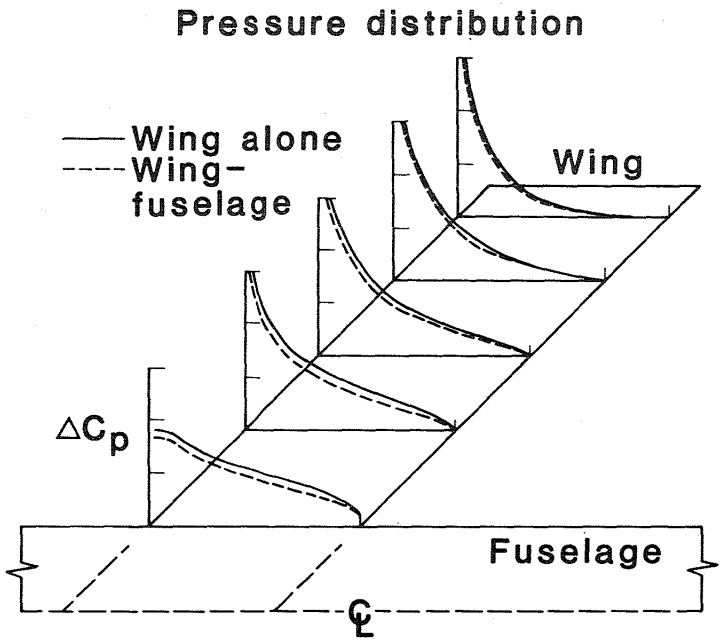

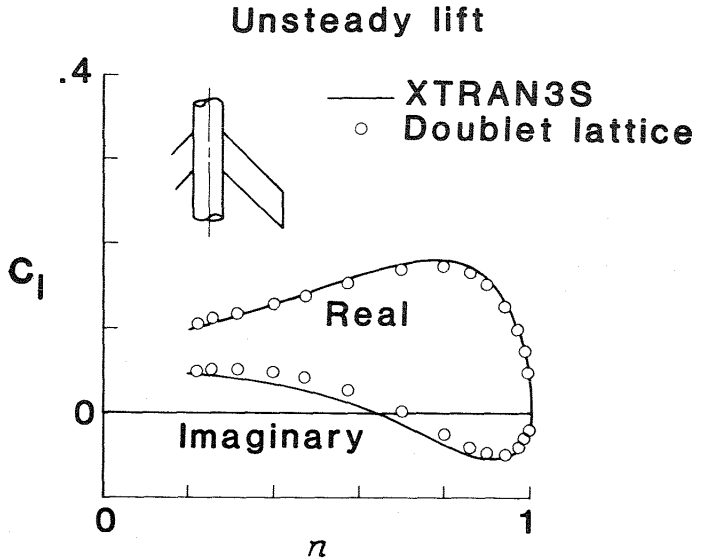

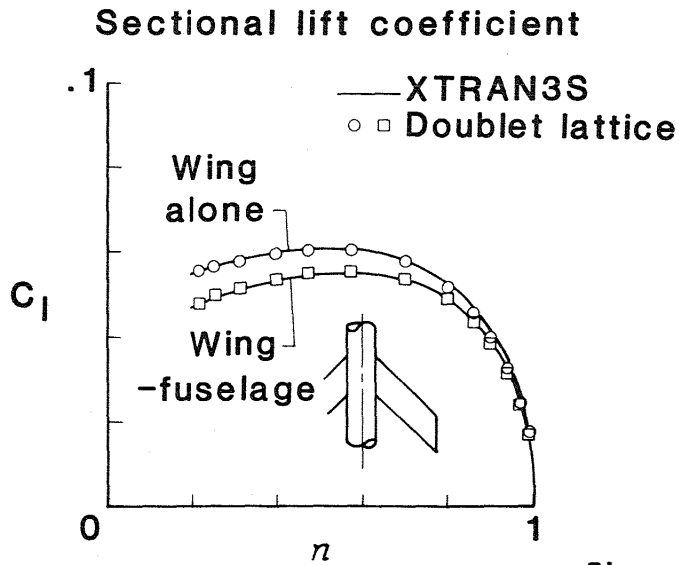

● Nonlinear transonic application
M = 0.93, α = 0°

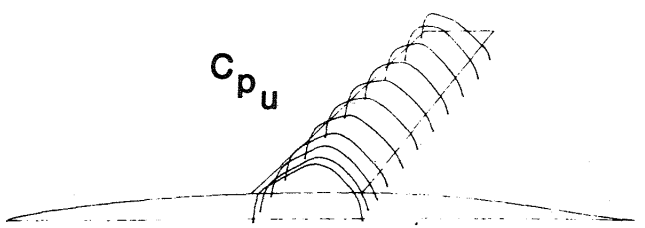

Figure 14(b).

XTRAN3S EXTENDED TO INCLUDE OSCILLATING CONTROL SURFACE

John T. Batina
Unsteady Aerodynamics Branch
Ext. 4236

RTOP 505-63-21

Research Objective - The objective of this research was to extend the XTRAN3S transonic code to allow the treatment of a trailing edge oscillating control surface.

Approach - The three-dimensional finite-difference code XTRAN3S provides a time-marching solution to the nonlinear, small-disturbance, potential equation for transonic flow. The wing flow tangency boundary condition has been modified to include a trailing edge oscillating control surface as a user specified program option. The XTRAN3S code is now capable of computing unsteady transonic flowfields about wings containing a trailing edge control surface with constant percent chord hinge line and side edges parallel to the freestream.

Accomplishment Description - Results were first obtained for an oscillating control surface with 75% chord hinge line on a two-dimensional flat plate wing. Two-dimensional flow is simulated in XTRAN3S by an appropriate choice of spanwise gridpoints. The calculations were performed at $M = 0.8$, a reduced frequency of $k = 0.2$, and an oscillation amplitude of $\delta = 1.0°$. Although not shown, the XTRAN3S lifting pressure coefficients are in excellent agreement with linear theory. Sample three-dimensional results are presented in figure 15(b) for the NLR wing which has a leading edge sweep angle of 50.1°, an aspect ratio of 1.5, and a taper ratio of 0.573. The wing has an inboard partial span control surface with hinge line at 75% chord, inboard side edge at the wing root, and outboard side edge at 59% semispan. Results were obtained with the control surface oscillating at $M = 0.8$, $k = 0.5586$, and $\delta = 1.0°$. Real and imaginary components of the lifting pressure coefficients, ΔC_p, are plotted for the 45% semispan station in the figure. The XTRAN3S pressures are in very good agreement with the linear theory results and also with the NLR experimental data.

Future Plans - Further modifications are being made to the XTRAN3S code to allow for multiple controls as well as leading edge control surfaces for unsteady aerodynamic, aeroelastic, and active controls applications.

Figure 15(a).

XTRAN3S EXTENDED
TO INCLUDE OSCILLATING CONTROL SURFACE

Unsteady lifting pressure for NLR wing at M = 0.8, k = 0.56, $\delta = 1^{o}$

- Comparison of linear theory, XTRAN3S and experiment

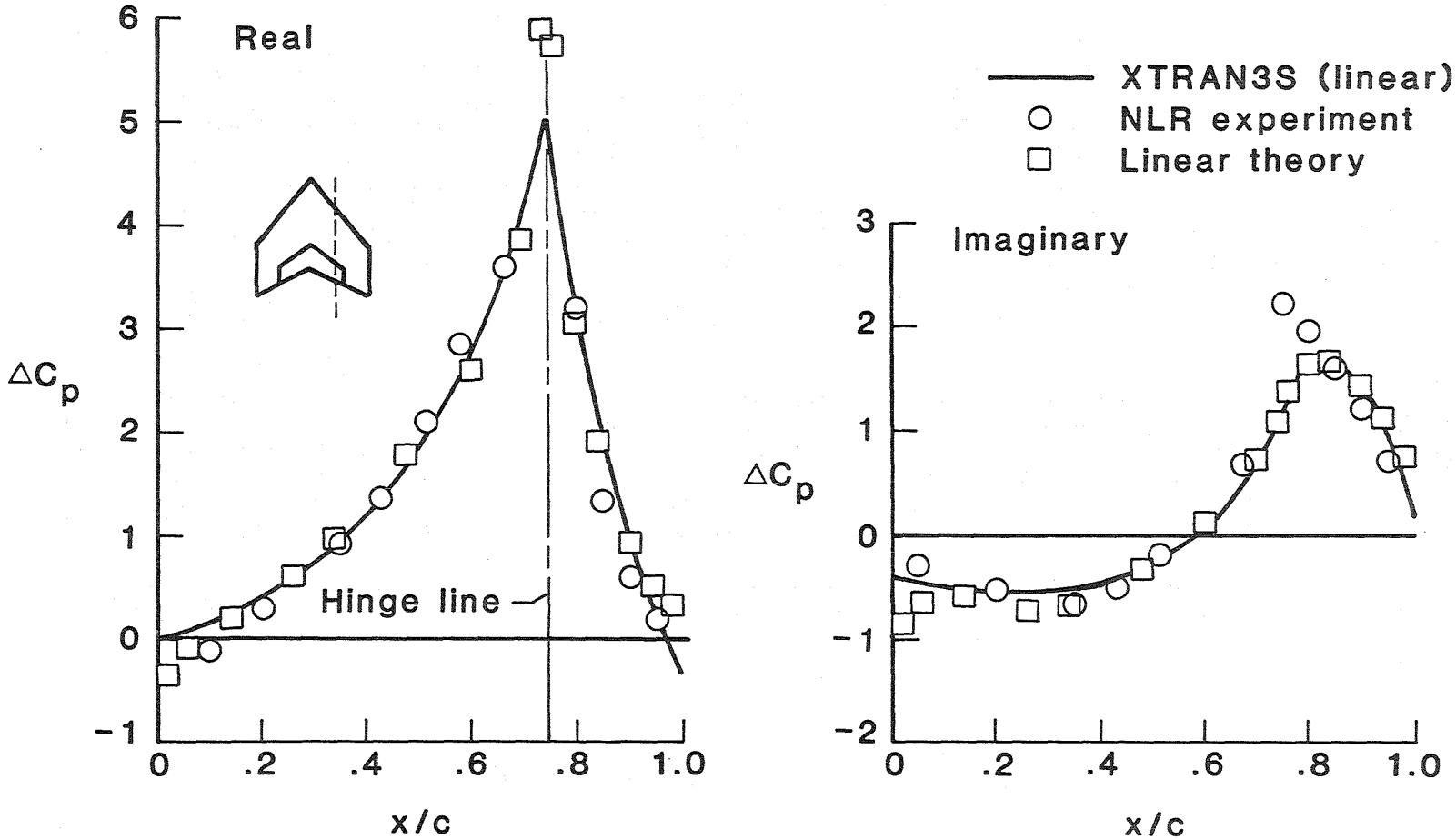

Figure 15(b).

COMPUTATIONAL TRANSONIC FLUTTER BOUNDARY TRACKING

John W. Gallman and T. Y. Yang
Purdue University

John T. Batina
Unsteady Aerodynamics Branch
Ext. 4236

RTOP 505-63-21

Research Objective - The objective of this research was to develop an efficient automated flutter boundary tracking procedure which utilizes a time-accurate unsteady aerodynamic code.

Approach - The flutter boundary tracking procedure uses a first order Taylor series expansion of the flutter speed in terms of Mach number to represent the flutter boundary. The top part of the figure shows the linear approximation and the expansion of the slope as a ratio of derivatives. The transonic small-disturbance code, XTRAN2L, is used to calculate the aeroelastic response histories for airfoil pitching and plunging from which damping values are obtained. Damping estimates from the aeroelastic response histories are used to calculate the local slope of the flutter boundary, and hence, allow the prediction of successive flutter speeds.

Accomplishment Description - A graphical representation of the flutter boundary tracking procedure and a typical set of results are shown in figure 16(b). In the left half of the figure, the circles represent the aeroelastic responses calculated to track the flutter boundary, the squares are the flutter speeds predicted from the linear equation, and the diamonds represent the flutter speeds interpolated from the damping values determined from the aeroelastic response (circles). The transonic flutter boundary results for the NACA 64A010A airfoil at $\alpha = 1.0°$ are shown in the right half of the figure. The flutter boundary tracking solution is in very good agreement with the exact solution, obtained from a traditional, brute-force, time-marching method. The absolute mean error for the boundary is 0.72%. If it is assumed that four response calculations per flutter point for the brute-force time-marching method, the flutter boundary tracking solution is obtained in a single job submission with an estimated savings of a factor of two in CPU costs.

Future Plans - This work was undertaken to develop a flutter boundary tracking procedure that might be incorporated into a three-dimensional transonic code, such as XTRAN3S. The development of such a capability might significantly reduce the cost and complexity of flutter boundary calculations for complete aircraft configurations.

Figure 16(a).

AUTOMATED TRANSONIC FLUTTER BOUNDARY TRACKING PROCEDURE DEVELOPED

- Only two response calculations required per Mach number
- Complete flutter boundary in single job submission

$$U_{f_{i+1}} = U_{f_i} + \frac{\partial U_f}{\partial M}\left(M_{i+1} - M_i\right); \quad \frac{\partial U_f}{\partial M} \approx \frac{(\Delta\sigma/\Delta M)_U}{(\Delta\sigma/\Delta U)_M}$$

- Graphical procedure description
- Airfoil application NACA 64A010A airfoil at $\alpha = 1.0^o$

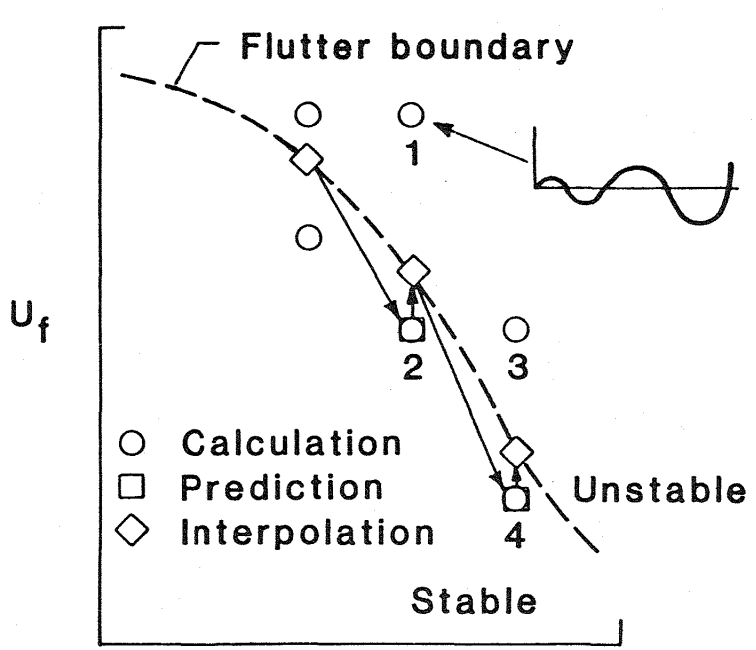

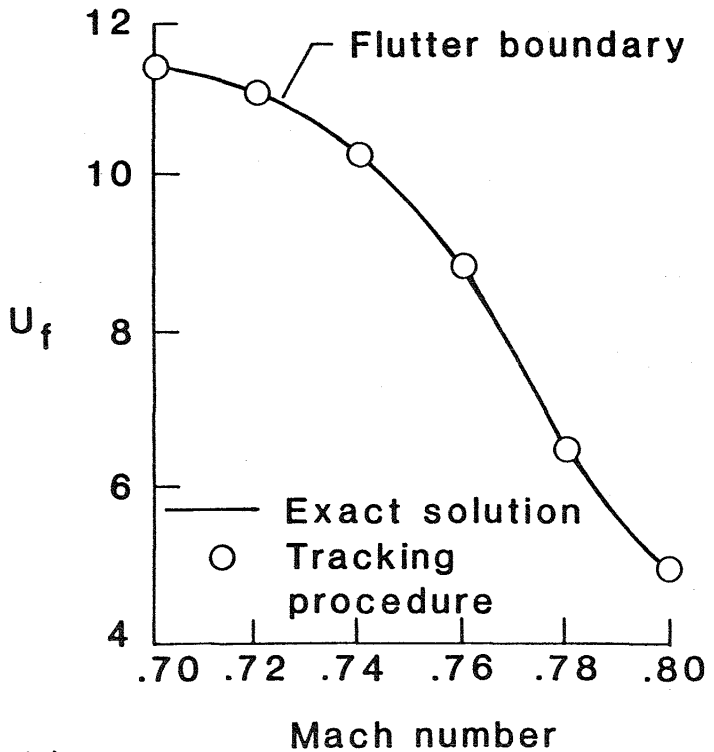

Figure 16(b).

LIFTING SURFACE THEORETICAL RESULTS CORRELATE WELL WITH EXPERIMENTAL DATA FOR HELICOPTER ROTOR IN FORWARD FLIGHT

Harry L. Runyan
William and Mary
Ext. 4236

Hsiang Tai
Polymeric Materials Branch
Ext. 3041

RTOP 505-63-21

Research Objective - The standard procedure for predicting the airloads on a rotor blade is to utilize experimentally derived, two-dimensional airforces which were obtained through a large range of angles of attack up to and through the stalled region. These data are usually put in tabular form and used in an iteration procedure to determine stability and performance. This process neglects the effect of the wake as well as the three-dimensional effects. Approximations are usually made to try to correct for the wake and three-dimensional, compressible effects applicable to both steady and unsteady flow for helicopter rotors in forward flight.

Approach - The formulation of the aerodynamic equations used here is based on the linearized acceleration potential approach. The fluid is considered perfect, with no separation, and the formulation is based upon the assumption of small pertubations. The blade is treated as a very thin surface of discontinuity across which a pressure jump occurs. The effect of compressibility is accounted for by utilizing the complete linearized potential for a lifting doublet. The acceleration potential approach was chosen because the pressure discontinuity occurs only on the surface of the blade and thus the boundary conditions need only be applied on the blade surface and not throughout the wake although wake effects are accounted for. The problem is formulated in an inertial coordinate system as shown on the left of figure 17(b). The rotor is moving in the negative x-direction with velocity U, and in the positive z-direction with velocity W and is rotating counter clockwise with constant angular velocity Ω. The helical path of the rotor is indicated by the dashed curve. A point of interest on the blade is designated by the vector $X_0(\tau)$ from the origin of the ground based coordinate system.

Accomplishment Description - Some parametric studies have been made including calculations for a 4-bladed rotor. Previously, it was shown that in going from the one-blade to the two-blade case, a large degradation in lift was found in the region of azimuth angle Ψ = 260° to 330°. A similar but even larger loss in lift occured for the 4-bladed rotor in the same azimuth range. A correlation with an experiment has been made and the results are shown on the figure for a two-bladed rotor. The experiment by Meyer et al (NACA TN 2953) was conducted on a rotor having 2.5 ft. radius and 1/4 ft chord. For the blade located at Ψ = 150°, the theory is about 9% lower than the experiment in the neighborhood of the peak load. For Ψ = 330°, the agreement is very good. Thus, it appears that the theory is adequate for predicting airloads on such rotors.

Future Plans - In addition to continuing parametric studies and correlations with other experiments, emphasis will be placed on studies of the wake generation. Preliminary calculations have already been done which show some promise in determining the velocities in the wake. Also, incorporation into an aeroelastic analysis will be initiated.

Figure 17(a).

LIFTING SURFACE THEORY FOR ROTOR IN FORWARD FLIGHT CORRELATES WELL WITH EXPERIMENTAL DATA

$U = 45.8$ ft/sec, $\alpha_r = 5$ deg, $\Omega = 83$ rad/sec, $\mu = 0.22$

INERTIAL COORDINATE SYSTEM

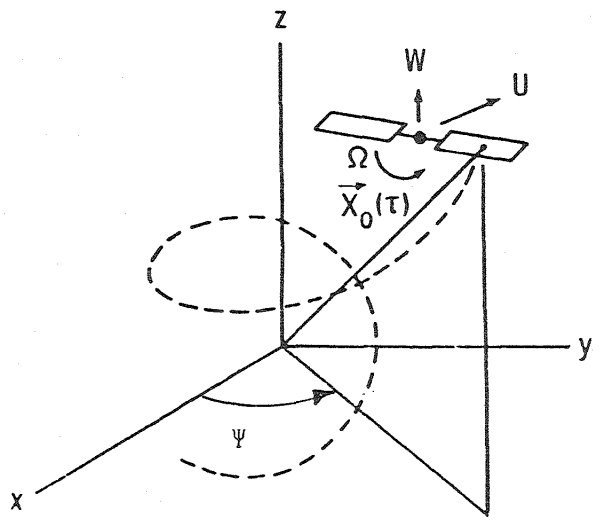

SPANWISE LIFT DISTRIBUTION

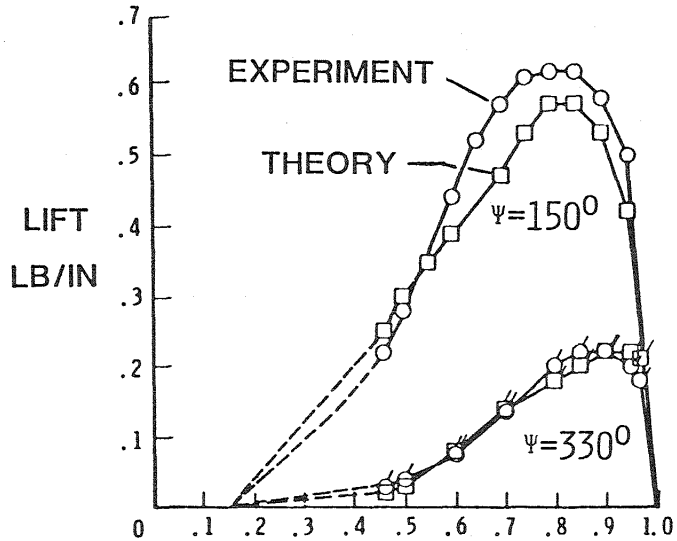

Figure 17(b).

NON-ISENTROPIC STRONG SHOCK CONDITIONS IMPLEMENTED IN XTRAN3S

Mike Gibbons and Marc Williams
Purdue University

Woodrow Whitlow, Jr.
Unsteady Aerodynamics Branch
Ext. 4236

RTOP 505-63-21

Research Objective - The goal of this research is to improve the reliability of the three-dimensional transonic small disturbance (TSD) code, XTRAN3S, specifically when strong shocks exist. This will be done by applying a set of corrections to the code accounting for the generation of entropy when shocks are present in the flow.

Approach - Three separate modifications were introduced by Fuglsang and Williams (AIAA Paper No. 85-0600) in the two-dimensional code XTRAN2L to account for non-isentropic effects; 1) a new streamwise flux, 2) convection of the shock generated entropy downstream, and 3) adding the entropy generated pressure to the total pressures. In the present work, corresponding changes to the XTRAN3S code have been made for each spanwise plane as though the flow were two dimensional. Finally, the type-dependent differencing, which originally used a Murman-Cole scheme, has been changed to use the Enquist-Osher method.

Accomplishment Description - Steady calculations have been made at M = 0.85 for an aspect ratio 12 rectangular wing with an NACA 0012 airfoil section. The left side of figure 18(b) shows the original and modified XTRAN3S root pressure distributions compared with results from an Euler equation code (FL057MG). The modified code improves the agreement with the Euler results; particularly aft of the shock. The right hand figure illustrates the importance of the entropy corrections for transonic calculations. The lift curve slope from the original code for moderate angles of attack, α, is in basic disagreement with the Euler results. The modified code corrects a significant portion of this discrepancy as indicated by the point at α = 2 degrees. Further calculations have shown that the modified code gives the expected linear lift curve versus angle-of-attack. Steady calculations have also been made for an RAE tailplane model for M = 0.95 where the shock position calculated by the modified code was 5 percent chord ahead of that from the unmodified code and in better agreement with experiment.

Future Plans - Further calculations will be made for several values of Mach number to assess the importance of the entropy corrections. Also, their effect upon unsteady airloads due to wing pitching oscillations will be assessed. The results will be presented in a 1986 AIAA Structures, Structural Dynamics and Materials Conference paper.

Figure 18(a).

STRONG SHOCK CONDITIONS IMPLEMENTED IN XTRAN3S

M = 0.85, AR = 12, NACA 0012 rectangular wing

- Effect on root pressure distribution

$\alpha = 0^{o}$

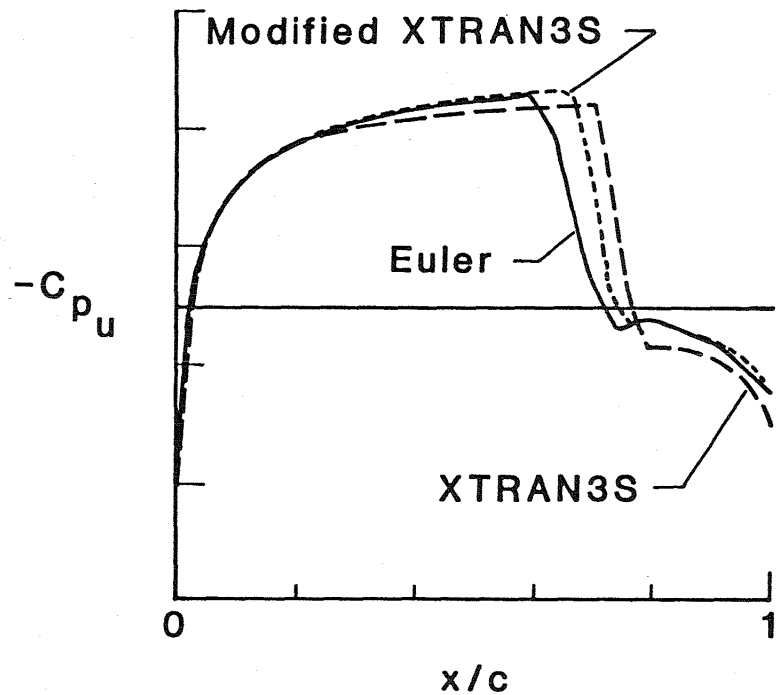

- Lift-curve slope overpredicted by XTRAN3S for strong shock cases

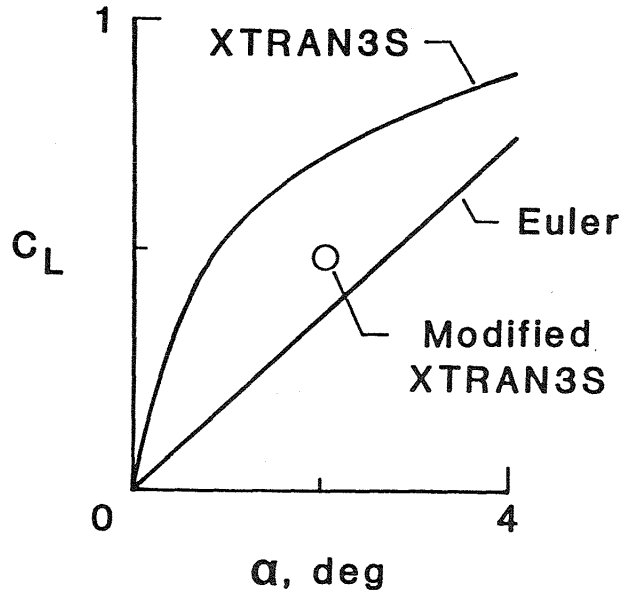

Figure 18(b).

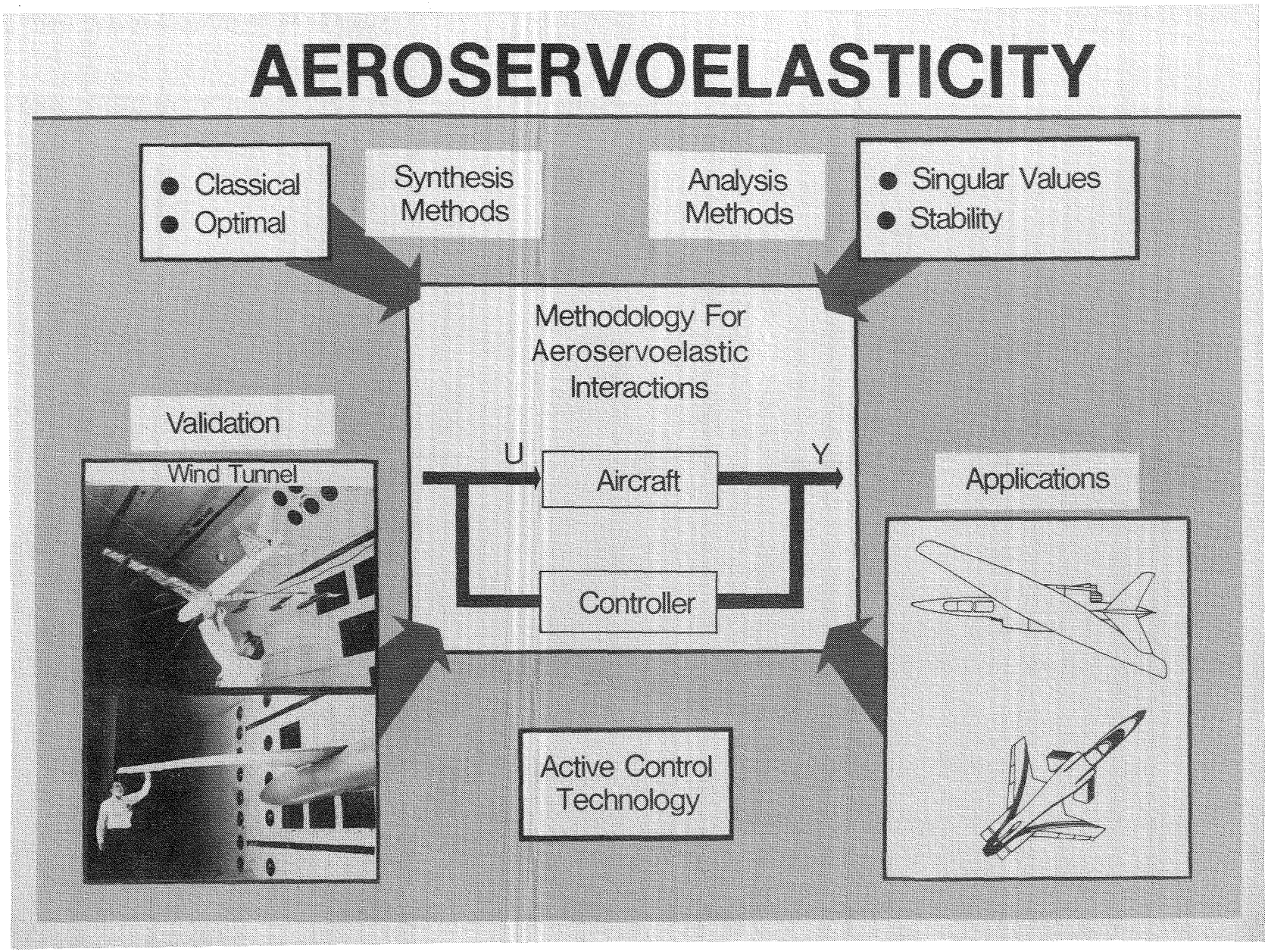
AEROSERVOELASTICITY
Classical
Optimal
Synthesis Methods
Analysis Methods
Singular Values
Stability
Methodology For Aeroservoelastic Interactions
U
Aircraft
Y
Controller
Validation
Wind Tunnel
Applications
Active Control Technology

Figure 19.

AEROSERVOELASTICITY

FIVE YEAR PLAN

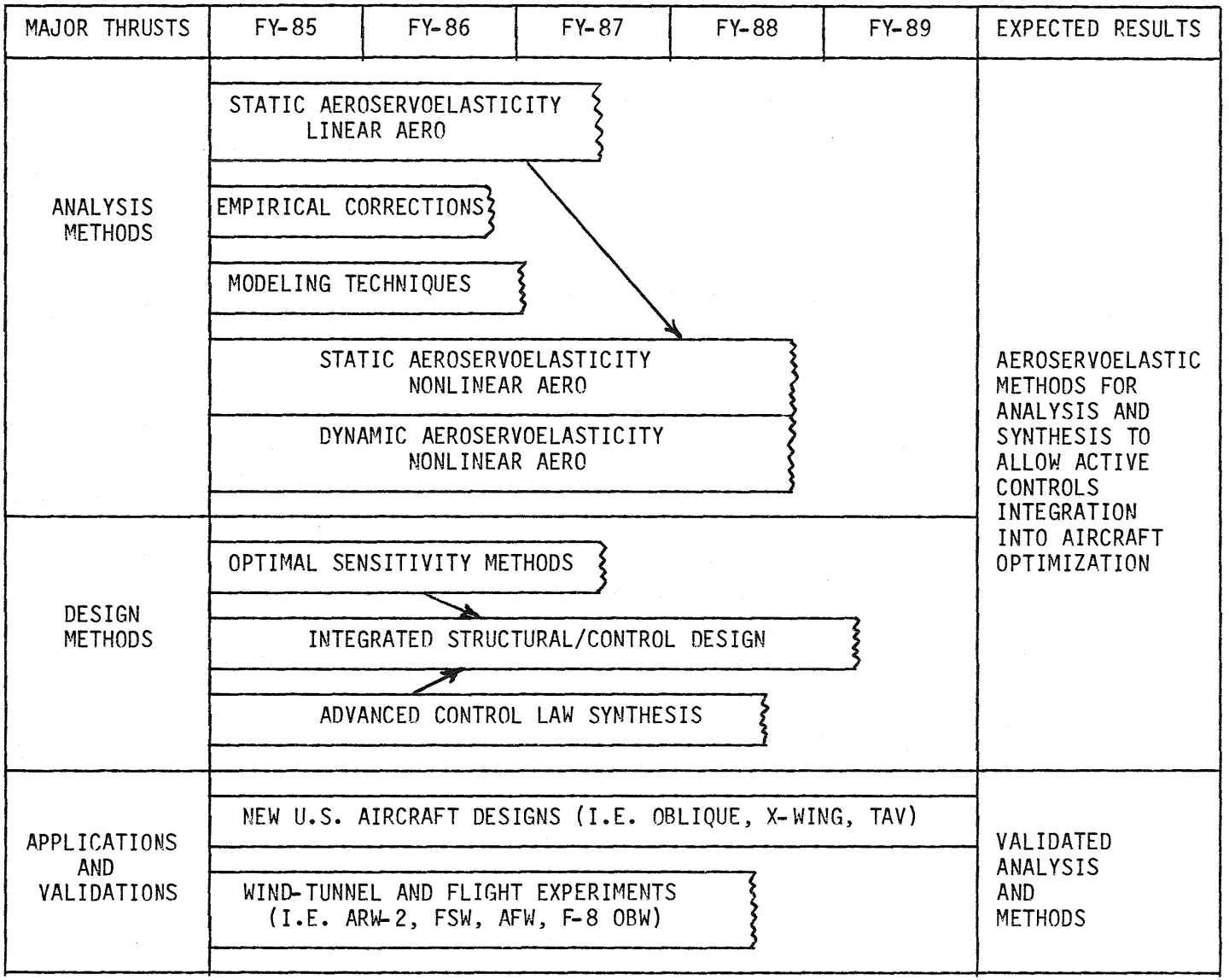

Figure 20.

COMPARISON OF CALCULATED AND EXPERIMENTAL BENDING MOMENT DUE TO CONTROL DEFLECTION

Boyd Perry III
Aeroservoelasticity Branch
Extension 3323

RTOP 505-63-21

Research Objective - Bending moment reversal is a static aeroelastic phenomenon which is analogous to the more familiar static aeroelastic phenomenon of aileron reversal. The purpose of the present work is to investigate this phenomenon.

Approach - Because of the aerodynamic and stiffness characteristics of the particular airplane under investigation, the steady-state rolling moment produced by a differential deflection of the ailerons changes sign under certain conditions. All other quantities held constant, this aileron reversal is most often illustrated by examining the rolling moment (due to a unit differential deflection of the ailerons) as a function of dynamic pressure. Other quantities, such as airplane lift and pitching moment due to a symmetric deflection of the ailerons, may also reverse. In addition, it has been found that wing loads (such as shear and bending moment at various locations along the wing span) due to symmetric deflection of the ailerons will also reverse. Bending moment reversal may be predicted analytically by removing the dynamic terms (those associated with time derivatives and non-zero reduced frequencies) from the modal dynamic equations of motion and load equations.

Accomplishment Description - In the present work, a cantilever wind tunnel model of the right semispan of the DAST ARW-2 wing (depicted in the upper left and corner of figure 21(b)) is used as the example configuration. The plot in the upper right shows a comparison of analytical and wind-tunnel results of incremental wing-root bending moment due to incremental control deflection as a function of dynamic pressure. The magnitude and trend are correctly predicted by analysis. Analysis also predicts that wing-root bending moment will reverse at a dynamic pressure of about 500 psf. The two plots at the bottom of the figure present, for dynamic pressures above and below reversal, the two components of bending moment and their total as functions of fraction of wing semispan. (At the lower dynamic pressure there are two experimental points available for comparison.) The two components of bending moment are: that due to the deflection of the control surface, treating the wing as if it were rigid; and that due to the deformation of the flexible wing. The two components are opposite in sign, and the reason that total bending moment reverses is that, with increasing dynamic pressure, the "control" component increases proportional to dynamic pressure, while the "flexible" component increases more rapidly.

Future Plans - There are plans to investigate the effects and implications that this static aeroelastic phenomenon has on certain dynamic phenomena. In addition, an AIAA paper and a NASA TP are proposed.

Figure 21(a).

COMPARISON OF CALCULATED AND EXPERIMENTAL BENDING MOMENT DUE TO CONTROL DEFLECTION

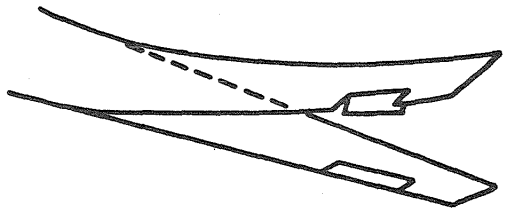

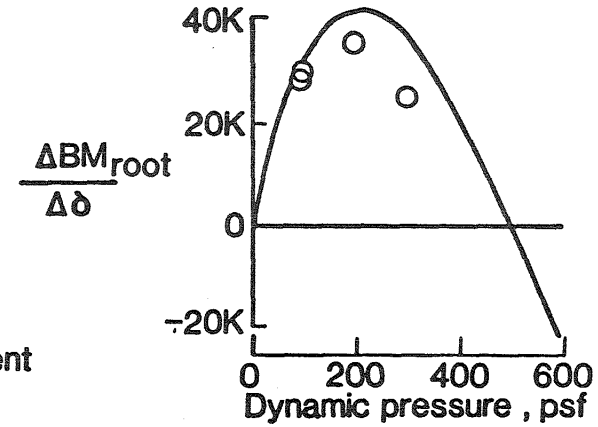

O Experiment

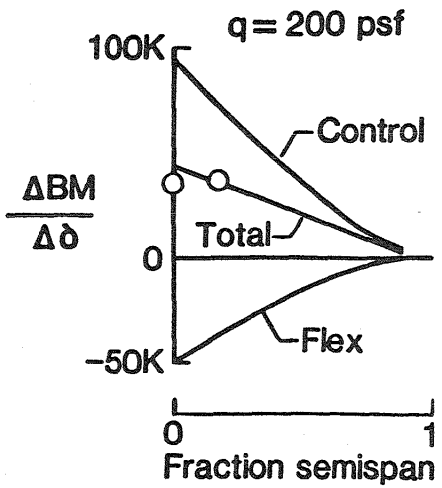

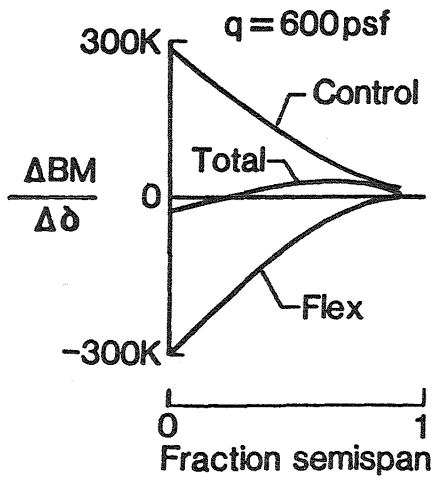

Figure 21(b).

ENGINEERING WORKSTATIONS USED IN ASE COMPUTATIONS

H. J. Dunn
Aeroservoelasticity Branch
Extension 3527

RTOP 505-63-21

Research Objective - High performance engineering workstations that can perform a large amount of the aeroservoelastic calculations now being done on mainframes can be obtained for an investment of less than $50,000. The purpose of this present work is to demonstrate the effectiveness and to identify problem areas that arise when the computing "facility" is located in the researcher's work area.

Approach - A high performance engineering workstation was procured and placed in a researcher's work area. The engineering source codes, that were being used on mainframes, were transferred to the workstation. These source codes were then modified accordingly to function on the workstation.

Accomplishment Description - Figure 22(b) illustrates the measured clocktime and the amount of actual CPU time used by the workstation to perform a flutter calculation. Although the mainframe is faster in terms of CPU time in calculating the root locus of the flutter, the workstation environment is faster in returning the results to the researcher. Since engineering decisions can be made in near real time with the workstation, the productivity of the researcher is increased.

Future Plans - Future plans are to connect the workstation to the LaRC LAN so that information can be transferred between different disciplines. Additional engineering source code is to be transferred to the workstation in order to determine the full potential that can be obtained.

Figure 22(a).

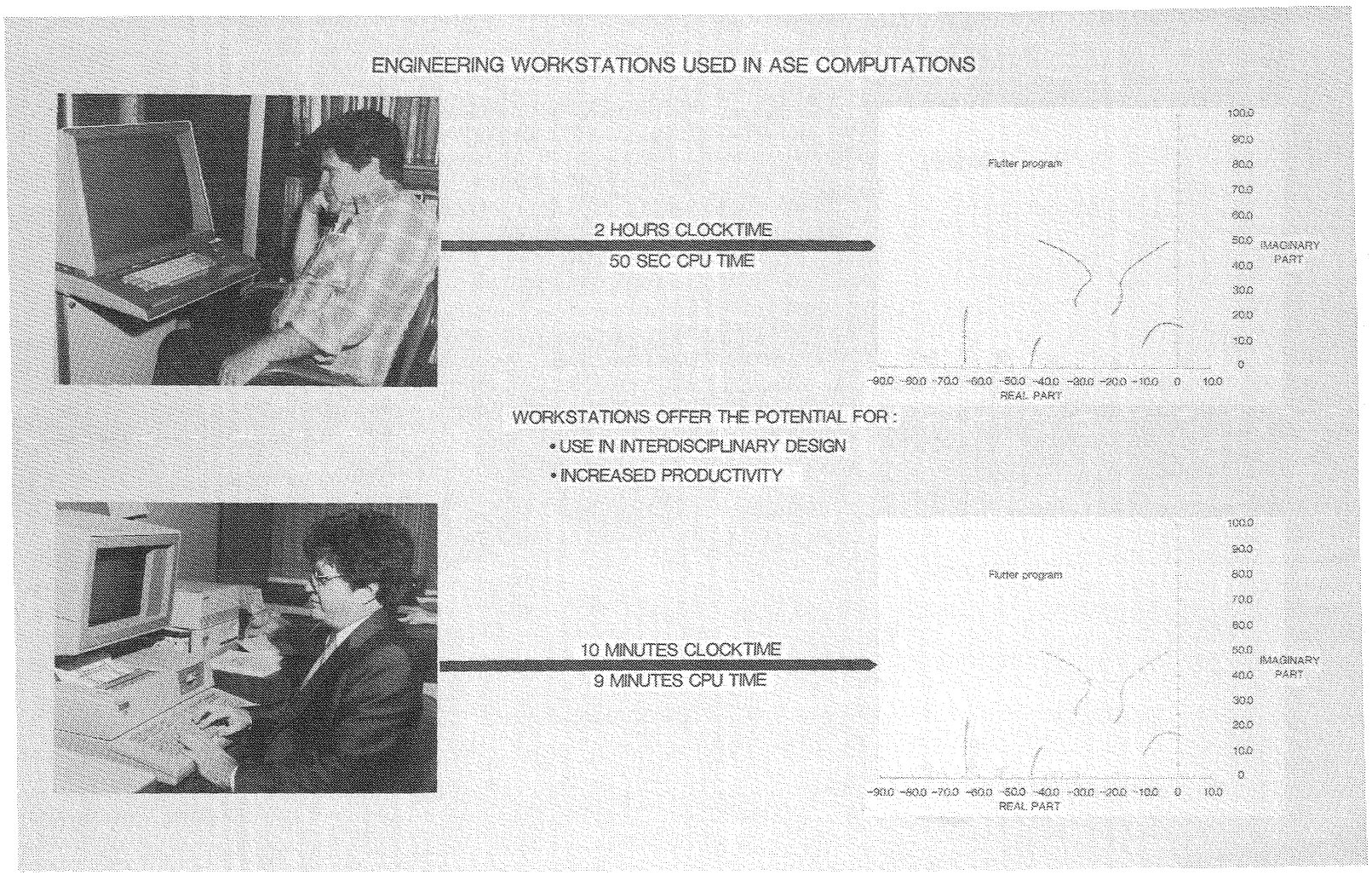
ENGINEERING WORKSTATIONS USED IN ASE COMPUTATIONS
2 HOURS CLOCKTIME
50 SEC CPU TIME
Flutter program
IMAGINARY PART
REAL PART
WORKSTATIONS OFFER THE POTENTIAL FOR :
• USE IN INTERDISCIPLINARY DESIGN
• INCREASED PRODUCTIVITY
10 MINUTES CLOCKTIME
9 MINUTES CPU TIME
Flutter program
IMAGINARY PART
REAL PART

Figure 22(b).

INTEGRATED STRUCTURE/CONTROL DESIGN METHODOLOGY

Michael G. Gilbert
PRC Kentron Inc.
Aeroservoelasticity Branch

RTOP 505-63-21

Research Objective - One key result of recent advanced flight vehicle demonstration programs has been the identified need for integrated analysis and design methods which accurately predict the interactions between traditionally separate aeronautical disciplines. For example, severe aeroservoelastic (aerodynamic, servo control, elastic structure) interactions have been encountered on several programs, leading to expensive delays and vehicle redesign efforts. In order to avoid these problems, and possibly to begin using the interactions to advantage, new integrated analysis and design methods are being developed, with the particular goal of achieving better overall system design through the early coordination of vehicle design disciplines.

Approach - Formal mathematical optimization techniques are a recognized means of finding superior solutions to many design problems. One recent advance in this field is the use of optimum sensitivity analysis to predict the change in the optimum solution to a change in a fixed parameter of the problem. These techniques have been used successfully in structural optimization and in the decompositions of extremely large optimization problems. Here, optimum sensitivity analysis is being used to develop an integrated structure/active control design capability, as shown in figure 23(c). The method treats structural quantities P as fixed parameters in an optimal control problem, where the control u is selected to minimize a scalar performance index J. Optimum sensitivity analysis is then used to alter the structural quantities so as to further improve the optimal control law performance. The ability of optimum sensitivity analysis to provide this capability is illustrated in the lower half of Figure 1. Shown is the change in the performance index J due to a change in the structural parameter ω from ω_1 to ω_2, at the solution of the optimal control problem for ω_1. The key advantage of optimum sensitivity analysis is that this gradient is calculated analytically from the necessary mathematical conditions for optimality, dramatically reducing the number of solutions of the optimal control problem that are required.

Figure 23(a).

INTEGRATED STRUCTURE/CONTROL DESIGN METHODOLOGY

CONTINUED

Accomplishment Description - The integrated structure/control design method has been demonstrated on a simple 2-dimensional aerodynamic section, as shown in figure 23(d). The objective of the example is to optimally deflect the trailing edge control surface such that the performance index J, which is the sum of the squared section angle-of-attack and control deflection weighted by r, is minimized. The structural plunging and pitching natural frequencies were treated as the structural parameters. It was found, unlike the usual optimal control problem where the weight r is varied to trade off angle-of-attack and control deflection, that changing the pitch natural frequency could reduce both the angle-of-attack and control deflection. The optimum sensitivity gradients were used to find the necessary change in pitch stiffness to reduce the normalized control deflection from 7.25 to 6.00, and the optimal control deflection with the new pitch stiffness was found to be 6.30.

Future Plans - The methodology is being adapted to better reflect realistic integrated design objectives, particularly in terms of performance assessment of the controlled system. These include multi-input, multi-output control law designs, control system stability margins, and performance requirements not easily quantified in a scalar performance index. The method then will be exercised on current advanced research aircraft models. Follow-on work is anticipated in the areas of reducing the required dynamic order of the optimal control law, and incorporating more fundamental structural design parameters.

Figure 23(b).

INTEGRATED STRUCTURE/CONTROL DESIGN METHODOLOGY DEVELOPMENT USING OPTIMUM SENSITIVITY TECHNIQUES

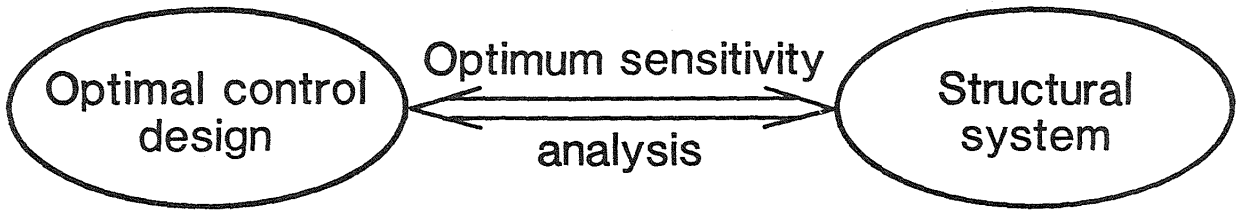

$\dot{X} = A(p)X + B(p)u$

u^* minimizes

$J(u,p)$

Structural parameters

$p = \begin{cases} \text{Mode shapes } \Phi \\ \text{Natural frequencies } \omega \end{cases}$

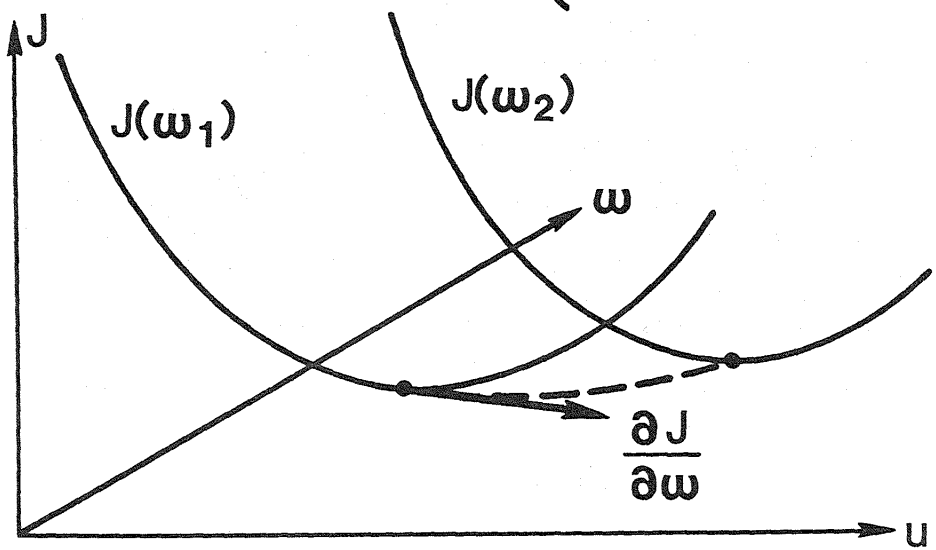

Figure 23(c).

INTEGRATED STRUCTURE/CONTROL DESIGN EXAMPLE

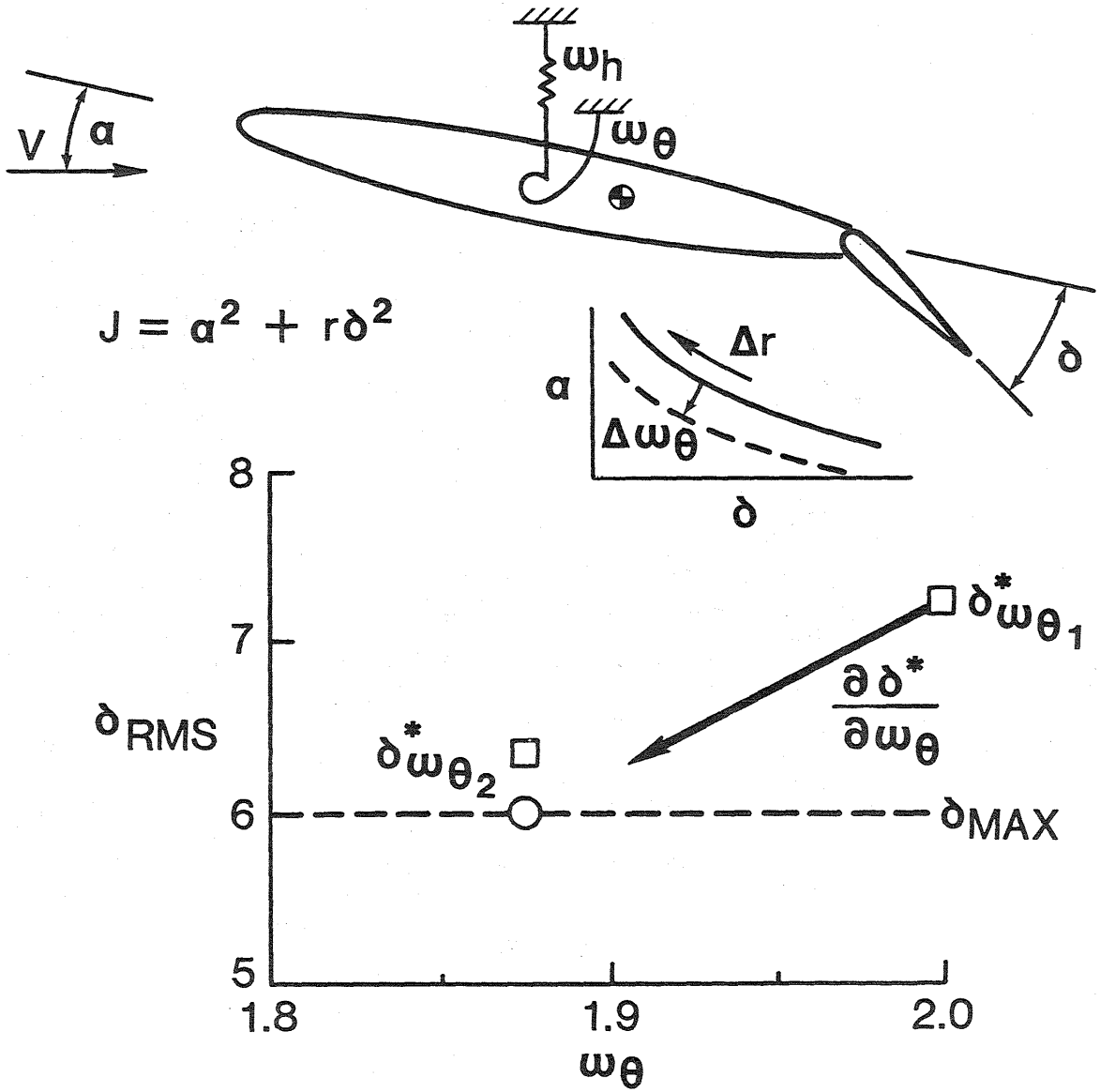

Figure 23(d).

X-WING AEROSERVOELASTIC ANALYSES

Michael G. Gilbert
PRC-Kentron Inc.
Aeroservoelasticity Branch

RTOP 505-61-51

Research Objective - The X-Wing rotor concept has been conceived as a means of providing for high speed, high altitude flight capability in a vertical takeoff and landing aircraft. Using a stiff, four bladed rotor with circulation control blowing, the X-Wing would takeoff, land, and hover like a conventional helicopter, but would stop the rotor for high speed forward flight, transforming the rotor blades into two forward-swept and two aft-swept wings. As a means of assessing the required technology for such a vehicle, a program has been initiated to demonstrate conversion and fixed-rotor flight of an X-Wing rotor on the NASA/Army Rotor Systems Research Aircraft (RSRA). NASA LaRC is providing aeroservoelastic stability analyses of the X-Wing/RSRA aircraft, shown in figure 24(b) in the fixed rotor mode as means of verification of vehicle contractor predicted flight stability boundaries.

Approach - Aeroservoelastic stability analyses of the X-Wing/RSRA require the interdisciplinary study of the elastic structure, circulation control aerodynamics and associated blowing pneumodynamics (since blowing is an aircraft control input), unsteady wing aerodynamics, and the fixed rotor aircraft flight control laws. Mathematical model development and stability analyses are being conducted using the Interaction Structures, Aerodynamics and Controls (ISAC) computer codes.

Accomplishment Description - An initial aeroelastic (step 1) model was developed using vibration data for a rigid RSRA with an elastic representation of the X-Wing rotor. Open-loop longitudinal vehicle stability analyses were conducted for four nominal vehicle center-of-gravity (c.g.) locations as a function of flight altitude and true airspeed. These results are shown in the figure, with flight to the left of a boundary stable and flight to the right of the same boundary unstable. An analysis of the unstable motion indicated that the longitudinal instability was due to elastic deformations of the X-Wing rotor blades, with the deformations causing a net shift in the vehicle center-of-pressure in the forward direction, thereby reducing the vehicle static margin. The magnitude of this effect is illustrated in the figure. A second aeroelastic model has now also been developed which adds the vibration characteristics of the elastic RSRA. These vibration data do not exhibit the traditional separation of the vehicle longitudinal dynamics from the lateral dynamics, forcing the vehicle aeroelastic stability analyses to consider the longitudinal and lateral motions simultaneously. Results have indicated that the longitudinal instability speeds are further reduced from the initial model.

Future Plans - The effects of the circulation control blowing and the pneumodynamic representation will be added to the second aeroelastic model. Closed-loop stability analyses of the vehicle will begin when the flight control law design effort is completed and the control laws are received by NASA LaRC. The results are to be used to verify the flight control law designs before first flight.

Figure 24(a).

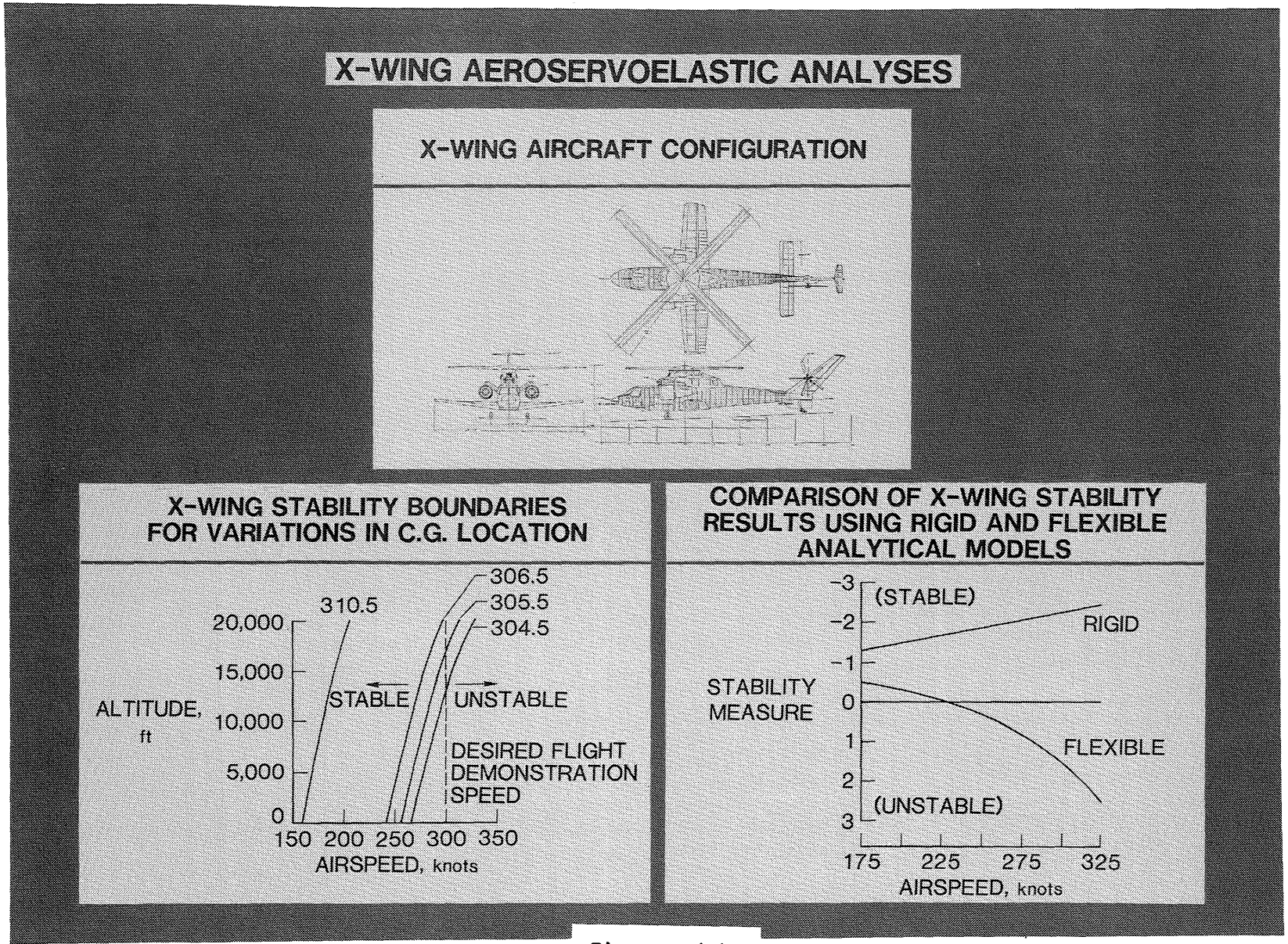
X-WING AEROSERVOELASTIC ANALYSES
X-WING AIRCRAFT CONFIGURATION
X-WING STABILITY BOUNDARIES FOR VARIATIONS IN C.G. LOCATION
306.5
310.5
305.5
304.5
20,000
15,000
10,000
5,000
0
ALTITUDE, ft
STABLE
UNSTABLE
DESIRED FLIGHT DEMONSTRATION SPEED
150 200 250 300 350
AIRSPEED, knots
COMPARISON OF X-WING STABILITY RESULTS USING RIGID AND FLEXIBLE ANALYTICAL MODELS
-3
-2
-1
0
1
2
3
(STABLE)
RIGID
STABILITY MEASURE
FLEXIBLE
(UNSTABLE)
175 225 275 325
AIRSPEED, knots

Figure 24(b).

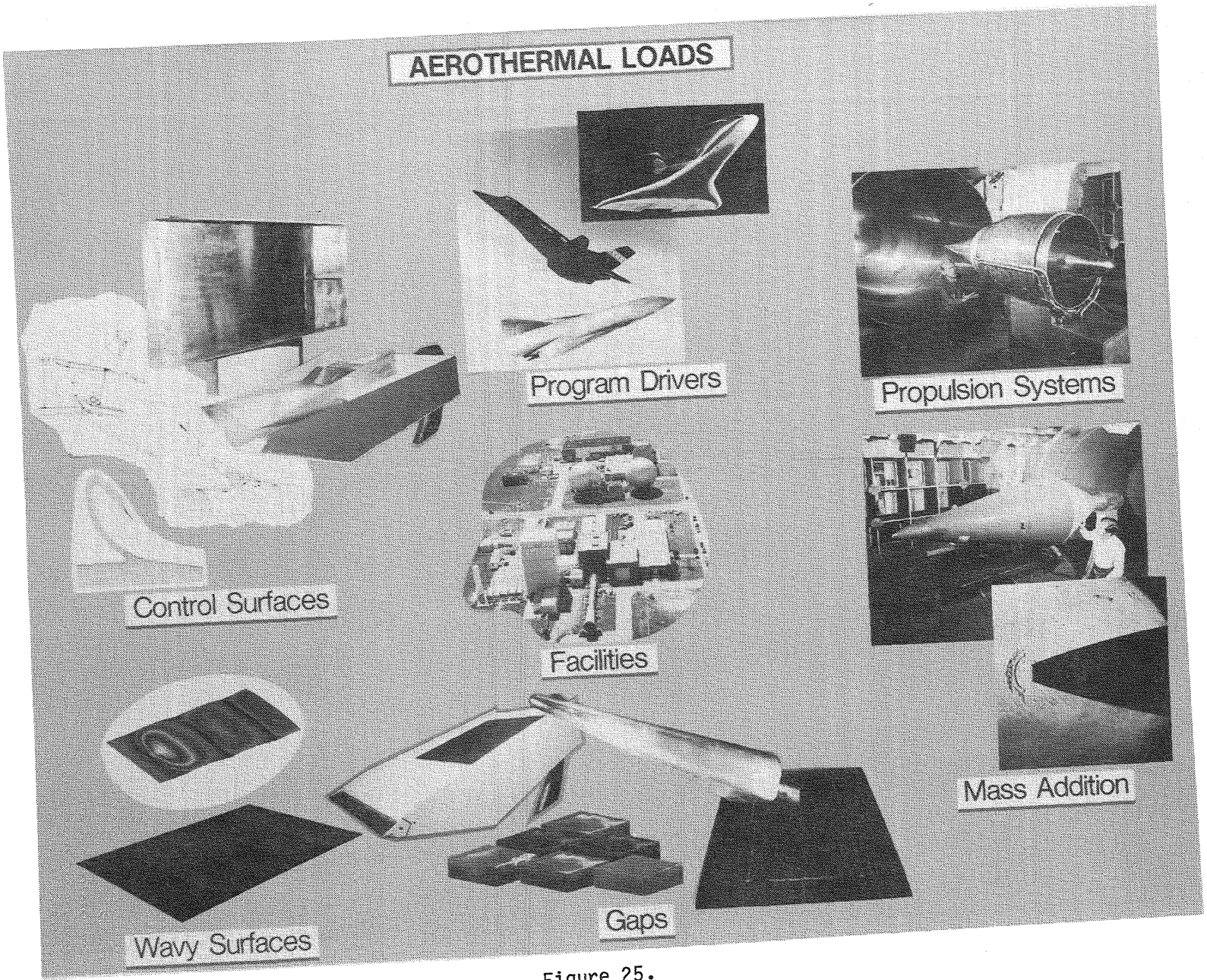
AEROTHERMAL LOADS
Program Drivers
Propulsion Systems
Control Surfaces
Facilities
Mass Addition
Wavy Surfaces
Gaps

Figure 25.

AEROTHERMAL LOADS

FIVE YEAR PLAN

MAJOR THRUSTS	FY 85	FY 86	FY 87	FY 88	FY 89	EXPECTED RESULTS
EXPERIMENTAL	WAVEY SURFACES/PROTUBERANCES					DETAILED DESIGN DATA BASE
	COMPRESSION/AXIAL CORNER FLOWS					
	SHOCK-SHOCK/SHOCK BOUNDARY LAYER					
	MASS ADDITION FLOW EFFECTS					VALIDATED CODES
ANALYTICAL	EULER ALGORITHMS					
	NAVIER-STOKES COMPRESSIBLE VISCOUS FLOW ALGORITHM					INTEGRATED ANALYSIS CAPABILITY
	ADAPTIVE TECHNIQUES					
	INTEGRATED FLOW-THERMAL-STRUCTURAL					
FACILITIES AND TEST TECHNIQUES	OPERATION AND MAINTENANCE					EFFICIENT RELIABLE FACILITIES AND TECHNIQUES
	HIGH TEMPERATURE INSTRUMENTATION					
	FACILITY ENHANCEMENTS					
	8' HTT MODIFICATION FOR AIRBREATHING PROPULSION					

Figure 26.

AEROTHERMAL TEST OF SHUTTLE SPLIT-ELEVON MODEL IN 8' HTT

L. Roane Hunt
Aerothermal Loads Branch
Ext. 3423

RTOP 506-40-21

Research Objective - The two elevons on each of the Shuttle wings are split and are separated with a chordwise gap of 6 inches where complex flow interactions are produced that are not amenable to proven analytical techniques. In the original Shuttle design, the specified aerothermal loads allowed the use of HRSI tiles in the gap for thermal protection; and earlier test results in the Langley 8' HTT supported the original design. However, test results from small-scale laminar test at ARC suggested that the HRSI tiles were not adequate and replaceable ablation panels were used on the first five Shuttle flights.When flight results indicated that the original HRSI design would be adequate, the original tile design was reinstated. Since flight data continues to indicate excessive heating on the windward edges of the elevons that is not fully understood, a 1/3 scale model of the Shuttle split elevon was modified for test in the 8' HTT to provide detailed aerothermal load distributions with critical test parameters varied.

Approach - The elevon portion of the previous model was replaced with a 1/3 scale replica of the Shuttle (figure 27(b)) and had a chord length of 24 inches and gap widths from 1 to 3 inches. Sharp and 1/4 inch radius rounded edges of the elevon gaps were used to define edge effects on the aerothermal loads to the elevon sidewalls. Tests were performed in the 8' HTT at a free-stream Mach number of 6.5, a unit Reynolds number range from 0.4 to 1.5 x 10^6, and a total temperature of 3500 R. The model wing angle was varied from 0 to 10 degrees and the elevon angles were varied from 0 to 20 degrees.

Accomplishment Description - The basic data from all 31 test runs have been reduced and preliminary data plots have been generated. A typical spanwise heating distribution across the elevon and into the gap is shown in the lower left plot. The windward heating on the elevon is normalized by the measured value QL and the heating decreases substantially near the edge. The maximum heating in the gap, QMAX, occurs near the edge and is driven by the elevon windward surface pressure, PL, as illustrated in the lower right plot. QL and QMAX for the various combinations of wing and elevon deflection angles are presented and both vary with the 0.8 exponential power of PL with QMAX consistently 25% of QL.

Future Plans - Experimental results will be presented in a NASA document and be available for comparison with analytical solutions when appropriate computer codes are identified to handle these flow details.

Figure 27(a).

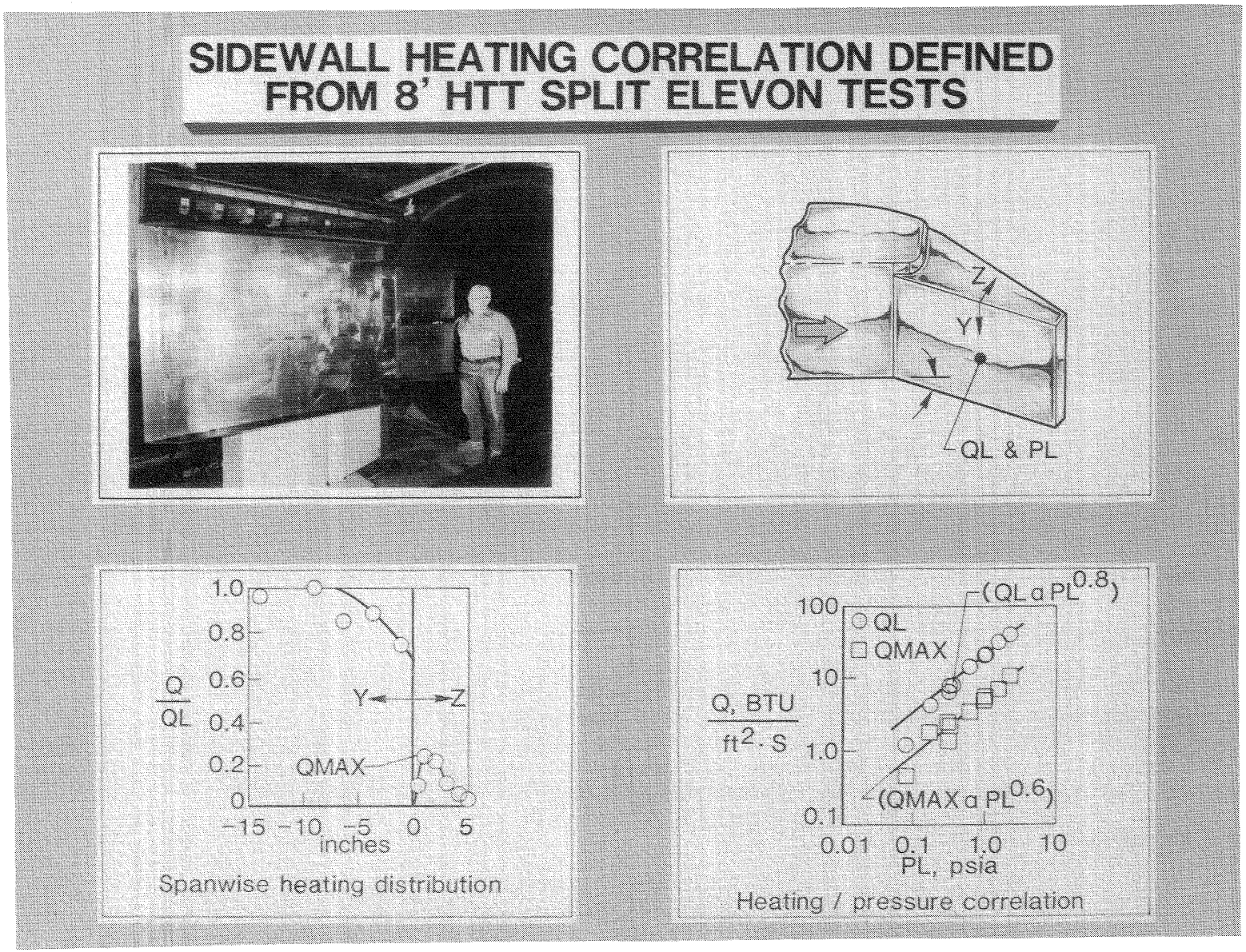
SIDEWALL HEATING CORRELATION DEFINED FROM 8' HTT SPLIT ELEVON TESTS
Z
Y
QL & PL
1.0
0.8
0.6
0.4
0.2
0
Q/QL
Y
Z
QMAX
−15 −10 −5 0 5
inches
Spanwise heating distribution
100
10
1.0
0.1
Q, BTU / ft2 · S
QL
QMAX
(QL α PL0.8)
(QMAX α PL0.6)
0.01 0.1 1.0 10
PL, psia
Heating / pressure correlation

Figure 27(b).

QUILTED TILE ARRAY SIMULATING THERMALLY BOWED METALLIC TPS

Christopher E. Glass and L. Roane Hunt
Aerothermal Loads Branch
Ext. 4441/3423

RTOP 506-40-21

Research Objective - Metallic TPS panels on high speed vehicles are subject to thermal distortions when they experience large through-the-thickness temperature gradients. The panel, anchored at the corners, bow up into the flow field altering a smooth vehicle moldline to a quilted surface configuration. Although the bowed height of the panels is expected to be less than the local boundary layer thickness, the complex interaction of the high-speed flow field and the bowed surface will effect the local and global aerothermal loads to the vehicle. An experimental aerothermal study has been completed which complements analytical studies of this problem.

Approach - A quilted array of ceramic tiles was designed and fabricated to fit the 8' HTT panel holder, as shown in figure 28(b), which provides two-dimensional laminar and turbulent boundary layer flow. The tiles were designed 10 inches square with protuberance heights of 0.1, 0.2, and 0.4 inches. The same tiles were designed to be tested in both aligned and staggered array configurations. The array includes two types of instrumented metallic tiles to be inserted into the ceramic tile array for surface pressure and thin-wall heat-transfer measurements. Aerothermal tests were performed at a free-stream Mach number of 6.5, a unit Reynolds number of 0.4×10^6 per foot, and a total temperature of 3500°R.

Accomplishment Description - The quilted dome array simulating thermally bowed metallic TPS was tested during FY85 in the 8' HTT and the preliminary data analysis have been completed. Preliminary results include pressure and cold-wall heating-rate distributions, boundary layer profiles, and temperature contours obtained from infrared thermographic measurements. In general, the laminar flow results agree qualitatively with previously obtained 3-D Navier-Stokes solutions for the quilted dome configuration.

Future Plans - Results will be documented and detailed comparisons with a 3-D Navier-Stokes solution for the laminar flow condition will be documented later in a NASA TP.

Figure 28(a).

AEROTHERMAL TESTS ON A SURFACE SIMULATING THERMALLY BOWED METALLIC TPS COMPLETED IN 8' HTT

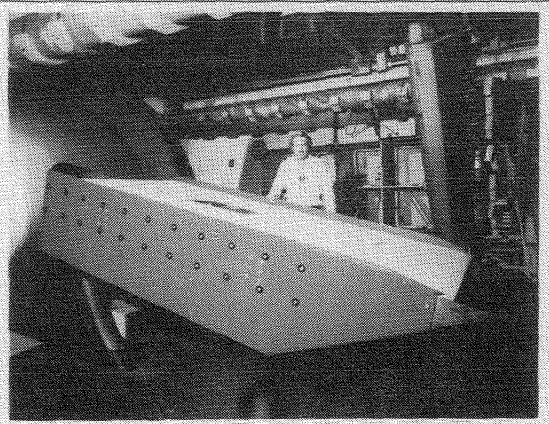

Test conditions

Mach No.	6.5
RE/ft x 10^{-6}	0.4
T_t	3500R
q	2.5psi
δ	0.81 in.–laminar
	1.42 in.– turbulent
H	0.1,0.2,0.4 in.
Test runs	21–laminar
	15–turbulent

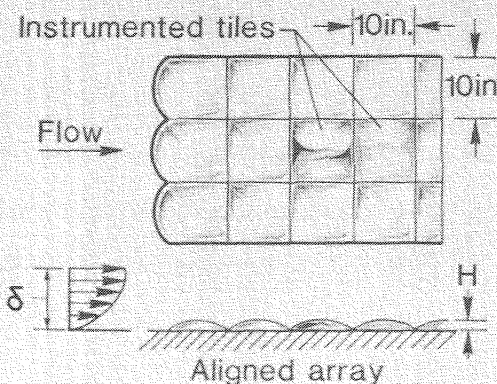

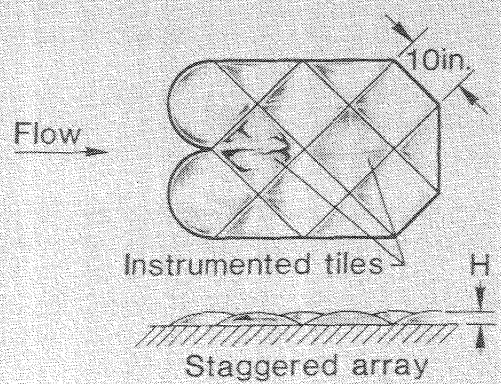

Figure 28(b).

INVISCID FINITE ELEMENT FLOW ANALYSIS APPLIED TO EXPERIMENTAL MODEL

Kim S. Bey
Aerothermal Loads Branch
Ext. 4441

RTOP 506-43-31 and 506-40-21

Research Objective - Demonstrate the capability of the finite element method to accurately and efficiently predict the aerothermal environment over complex configurations through comparisons with experimental results. Provide computational results to enhance understanding of the phenomena involved.

Approach - A two-dimensional inviscid finite element code for high-speed flow has been developed as an intermediate step in the development of a full Navier-Stokes code. The code is vectorized for efficient execution on the VPS 32 computer. To demonstrate and verify its capabilities to compute flow fields with complex geometries the code was applied to a wing-elevon cove experimental model tested at Mach 7 in the LaRC 8-Foot High Temperature Tunnel (8' HTT). Although the cove configuration has strong viscous dominated flow regions the inviscid analysis is valid in some regions and was applied as a precurser to the full viscous analysis to enhance understanding of the flow field phenomena and to validate the numerical algorithm. Computations for the experimental configuration, shown in the center figure, begin with the blunt leading edge of the panel holder where the impinging high-speed flow generates an entropy layer that persists downstream past the cove location. The flow approaching the cove region is used as the upstream boundary condition for the cove analysis. Results of the blunt leading edge analysis are compared to results obtained by two other analytical techniques, a shock capturing finite volume technique and a shock fitting method of lines technique, the results of the cove analysis are compared with experimental results.

Accomplishment Description - The predicted blunt leading edge flow field density distribution and outflow plane velocity profile are shown to the left of figure 29(b). The outflow plane velocity profile predicted by the finite element code is in good agreement with the profiles predicted by the other two techniques. Application of the code to the cove produced the flow field density distribution and elevon wall pressure distribution shown to the right of the figure. The predicted wall pressure agrees with the experimentally measured wall pressure inside the cove where the viscous effects are small but not at the mouth of the cove where viscous effects dominate. In the outer flow region the wall pressure increases to a value slightly greater than predicted by oblique shock theory for a compression corner because the flow expands slightly around the trailing edge of the wing. These results demonstrate the capability of the finite element technique to capture shocks and to resolve complex flow fields.

Future Plans - The viscous terms have been added to the code to provide a full Navier-Stokes analysis of the wing-elevon cove. Long range plans include the extension to three-dimensional flow fields for incorporation into an integrated finite element flow-thermal-structural analysis capability.

Figure 29(a).

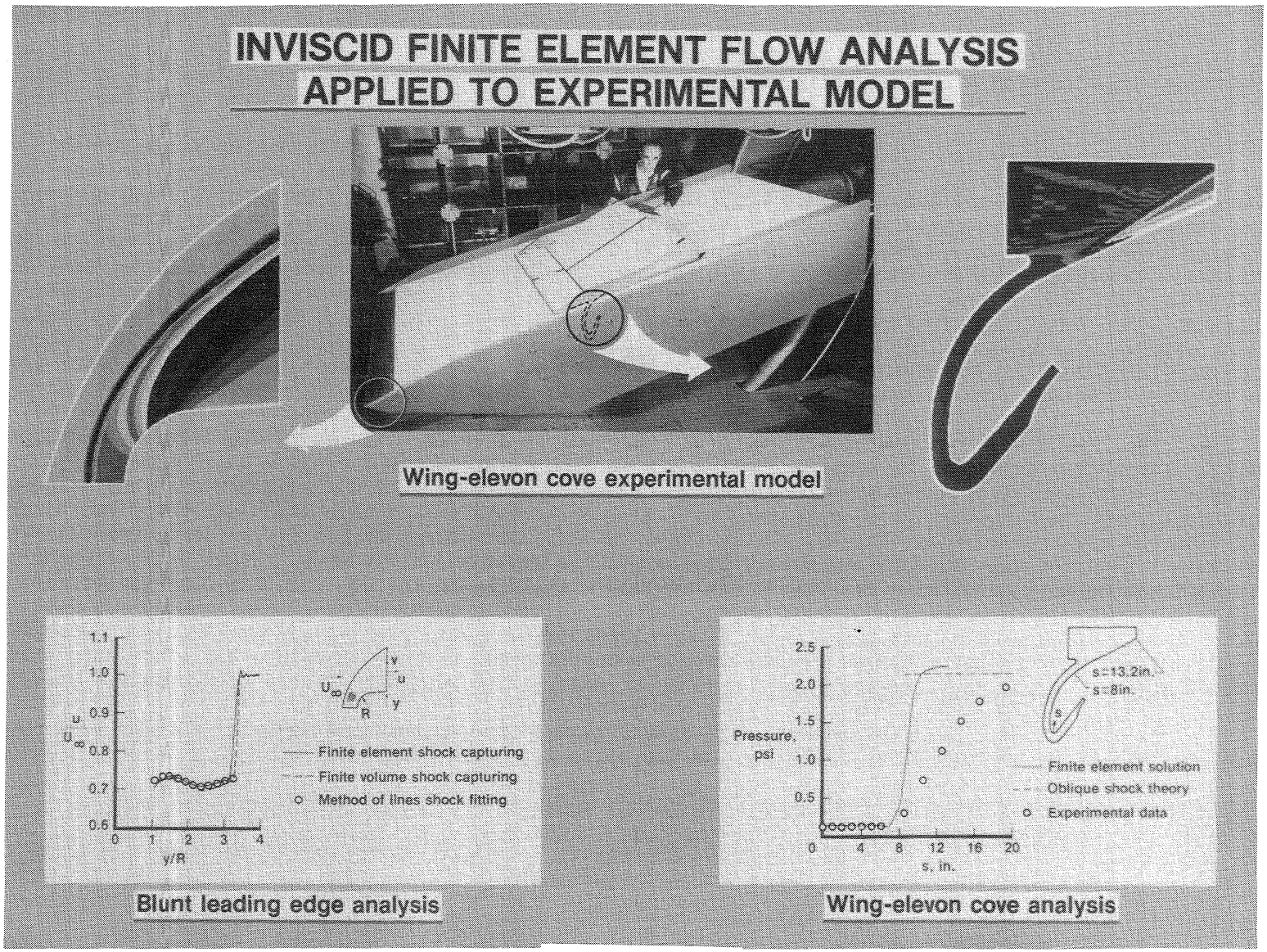
INVISCID FINITE ELEMENT FLOW ANALYSIS
APPLIED TO EXPERIMENTAL MODEL
Wing-elevon cove experimental model
1.1
1.0
0.9
0.8
0.7
0.6
u/U∞
0
1
2
3
4
y/R
v
u
U∞
R
y
Finite element shock capturing
Finite volume shock capturing
Method of lines shock fitting
Blunt leading edge analysis
2.5
2.0
1.5
1.0
0.5
Pressure, psi
0
4
8
12
16
20
s, in.
s=13.2in.
s=8in.
s
Finite element solution
Oblique shock theory
Experimental data
Wing-elevon cove analysis

Figure 29(b).

CLOSED FORM EVALUATION OF TAYLOR-GALERKIN FINITE ELEMENT MATRICES YIELDS AN ORDER OF MAGNITUDE SAVINGS ON COMPUTATIONAL RESOURCES FOR HIGH SPEED FLOW

Kim S. Bey
Aerothermal Loads Branch
Extension 4441

RTOP 506-43-31

Research Objective - To develop computationally efficient and accurate finite element algorithms for high speed flow to be integrated with thermal-structural finite element analyses.

Approach - A number of grants have been established to develop finite element algorithms for high speed flow. Algorithms are evaluated based on computational efficiency and solution accuracy by comparisons with other numerical techniques and experimental data.

Accomplishment Description - The Taylor-Galerkin algorithm was applied to high speed flow by grantees at the University of Wales. They implemented the algorithm with triangular elements and included automatic mesh refinement and multiple time domain marching to steady state. Triangular elements were chosen because the integrals which make up the element matrices can be evaluated in closed form. Quadrilateral elements, on the other hand, usually require numerical integration to compute element matrices. Quadrilateral elements offer a storage advantage in that it takes two triangles to form a quadrilateral. This savings is increased in 3D as it takes five tetrahedrons to form one hexahedron.

An element matrix for a quadrilateral element consists of four integrals and for a hexahedron consists of eight integrals (one for each node). When the compact expression for one integral (figure 30(b)) is expanded completely, it contains 128 terms for a quadrilateral and almost 200,000 terms for a hexahedron. Upon implementing the Taylor-Galerkin algorithm for quadrilateral elements it was found that the 128 terms could be algebraically simplified to 4 terms and the integral could then be evaluated in closed form. In 3D the simplification of 200,000 terms is impossible to do by hand, so that closed form expressions for 3D integrals were obtained using the symbolic manipulation program MACSYMA. The computational savings achieved in the evaluation of two types of hexahedral element matrices (the consistent mass matrix and other element matrices) are shown in the figure. The computational savings achieved by closed form integration for both types of element matrices is in excess of an order of magnitude over the numerical integration necessary to obtain the equivalent exact result.

Future Plans - The computational savings derived from closed form evaluation of the finite element matrices is an important step towards developing computationally efficient finite element algorithms for high speed flow. The closed form integration has been implemented in a vertorized Taylor-Galerkin code which is being applied to a number of 2D and 3D flow problems on the Langley VPS 32.

Figure 30(a).

COMPUTATIONAL SAVINGS FROM CLOSED FORM EVALUATION OF FINITE ELEMENT MATRICES FOR TAYLOR-GALERKIN ALGORITHM

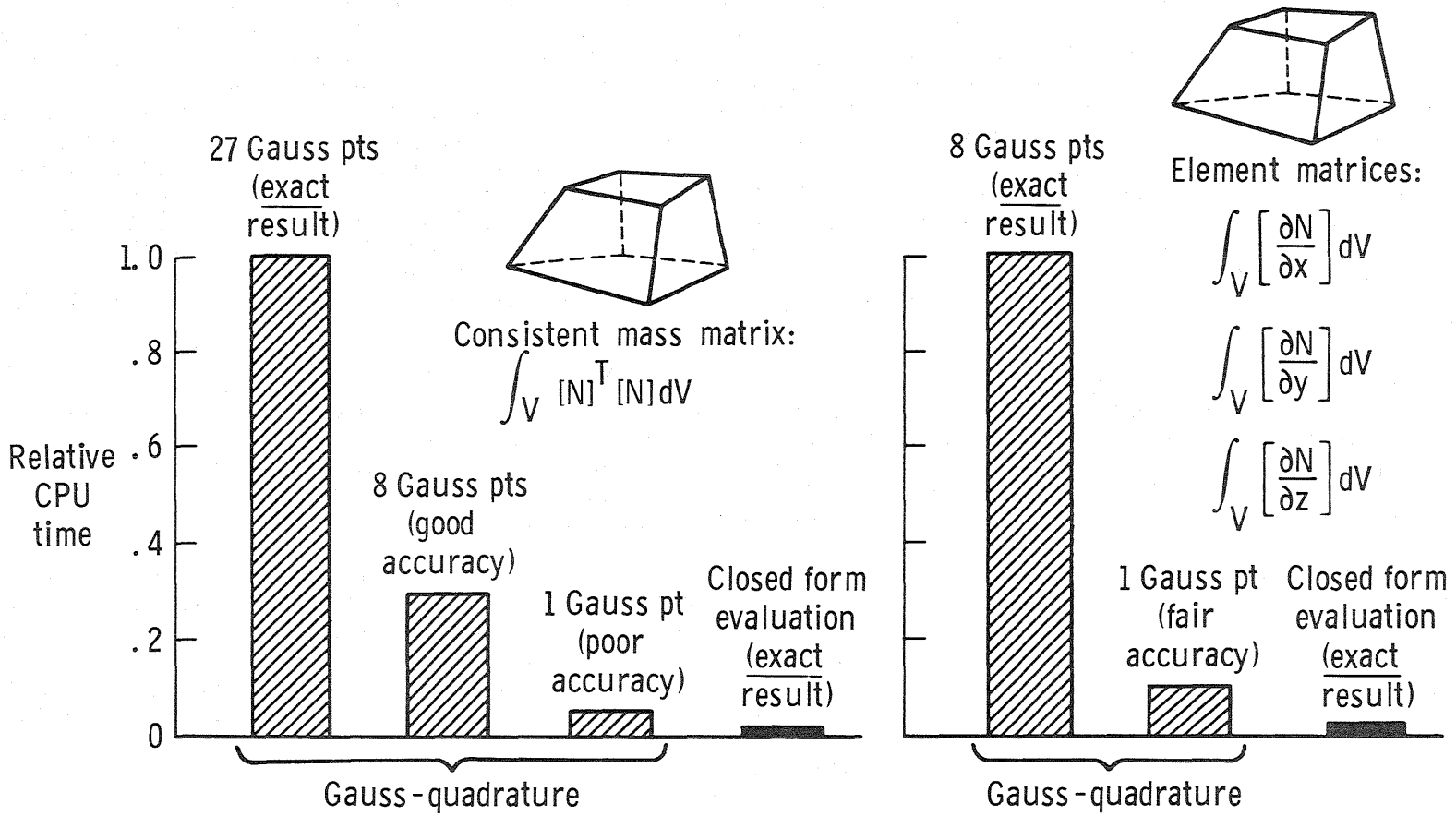

Figure 30(b).

IMPROVEMENTS IN SPECTRAL COLLOCATION THROUGH A MULTIPLE DOMAIN TECHNIQUE

Michele G. Macaraeg
Aerothermal Loads Branch
Ext. 2325

Craig L. Street
Theoretical Aerodynamics Branch
Ext. 2627

RTOP 506-43-31 and 506-40-21

Research Objective - Develop spectral collocation methods for application to high-speed viscous flow problems that maintain the high accuracy, resolution and convergence rates possible with spectral techniques. The exceptional attributes of spectral methods are severely degraded when complex geometries are mapped into a simple computational domain or when the mappings have severe stretching, as would be required to capture a boundary layer in high-speed viscous flow. Eliminating this degradation will provide a powerful tool for the accurate prediction of aerothermal loads on future high-speed structures.

Approach - Divide the computational domain into subdomains such that each subdomain will map smoothly onto a simple computational subdomain without severe internal stretching. However, the mesh sizes in adjacent subdomains can vary by several orders of magnitude. By this means, complex geometries and high gradient regions can be captured without degrading the spectral accuracy and convergence rate within a subdomain. Subdomain solutions are interfaced by enforcing a global flux balance which preserves the high-order continuity of the solution. In addition, division into subdomains makes this technique amenable to parallel processing.

Accomplishment Description - Preliminary evaluation of the spectral collocation method with multiple subdomains was done on several fundamental equation types. The first is the solution of the viscous Burger's equation with very small viscosity, similar to a one dimensional shock. The domain is divided into three subdomains, with the grid size of the center subdomain ($-.02 \leq x \leq +.02$), where the shock forms, being six orders of magnitude smaller than the two outer subdomains. The results, on left of figure 31(b), show the development of the shock-like structure with time, the smooth transition between subdomains and the sharp resolution of the shock-like structure. The second is the solution of steady-state two-dimensional heat conduction problem with an interface between two materials with thermal conductivities differing by an order of magnitude. The domain is divided into two subdomains at the intersection of the two materials. The results, center, show that the solution is smooth within each subdomain and that the gradient jump at the interface of the two materials is automatically enforced by the global flux balance. The third is the solution of the two-dimensional Poisson equation on a square domain divided into four equal subdomains. The results, right, show that the solution is just as smooth at the interfaces of the subdomains as if they had been obtained on a single domain. These are preliminary evaluations, but they indicate that the multiple domain methodology may be capable of maintaining the desired spectral properties in the complex domains encountered in high-speed viscous flow problems.

Future Plans - Extend the application of the method to the Navier-Stokes equation system and evaluate its effectiveness on real flow problems. Continue efforts to reduce storage requirements and increase convergence rates of the algorithm. This method has been targeted for use as a prototype method for the large-scale parallel-processor Navier-Stokes computer under construction at Princeton University.

Figure 31(a).

IMPROVEMENTS IN SPECTRAL COLLOCATION THROUGH A MULTIPLE DOMAIN TECHNIQUE

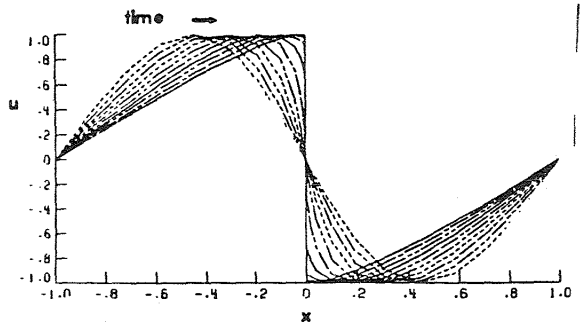

VISCOUS BURGER'S EQUATION

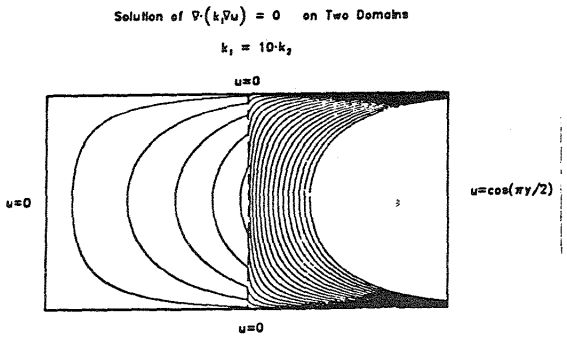

HEAT TRANSFER EQUATION

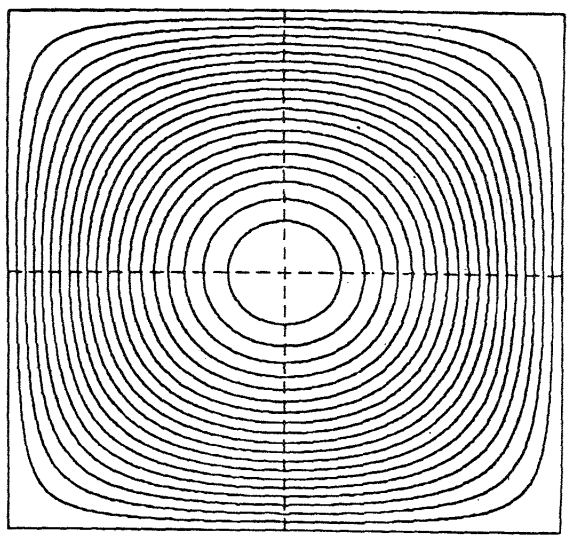

POISSON'S EQUATION

Figure 31(b).

1x3 HIGH ENTHALPY AEROTHERMAL TUNNEL COMBUSTOR LINER EVALUATION

Randy B. Heard
Aerothermal Loads Branch
Ext. 3423

RTOP 506-43-31

Research Objective - To evaluate the thermal structural response of a nickel heat sink liner and a solid nickel water cooled liner and pressure vessel at various operating conditions, and evaluate the design in terms of cyclic life.

Approach - The 1x3 HEAT had experienced severe fatigue and thermal stress problems with a tube-type water cooled combustor liner (figure 32(b)). Various tube-type constructed liners were tried and all failed in a similar manner, i.e. water leaks large enough to extinquish the combustion process. A solid heat sink liner was designed, fabricated, and used for short duration runs to expedite checkout and calibration of the facility. However, for research uses, a longer run time was needed. To meet this need, a solid water cooled liner was designed in-house at Langley. It is a nickel 201 cylinder with 88 grooves machined on the outside surface sealed with electroformed nickel. Both nickel liners and the pressure vessel were instrumented with thermocouples. The test section was instrumented with pitot probe, thermocouples, and Gardon heat gages. The tunnel was run with a methane/air mixture at approximately 3000°F and 130 psi in the combustor.

Accomplishment Description - Several hot runs were made with the heat sink liner and the data was compared to theoretical analysis. The data revealed that the pressure vessel would not reach its maximum allowable temperature as quickly as expected and therefore the heat sink liner was the limiting item. The data in the liner indicated a run time of approximately 70 seconds was possible before exceeding the maximum use temperature of 800°F at a gas temperature of 3000°F. These results agreed surprisingly well with the theoretical analysis. The heat sink liner was removed and the water cooled liner was installed and instrumented. Several runs of one minute were made and no sign of overheating or water leaks were evident. This was followed with two 5 minute runs with the same results. The tunnel was then run for 10 minutes and the tunnel data revealed no sign of overheating or any degradation of the tunnel components. The design of the water cooled liner appears to be capable of long duration runs. The table below summarizes the past and present water cooled combustor liners.

	Runs	Longest	Total Run Time	Condition at End of Tests
Contractor, Discrete Tube	19	76 seconds	280 seconds	Failed
Contractor, Discrete Tube	36	180 seconds	642 seconds	Failed
Contractor, Discrete Tube	6	146 seconds	412 seconds	Failed
Solid, Water Cooled	8	600 seconds	1257 seconds	Operational

Future Plans - The data from the hot tunnel runs will be reduced and documented in report form. The tunnel has been closed and is being mothballed due to lack of adequate staffing.

Figure 32(a).

1x3 HIGH ENTHALPY AEROTHERMAL TUNNEL COMBUSTOR LINER EVALUATION

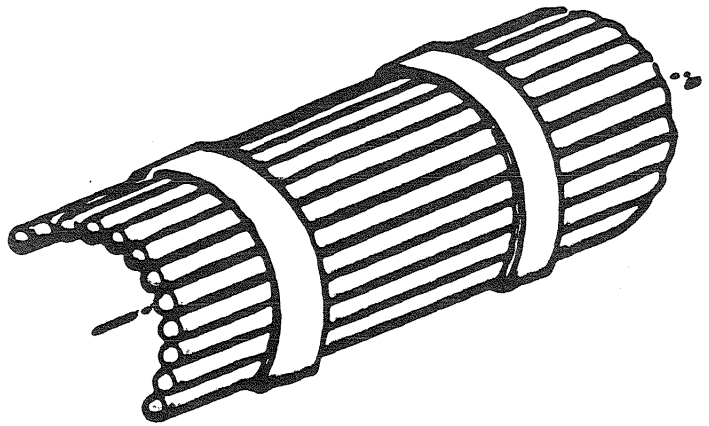

TUBE BUNDLE (WATER COOLED)
1975-1979

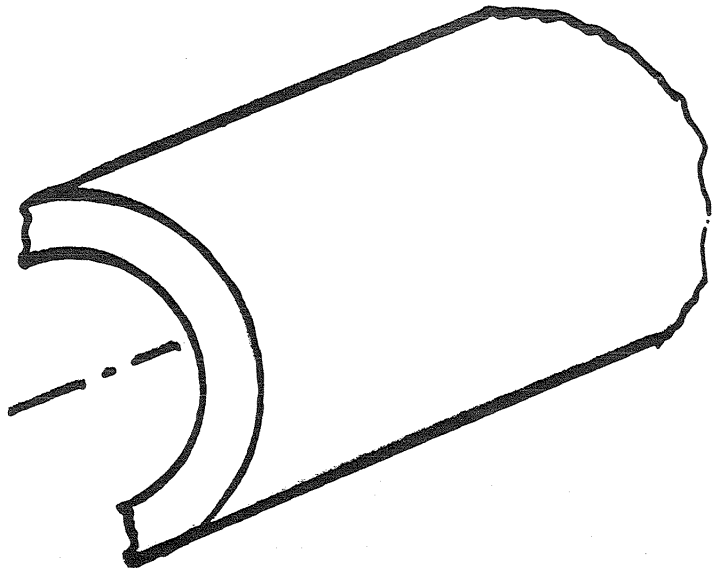

SOLID LINER (HEAT SINK)
1982-1983

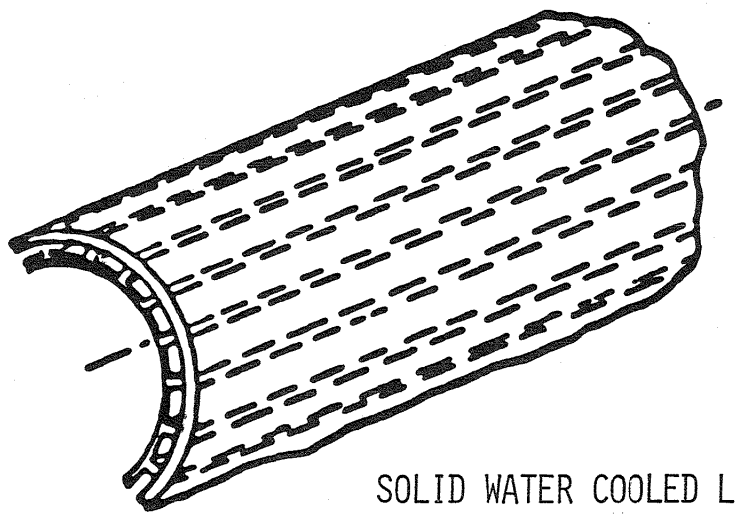

SOLID WATER COOLED LINER
1983-?

Figure 32(b).

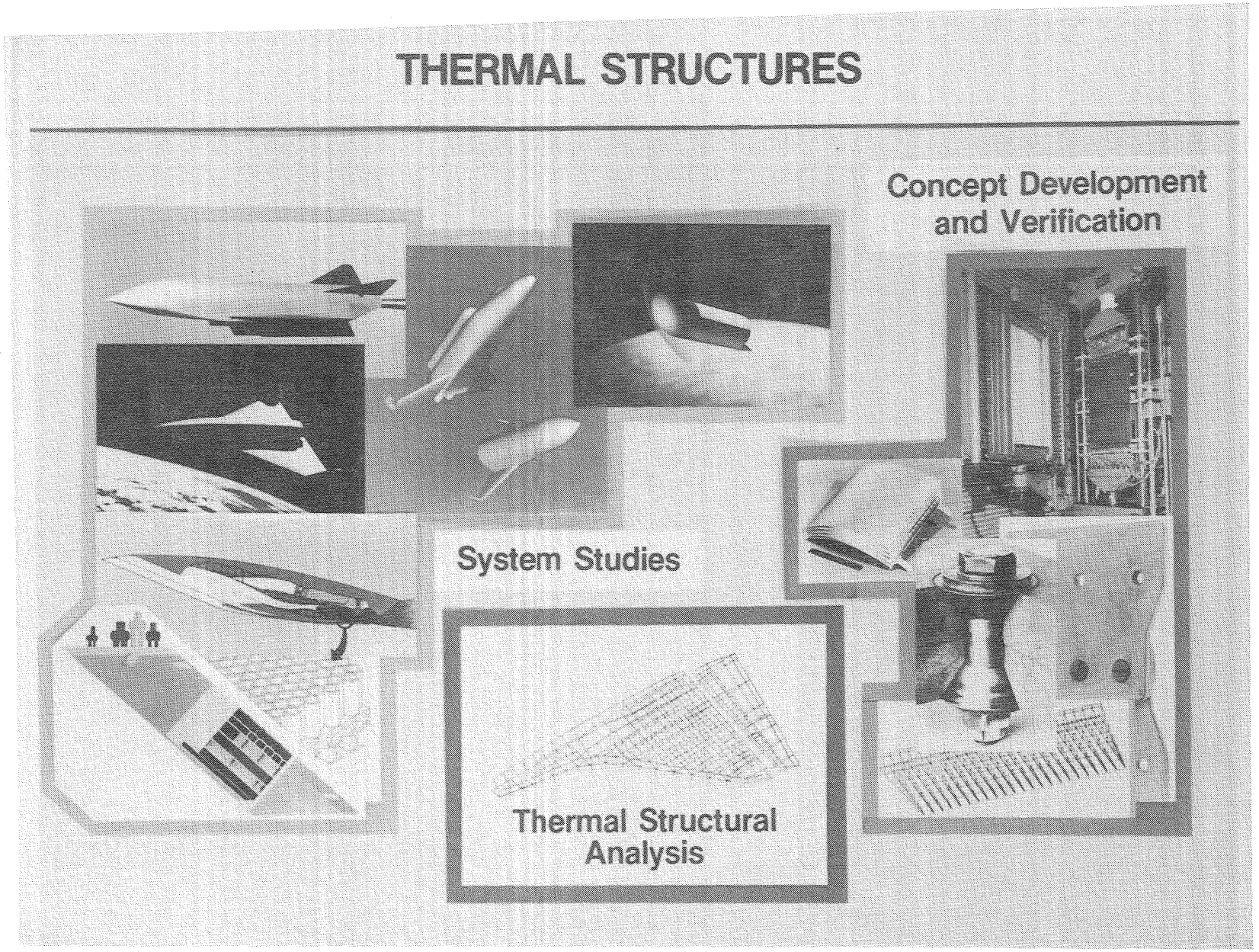
THERMAL STRUCTURES
Concept Development and Verification
System Studies
Thermal Structural Analysis

Figure 33.

THERMAL STRUCTURES

FIVE YEAR PLAN

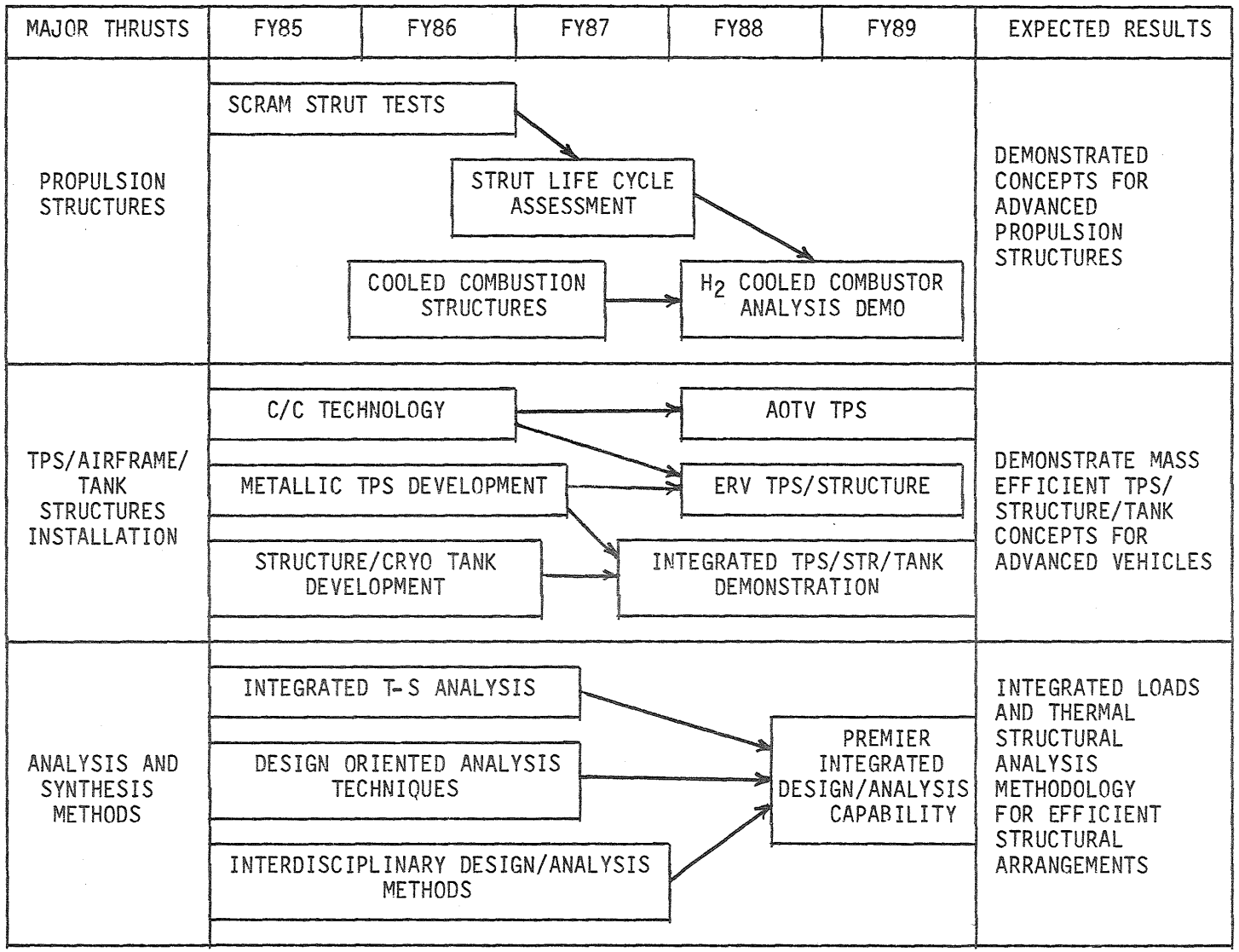

Figure 34.

This Page Intentionally Left Blank

BALLUTE SHAPE ANALYSIS REVEALS POTENTIAL INSTABILITY

S. J. Scotti
PRC Kentron Inc.
Ext. 4297

Max L. Blosser
Thermal Structures Branch
Ext. 4295

RTOP 506-43-31

Research Objective - Investigate the limits of shape change (required to accommodate atmospheric density variations) for the ballute aeroassisted orbital transfer vehicle (figure 35(c)) that can be achieved by varying internal pressure; and determine the impact of these limits on ballute stability and vehicle controllability.

Approach - Develop a method to predict the shape, drag, center of pressure location, and the pressure difference across the fabric of the partially deflated ballute as a function of the ratio of internal to stagnation pressure and use the method to identify potential limitations to shape change.

Accomplishment Description - A method for predicting the shape of ballute for various internal pressures has been developed. The method calculates the equilibrium position of a meridional tape of the ballute with the following assumptions: the tape is inextensible, the net fabric hoop stress has a negligible effect on the shape, and the external pressure is modified Newtonian.

Calculated ballute shapes are shown in figure 35(d). The design shape of the meridional tapes, indicated by a solid line, was calculated assuming an initial angle of 60 degrees, a radius of 25 feet. To find the effect of varying the internal pressure on the shape, the design meridional tape length and attachment point locations were preserved and the equilibrium position of the meridional tape, loaded by a uniform internal pressure and modified Newtonian external pressure, was calculated. The internal pressure was reduced below the design pressure (initial angle = 60 degrees) to obtain shapes with initial angles of 48, 40 and 35 degrees. As shown in the figure, the tapes become almost straight on the windward side of the ballute at low internal pressure. The internal pressure was increased above design to produce a shape with an initial angle of 70 degrees. Increasing the internal pressure will decrease the lobing of the fabric between the tapes, the fabric will carry a larger share of the load and the shape of the ballute will be affected. Because this analysis assumes zero fabric stresses, it cannot predict the contribution of the fabric to the shape. However, for the design pressure and below, the fabric stress does not greatly affect the ballute shape. For each shape, the turn down ratio, which is the ratio of the drag of the design shape to the drag of the off-design shape, is shown. Even for the 35 degree ballute shape, the turn down ratio is only 2.4:1 and several researchers have indicated that a minimum of 3:1 is required. The center of pressure location for each shape is also shown. The center of pressure moves forward as the ballute is deflated. Therefore, the ballute AOTV must be designed to be aerodynamically stable at its lowest inflation pressure.

Figure 35(a).

BALLUTE SHAPE ANALYSIS REVEALS POTENTIAL INSTABILITY

CONTINUED

The ballute fabric acts as a membrane which is stabilized by a pressure difference across it. There is excess fabric between the meridional tapes which is lobed and held in place by the pressure difference. As the internal pressure is decreased, the circumference of the ballute decreases and the lobes deepen considerably. Figure 35(e) shows the pressure difference across the fabric for each shape as a function of meridional position. On the back half of the ballute there is a relatively large pressure difference stabilizing the fabric. However, on the front or windward side of the ballute there is only a small pressure difference, even on the design shape. For the 48 degree ballute shape, the pressure difference goes to zero at the forward attachment point. For the 40 and 35 degree ballute shapes there are large areas of fabric that have zero pressure difference. These areas of fabric with no pressure difference to provide a stabilized shape will likely flutter. Although tests will be required to determine if the flutter will cause failure of the fabric or insulation, the unstabilized fabric is not desirable.

Plans - The results of this study will be documented in a memo to the AOTV Project Office and in a NASA Quick Release Technical Memorandum describing a comparative study of a ballute, a lifting brake, and a slant-nosed-cylinder configuration.

Figure 34(b).

BALLUTE AEROASSISTED ORBITAL TRANSFER VEHICLE

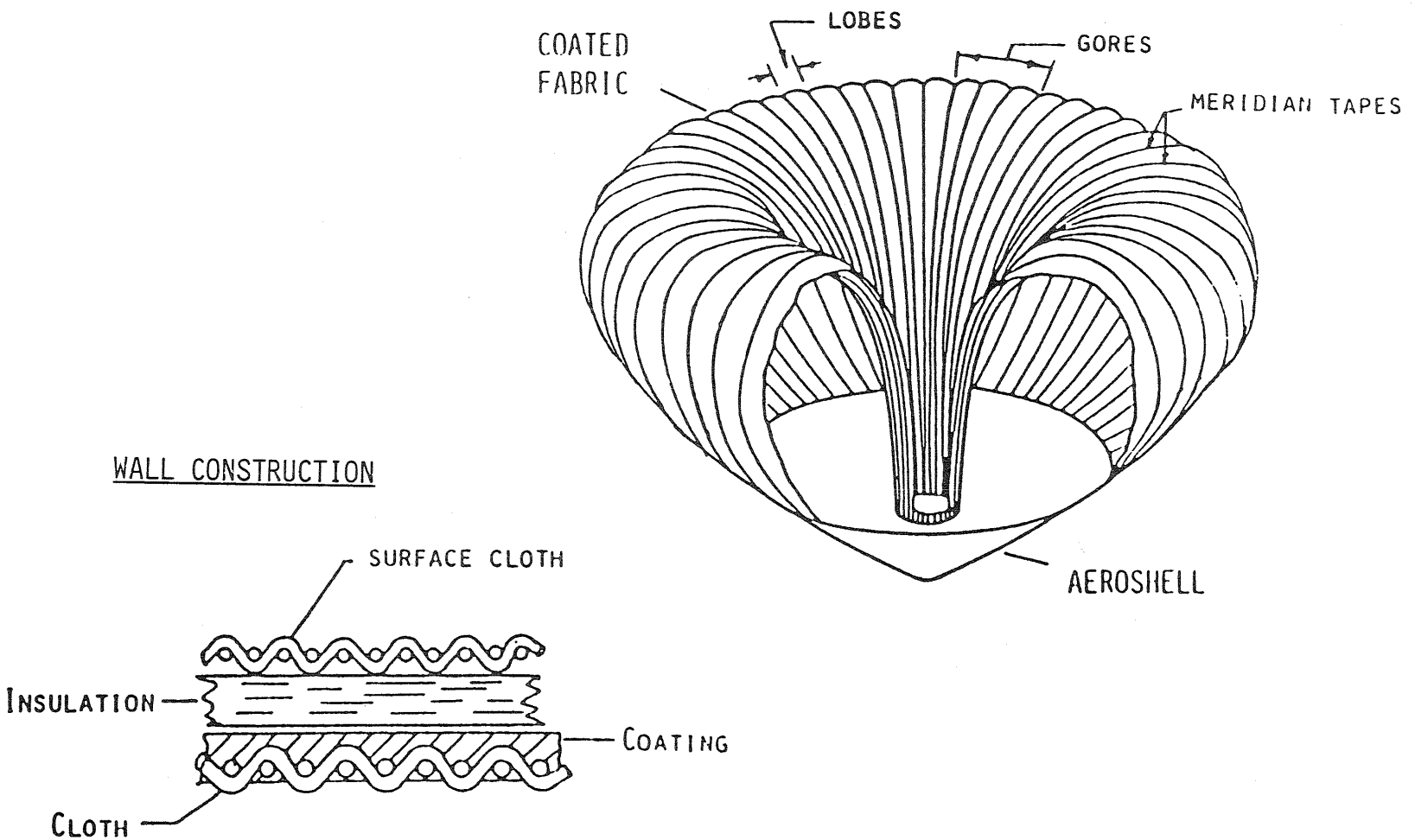

Figure 35(c).

BALLUTE SHAPES FOR VARIOUS INTERNAL PRESSURES

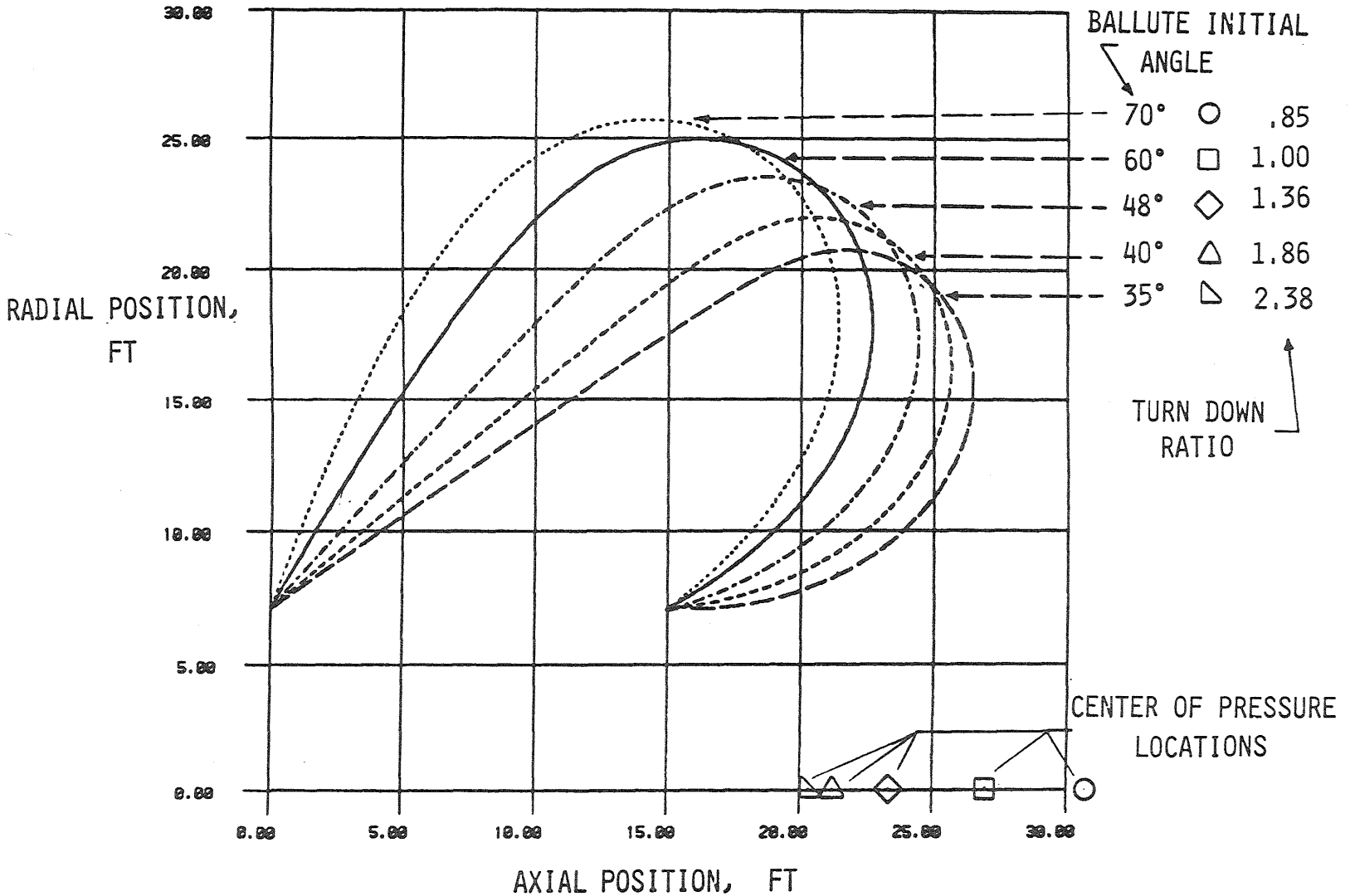

Figure 35(d).

PRESSURE DIFFERENCE ACROSS BALLUTE FABRIC AS A FUNCTION OF MERIDIONAL POSITION

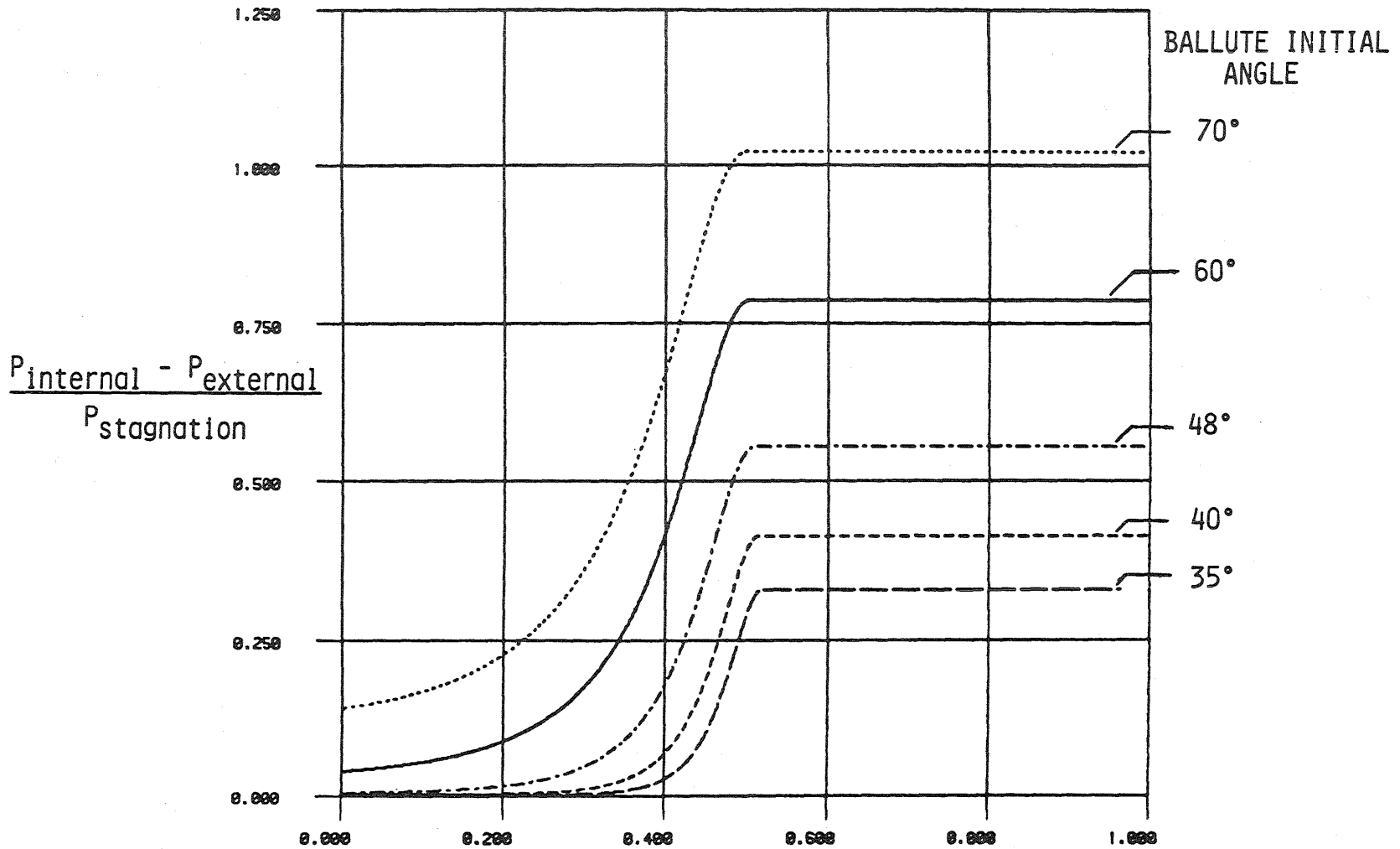

Figure 35(e).

REUSABLE HIGH-TEMPERATURE CRYOGENIC FOAM INSULATION SYSTEM

Allan H. Taylor and Randall C. Davis
Thermal Structures Branch
Ext. 4142

RTOP 505-63-81

Research Objective - To design, fabricate and test an advanced flightweight cryogenic insulation system for aerospace vehicles that could reusably withstand service temperatures of 400°F on the one face and -423°F on the other.

Approach - Under contract NAS1-17857 to Lockheed California Company, a series of material evaluation and processing experiments were conducted to establish a viable manufacturing process for a flightweight high-temperature cryogenic foam insulation system. Insulation blocks were fabricated, bonded to simulated tank wall structure and tested under conditions that simulated the expected service environment.

Accomplishment Description - A flightweight reusable high temperature cryogenic foam insulation system (as shown in figure 36(b)) has been developed and successfully demonstrated. The cryogenic foam block consists of two discrete layers of a 6.9 lb/cu ft closed cell polymethacrylimide foam (Rohacell 110 WF) bonded together with an epoxy adhesive. The bond line is additionally reinforced with an 0.003 in. thick layer of fiberglass cloth. The foam block is wrapped with a precut and preformed vapor barrier cover made of the non-permeable, high-temperature material, Kapton-aluminum-Kapton (KAK). The covered insulation blocks are bonded to the cryogenic tank wall.

Several specimens, each 2 in. thick and 10 in. square, bonded to an aluminum panel, have been fabricated to verify the manufacturing techniques. One such specimen was successfully tested for 100 thermomechanical cycles, consisting of cooling the metal surface to -323°F, heating the outer surface of the foam insulation with 400°F air, while simultaneously applying a 15 kip tensile load in the aluminum panel. In a similar test of another specimen, the insulation was exposed to the 400°F air and metal tank surface exposed to -423°F for 20 cycles. In both test specimens there was no apparent damage or degradation of the cryogenic foam insulation system.

Future Plans - As part of the continuation of the current contract with Lockheed California Company, specimens will be fabricated and tested using a lower density version of the Rohacell material, Rohacell 51 WF, which has a density of 3.1 lb/cu ft. Also the conductivity and permeability of the cryogenic foam insulation system will be determined over the range of environmental conditions anticipated during service.

Figure 36(a).

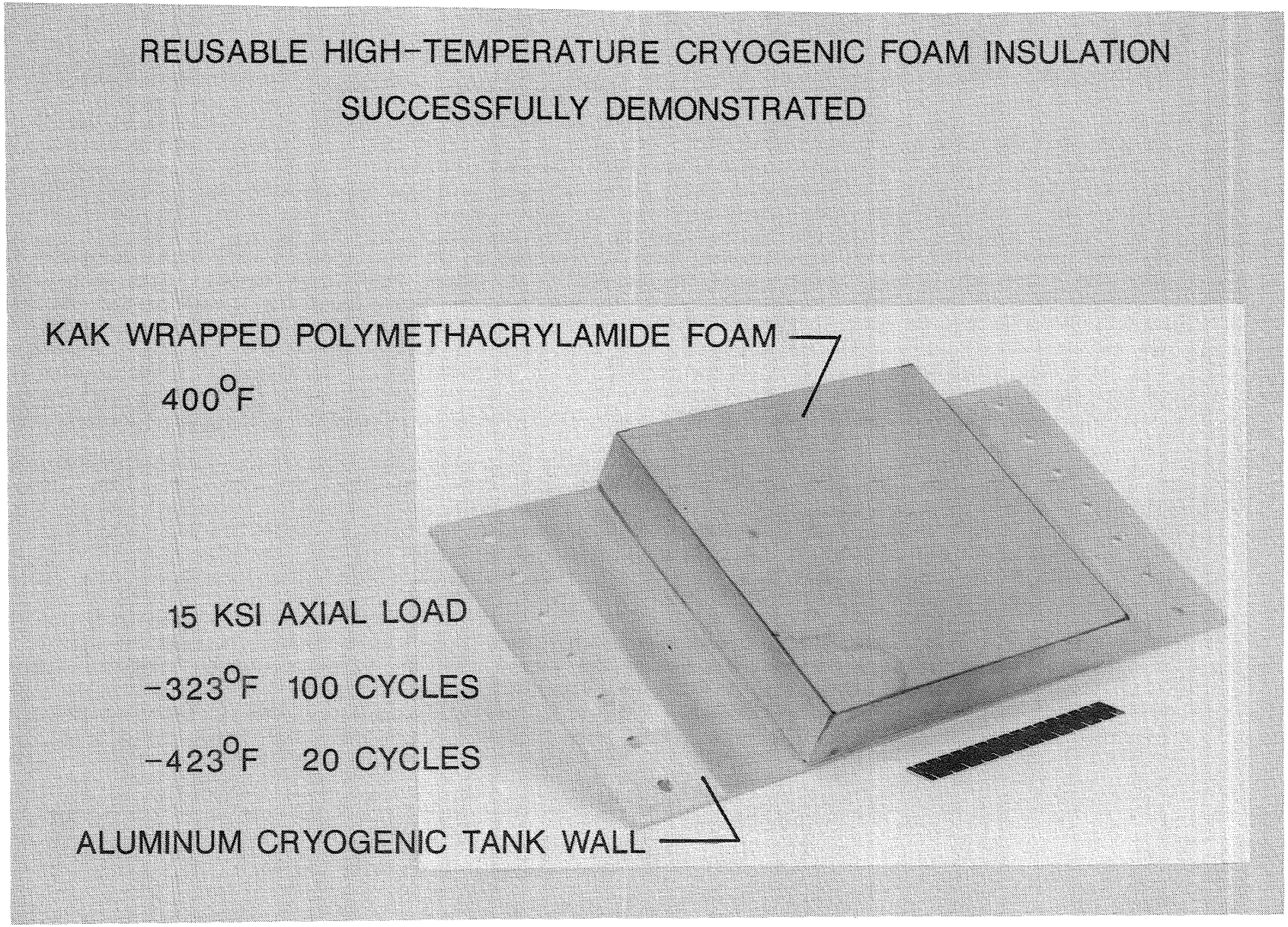
REUSABLE HIGH-TEMPERATURE CRYOGENIC FOAM INSULATION
SUCCESSFULLY DEMONSTRATED
KAK WRAPPED POLYMETHACRYLAMIDE FOAM
400°F
15 KSI AXIAL LOAD
-323°F 100 CYCLES
-423°F 20 CYCLES
ALUMINUM CRYOGENIC TANK WALL

Figure 36(b).

CURVED METALLIC TPS

John L. Shideler
Thermal Structures Branch
Ext. 2425

Mark P. Gorton
PRC Kentron Inc.
Ext. 2425

RTOP 506-43-31

Research Objective - While much of the surface of a typical Space Transportation System (STS) is flat or nearly flat, some areas are necessarily curved. Wind tunnel test data for flat Superalloy Honeycomb (SA/HC) prepackaged Thermal Protection Systems (TPS) have indicated that heating in the gaps between panels can occur and that surface pressure gradients may increase the severity of gap heating. Also, analysis indicates thermal stresses are much higher for curved TPS than for flat TPS. The objective is to evaluate gap heating between curved SA/HC panels under pressure gradient conditions, and to assess the severity of thermal stresses in curved panels.

Approach - An array of curved SA/HC panels has been fabricated for testing on the Curved Surface Test Apparatus (CSTA). The radii of the panels vary from 9 inches to 12 inches. A section of the CSTA was cut out so that the curved array could be inserted flush with the CSTA skin. Wind tunnel tests in the LaRC 8'HTT will provide temperature and pressure data to allow evaluation of gap heating under pressure gradient conditions. A single curved panel, instrumented with strain gages and thermocouples, will be tested under radiant heating to evaluate thermal stresses.

Accomplishment Description - After the windward panels were preheated to a surface temperature of 2000°F, the array was exposed for seven seconds to the most severe conditions that are within the normal operating range of the 8'HTT. Preliminary evaluation of test data indicated heating occurred in the gaps between panels. Removal of several panels revealed that the edges of the Nomex felt strips beneath the panel perimeters were not properly coated with RTV to eliminate porosity. Part of the felt beneath the panels was sealed with RTV and the model was retested for 34 seconds at the same tunnel conditions as for the previous test. Figure 37(b) shows the model in the stream at t = 0 sec. and t = 34 sec. Unacceptably high temperatures were again measured in the gaps between panels. Examination of the model revealed that the aft seal of the cavity into which the panels were installed had failed. Failure of this seal would allow the hot gas on the surface of the panels to flow through the gaps between panels and through the cavity seal to the base of the model. This condition (pressure difference of about 4 psi) is even more severe than the severe 2 psi-per-foot surface pressure gradient purposely imposed on the model. Preliminary results indicate that the cause of the high gap temperatures cannot be distinguished between the imposed surface pressure gradient or leakage through the cavity seal.

Future Plans - Before making additional areothermal tests, which are scheduled for CY 1986, the model and cavity seal will be repaired and modification of the concept to further inhibit gap heating will be considered.

Figure 37(a).

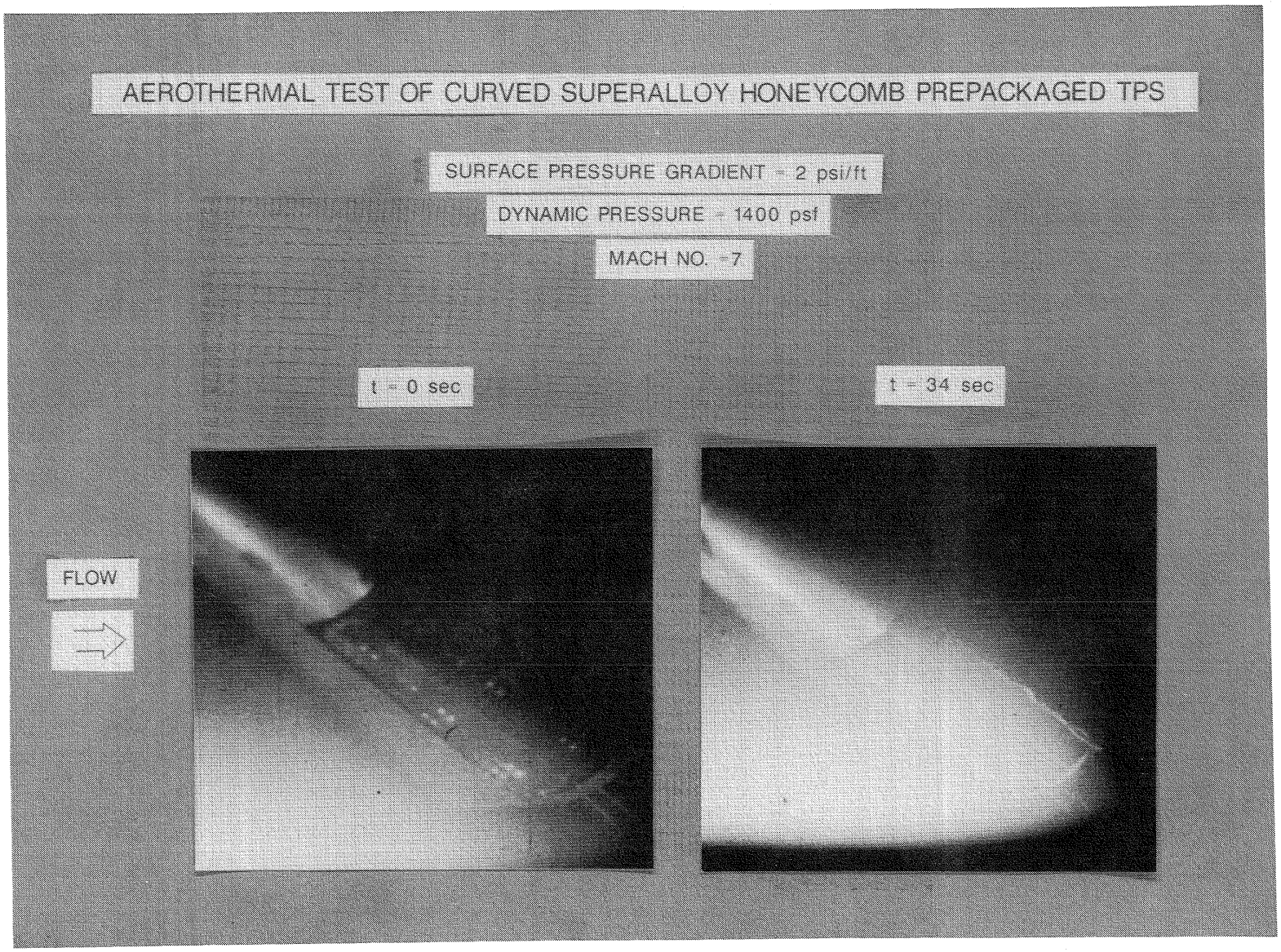
AEROTHERMAL TEST OF CURVED SUPERALLOY HONEYCOMB PREPACKAGED TPS
SURFACE PRESSURE GRADIENT = 2 psi/ft
DYNAMIC PRESSURE = 1400 psf
MACH NO. =7
t = 0 sec
t = 34 sec
FLOW

Figure 37(b).

This Page Intentionally Left Blank

CARBON-CARBON HEAT SHIELD FOR AEROASSISTED ORBITAL TRANSFER VEHICLE

Max L. Blosser
Thermal Structures Branch
Ext. 4295

RTOP 506-43-31

Research Objective - A previous structural system study has identified a slant-nose-cylinder aeroassisted orbital transfer vehicle (AOTV) which has many attractive features compared to current large diameter vehicle concepts. One of the key technology needs for the slant-nose-cylinder AOTV is a reusable thermal protection system (TPS) for the highly heated nose region. The objective of this study is to define and analyze this thermal protection system.

Approach - A one-dimensional thermal analysis was was used for a preliminary assessment of the thermal performance of three different TPS concepts. One of these concepts, a thick carbon-carbon heat shield, was selected for further investigation.

Accomplishment Description - The feasibility of using carbon-carbon as a thermal protection system for the nose of the slant-nose-cylinder AOTV was investigated using one-dimensional transient thermal analysis. This analysis was used to size the thickness of the carbon-carbon heat shield required to maintain the surface temperature below 3000°F, the current maximum reuse temperature of the carbon-carbon coating, and the thickness of fibrous insulation required to maintain the temperature of the aluminum structure below 350°F. Even though these thicknesses have been calculated, considerable work remains to define a workable thermal protection system. Details such as; size and shape of heat shields, method of attaching heat shield to cooler structure, and joint design to prevent flow through gaps between heat shields into the flexible insulation, must be addressed.

Two shapes were considered for the heat shields, square and hexagonal. The hexagonal shape is favored (figure 38(c)) for several reasons: only three attachments rather than four for a square, shorter straight-line gap length, and smaller deflections at corners due to thermal bowing. Optimum size for the heat shield has not been determined, but will depend on allowable surface roughness due to thermal bowing, stresses around attachments due to pressure loading, and maximum allowable clearance between tiles required to accommodate differential thermal expansion the carbon-carbon tile and the aluminum substructure.

Figure 38(a).

CARBON-CARBON HEAT SHIELD FOR AEROASSISTED ORBITAL TRANSFER VEHICLE

CONTINUED

Hot gas ingress between tiles must be minimized to prevent overheating of the underlying fibrous insulation and aluminum structure. One possible way to accomplish this is to sandwich a high temperature fibrous insulation between heat shields to seal the joint. However, a fibrous material which is compatible with the carbon-carbon coating and does not become embrittled at 3000°F must be identified or developed. The edges of the heat shields are shaped as shown so that: the fibrous material is held securely between the heat shields, the edges of the heat shields are free to rotate due to thermal bowing, the minimum possible gap (require to accommodate thermal expansion) is exposed to the flow, and a single heat shield can be installed or removed without disturbing surrounding heat shields by making half of the edges underhanging and half overhanging.

The most difficult challenge to overcome is to attach the 3000°F heat shield to the cool aluminum structure. Flexible metal (MA956) tabs arranged radially from the center of the heat shield accommodate thermal expansion difference by flexing to allow thermal bowing, yet can resist shear in any direction. These tabs must be sized to carry the compressive load due the pressure loading, yet minimize thermal conduction to the aluminum. Any material on the outer surface must retain its strength at 3000°F, yet be compatible with the carbon-carbon coating. Two threaded carbon-carbon pieces are assembled into a prefabricated hole in the heat shield, as shown, to provide a carbon-carbon cup which extends into the fibrous insulation. The bottom of this cup is then attached to the upper end of the metal tab (which was previously attached to the aluminum structure) using a low thermal stress conical fastener to complete the attachment of the heat shield to the aluminum structure. The cup can then be sealed by a threaded carbon-carbon or zirconia plug. This design therefore allows each heat shield to be installed or removed independently of surrounding shields. Also, the allowable surface temperature depends only on the maximum reuse temperature of the carbon-carbon coating, because the temperature of the metal to carbon-carbon joint can be controlled by varying the dimensions.

Future Plans - This concept is being considered for testing on the AOTV flight experiment. However, higher priority efforts may preclude further work on this concept in the near future.

Figure 38(b).

CARBON-CARBON HEAT SHIELD FOR AEROASSISTED ORBITAL TRANSFER VEHICLE

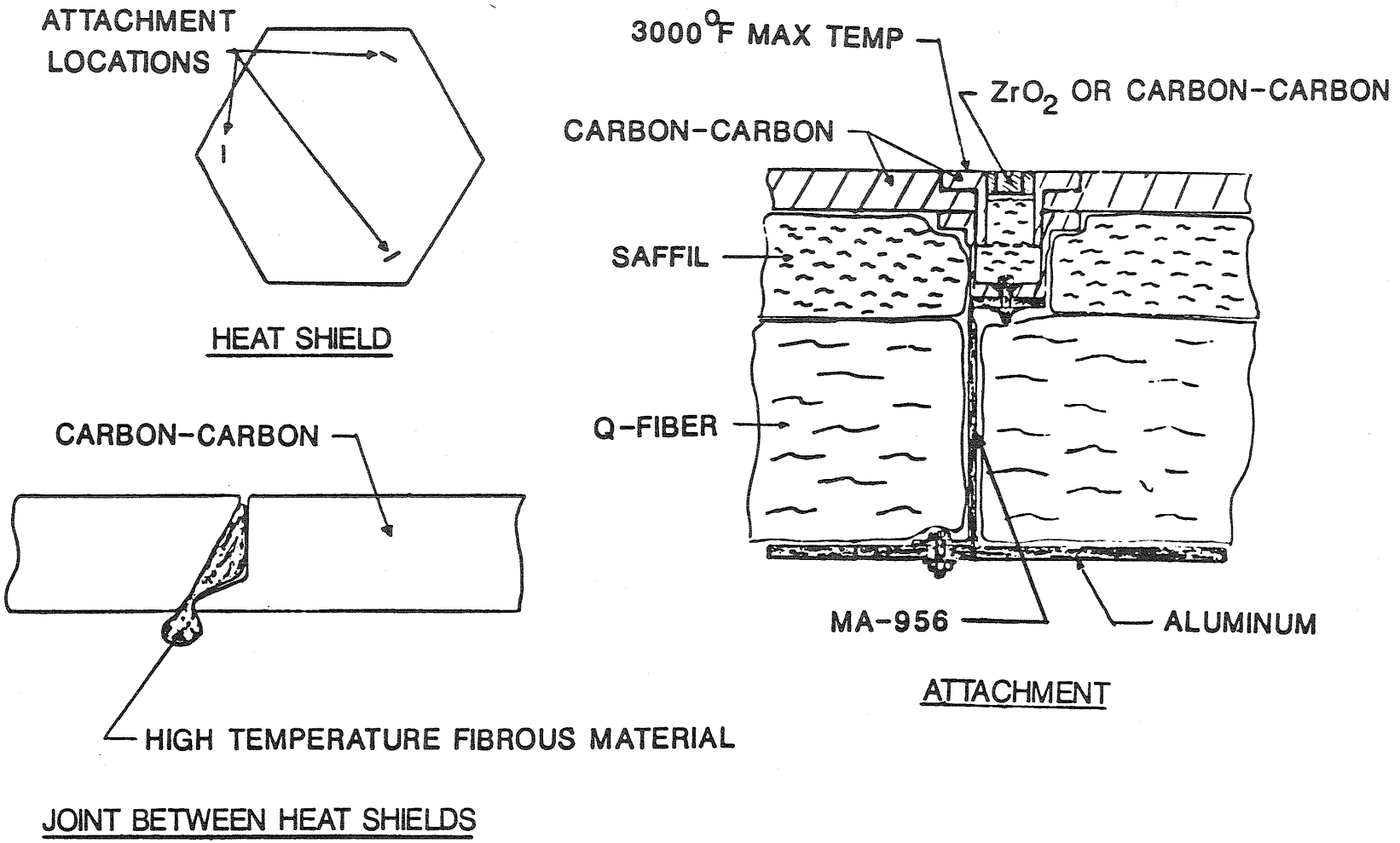

Figure 38(c).

EQUATIONS FOR THERMAL STRESS AROUND A CYLINDRICAL PIN

Max L. Blosser
Thermal Structures Branch
Ext. 4295

RTOP 506-43-31

Research Objective - High temperature materials such as carbon-carbon are being studied for use in lightly loaded hot structures. Many of these hot structures will be made of multiple pieces and fastened together. Typical metal fasteners have a much higher coefficient of thermal expansion than the material being fastened. The objective of this effort is to develop a quick and easy method to predict the thermal stresses around a cylindrical fastener at elevated temperature.

Approach - The general elasticity solution for an axisymmetric problem was applied to the specific case of a cylindrical pin in a sheet of material at elevated temperature.

Accomplishment Description - If the material around the cylindrical pin is assumed to be a disk and the temperature distribution is uniform, the problem is axisymmetric. The general elasticity solution for an axisymmetric problem, presented in Elasticity, by Robert Wm. Little, was used to obtain algebraic equations for the thermal stress distributions around the cylindrical pin. A thermal expansion term was added to the expression for radial displacement, and the following boundary conditions were applied: the radial stress at the outer edge of the disk of material was assumed to be zero, the radial stresses in the pin and in the material were assumed to be equal at the common boundary, and the radial displacements in the pin and material were also assumed to be equal at the common boundary. In addition, the pin was assumed to be in two-dimensional hydrostatic compression. These assumptions and boundary conditions were used to evaluate the constants in the general solution to produce the algebraic equations shown in figure 39(b).

A finite element model was generated to calculate stresses for a direct comparison with the exact algebraic equations. As expected, the finite element solution was found to approach the exact solution as the mesh was refined. For the finest mesh used (20 elements in the radial direction) the finite element and exact solutions agreed to within one percent.

These simple algebraic equations will give designers of high temperature joints the ability to quickly assess the stresses due to thermal expansion mismatch between the fastener and material. The equations can be easily modified to account for an initial clearance around the pin.

Future Plans - These equations will be included in a Master's thesis and will probably be published in a NASA TP.

Figure 39(a).

EQUATIONS FOR THERMAL STRESS AROUND A CYLINDRICAL PIN

THERMAL STRESSES IN MATERIAL

$$\sigma_r = \left[1 - \left(\frac{b}{r}\right)^2 \right] C_1$$

$$\sigma_\theta = \left[1 + \left(\frac{b}{r}\right)^2 \right] C_1$$

WHERE

$$C_1 = \frac{(\alpha_1 - \alpha_2)\ \Delta T\ E_2}{\left(\frac{b}{a}\right)^2 (1+\nu_2) + (1-\nu_2) + \frac{E_2}{E_1}\left[\left(\frac{b}{a}\right)^2 - 1\right](1-\nu_1)}$$

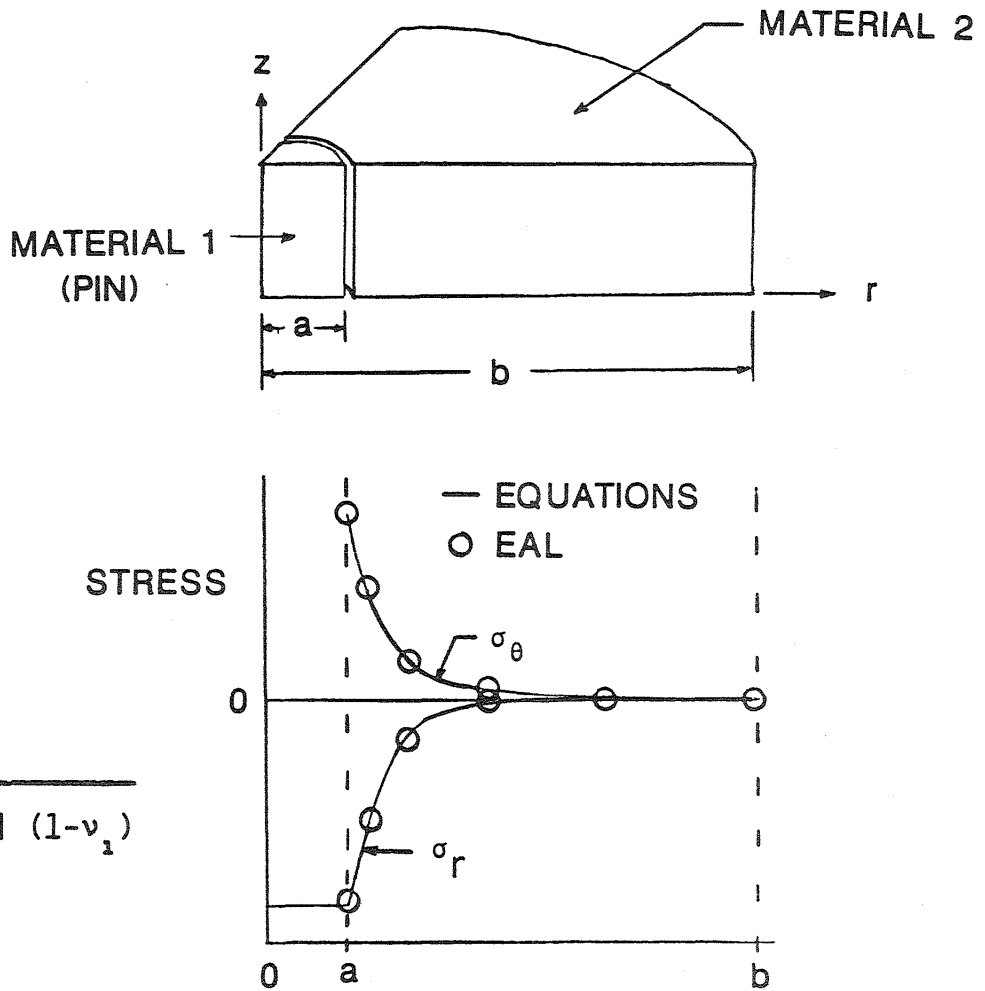

Figure 39(b).

This Page Intentionally Left Blank

CONFIGURATION AEROELASTICITY

FY86 PLANS

- SUPPORT USAF IN FLUTTER CLEARANCE STUDY OF JAS-39 AIRPLANE
- COMPLETE INITIAL PHASE IN EVALUATION OF FLEXIBLE ADAPTIVE WING CONCEPT
- COMPLETE EXPERIMENTAL STUDY OF ADAPTIVE ACTIVE FLUTTER SUPPRESSION
- COMPLETE INSTALLATION OF HARDWARE FOR TDT NEW DAS
- COMPLETE STUDY OF VIBRATION/AEROELASTIC STABILITY/PERFORMANCE OF BASELINE AND ADVANCED ROTOR BLADES FOR UH-60
- COMPLETE DESIGN OF VARIABLE SPEED RESEARCH ROTOR BLADES
- COMPLETE FINITE ELEMENT MODEL ANALYSIS AND EXPERIMENTAL CORRELATION FOR UH-60 AND AH-64
- COMPLETE THIRD INDUSTRY-WIDE REVIEW OF DAMVIBS PROGRAM

Figure 40.

AIRCRAFT AEROELASTICITY

Frank W. Cazier, Jr.
Configuration Aeroelasticity Branch
Extension 2661

RTOP 505-63-21

Research Objective - The primary objectives in Aircraft Aeroelasticity research area are (1) to determine and solve aeroelastic problems of current designs, and (2) to develop the aeroelastic understanding and prediction capabilities needed to apply new aerodynamic and structural concepts to future flight vehicles.

Approach - The types of research included in the Aircraft Aeroelasticity area are illustrated in figure 41(b). This research is a combination of experimental and complementary analytical studies. The experimental work focuses on the use of the Langley Transonic Dynamics Tunnel (TDT) which is specifically designed to meet the unique needs of aeroelastic testing. On occasion flight research programs are undertaken when it is necessary to simulate important parameters that cannot be accurately accounted for in ground-based facilities. Quite often the research is a cooperative effort with other government agencies and/or industry.

Status/Plans - Work for the coming year includes a variety of endeavors. Several will be mentioned here by way of illustration. Among the first will be a flutter clearance study of the new JAS-39 airplane. This TDT test will include testing both sting-mounted and cable-mounted dynamically scaled aeroelastic models of this advanced fighter type airplane. Two studies associated with the use of active controls to favorably change aeroelastic response will be conducted. One is an adaptive active flutter suppression endeavor, whereas the other is a study of the use of active controls along with aeroelastic tailoring of the structure to enhance roll control characteristics. Both of these efforts are the first in the series of two test entries in the TDT. The second entry in both cases will occur next year. Studies of self-induced oscillations are also planned. This study will include testing a series of wing models to examine transonic flutter characteristics at both low and high angles of attack.

Figure 41(a).

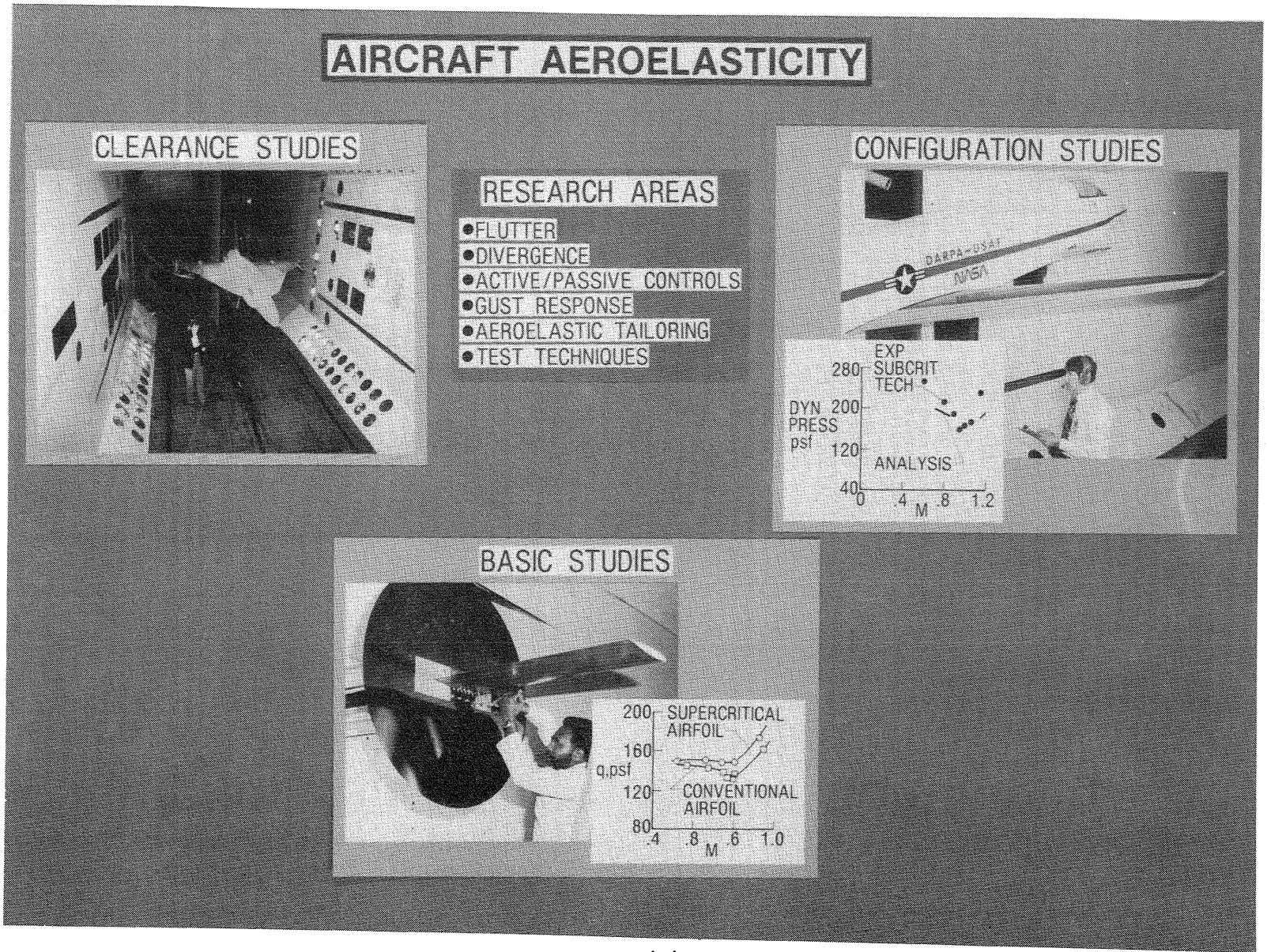
AIRCRAFT AEROELASTICITY
CLEARANCE STUDIES
RESEARCH AREAS
•FLUTTER
•DIVERGENCE
•ACTIVE/PASSIVE CONTROLS
•GUST RESPONSE
•AEROELASTIC TAILORING
•TEST TECHNIQUES
CONFIGURATION STUDIES
DARPA-USAF
NASA
EXP
SUBCRIT
TECH
280
DYN 200
PRESS
psf
120
ANALYSIS
40
0
.4
.8
1.2
M
BASIC STUDIES
200
SUPERCRITICAL
AIRFOIL
160
q,psf
120
CONVENTIONAL
AIRFOIL
80
.4
.8
.6
1.0
M

Figure 41(b).

This Page Intentionally Left Blank

UPGRADING THE DATA ACQUISITION SYSTEM FOR THE LANGLEY TRANSONIC DYNAMICS TUNNEL

Bryce M. Kepley
Configuration Aeroelasticity Branch
Extension 2661

Objective - The objective is to increase the productivity of the Langley Transonic Dynamics Tunnel (TDT) by replacing the existing computer-controlled data acquisition, display and control system with a new system that takes advantage of technological advances that have been made since the original system was designed over ten years ago. The new system will provide increased reliability, more flexibility, more data channels, faster data rates, and enhanced real time analysis as compared to the present system.

Approach - The conceptual design of the new system has been developed by a Langley in-house team. A simplified block diagram of the system's configuration is shown in figure 42(b). The three computer systems will provide the flexibility needed to perform multiple tasks. The two analog "front end" systems provide for support of multiple tests. The new system supports tests in the General Rotor Aeroelastic Laboratory (hover facility) adjacent to the TDT building. This facility is not connected to the present system.

Status/Plans - The development schedule for the system is presented in figure 42(c). The functional requirements for the system have been defined and documented. The top-level software design has been completed, and the detailed software design has been initiated. All major hardware components have been ordered. Although setup of the hardware in the TDT building will be completed by the end of this fiscal year, the system is not expected to be fully operational until 1987.

Figure 42(a).

BLOCK DIAGRAM OF NEW DAS FOR TDT

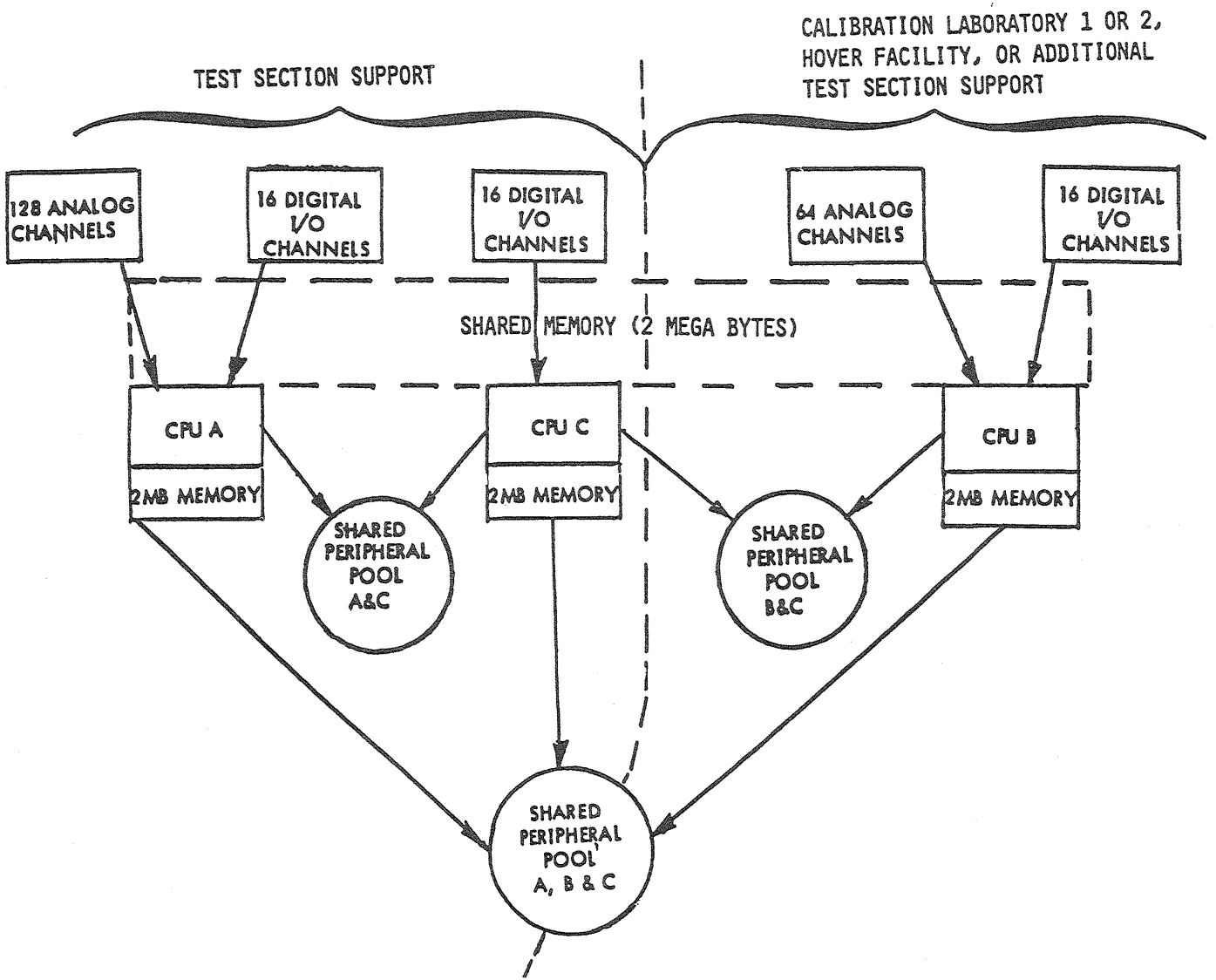

Figure 42(b).

TDT DATA ACQUISITION AND ANALYSIS SYSTEM PROJECT SCHEDULE

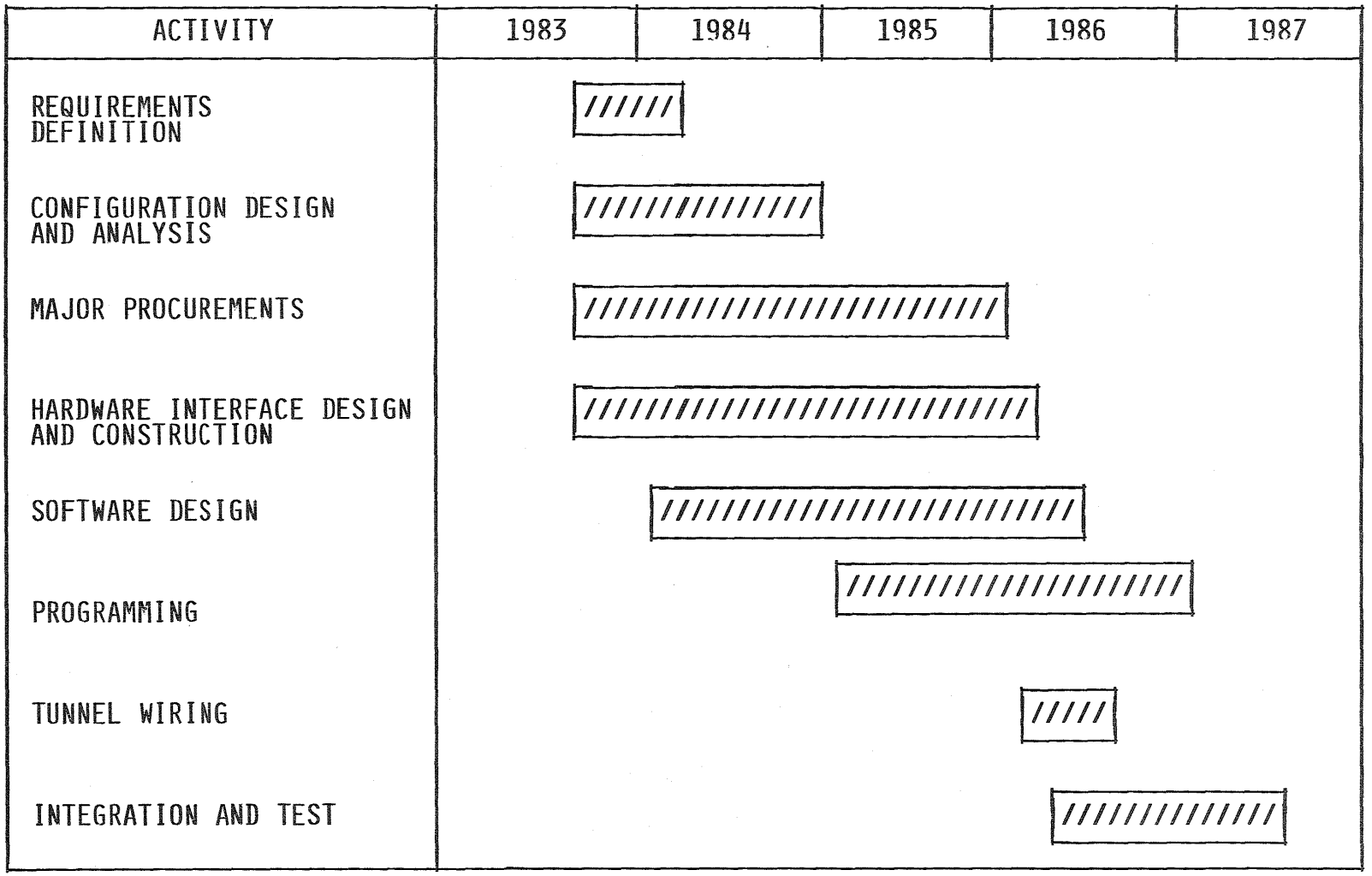

Figure 42(c).

ROTORCRAFT DYNAMICS AND AEROELASTICITY

Wayne R. Mantay
Configuration Aeroelasticity Branch
Extension 2661

RTOP 505-61-51

Research Objectives - The triad of research objectives in this area are (1) to conduct research in aeroelasticity, aerodynamics and dynamics of rotors; (2) to support design of advanced performance helicopters in the areas of loads, vibration and aeroelastic stability; and (3) to develop the experimental and analytical techniques necessary to extend TDT capabilities to future research opportunities, such as bearingless rotors.

Approach - This research area is a joint effort of the Loads and Aeroelasticity Division and the U.S. Army Structures Laboratory which is co-located at the NASA Langley Research Center. The work is a combination of experimental studies, tests in the TDT and the General Rotor Aeroelastic Laboratory (hover facility), and analytical studies. The Aeroelastic Rotor Experimental System (ARES) is a key test bed in the experimental studies. The in-house civil service research is supported and supplemented by industry contracts and university grants.

Status/Plans - Research during this year will address a variety of topics such as aeroelastic stability of hingeless rotors, rotor gust response, rotor optimization evaluations, advanced rotor track and balance characteristics, and a variable speed rotor concept. One illustrative project, namely, the advanced Blackhawk rotor study, is illustrated in figure 43(b). Langley personnel have designed an advanced rotor blade to increase the mission capabilities of the UH-60 Blackhawk helicopter. As part of a risk reduction approach, several technologies are being integrated into a model rotor test. The model blades utilize advanced airfoils with planform shape and twist to increase rotor performance. Additionally, aeroelastic tailoring concepts are being incorporated in the model blades for vibration reduction. Four model blade sets will be tested in the Langley Transonic Dynamics Tunnel (TDT). The test are expected to be completed early this fiscal year, after which an intensive effort will be placed on reducing what is expected to be a voluminous amount of data. Because of the unique capabilites of the TDT, these tests are expected to provide a means for quantifying advance rotor performance, loads, and vibration characteristics while properly addressing key model rotor scaling questions.

Figure 43(a).

ADVANCED BLACKHAWK PROGRAM

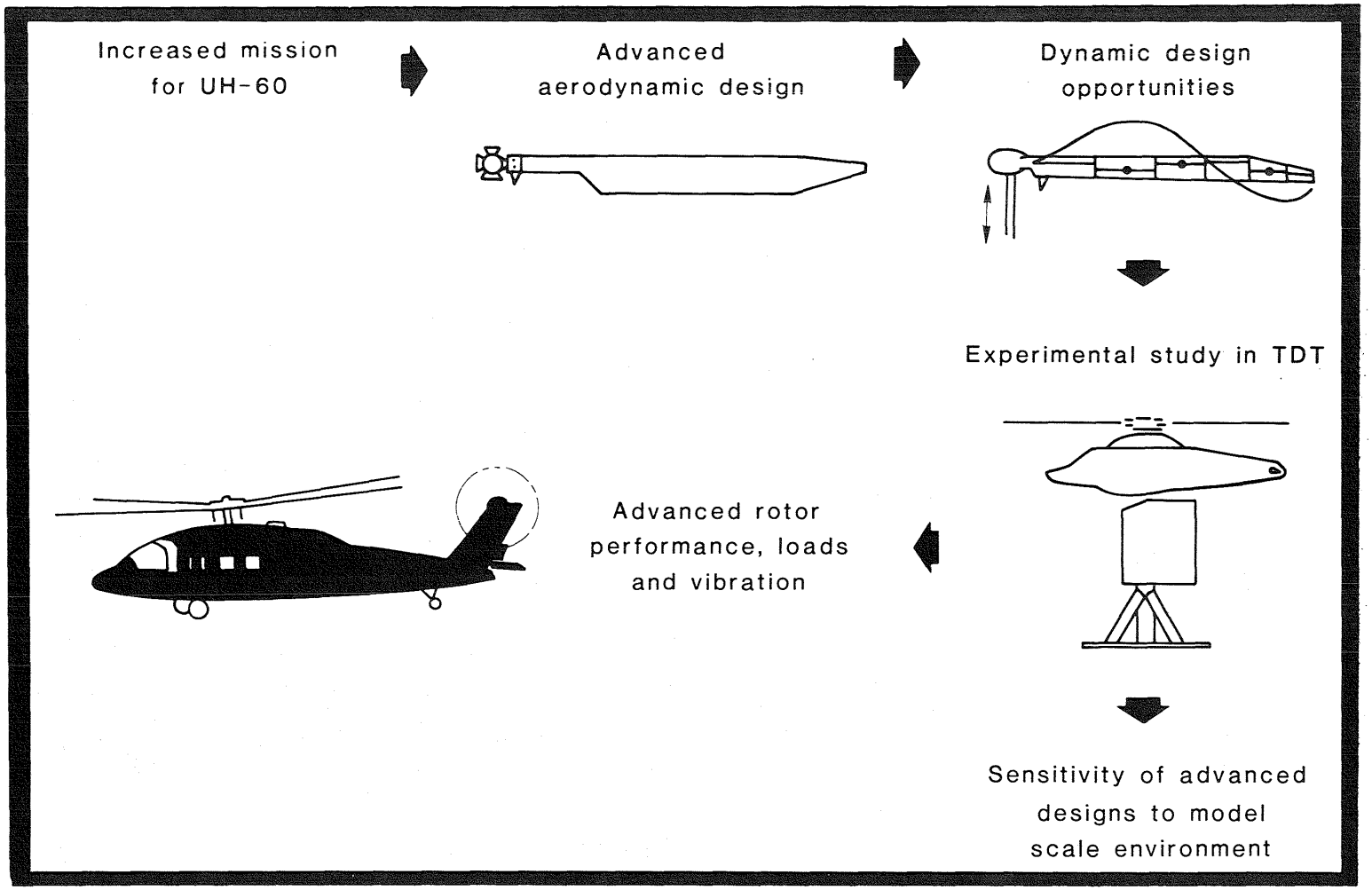

Figure 43(b).

A NATIONAL CAPABILITY TO ANALYZE VIBRATION AS PART OF HELICOPTER STRUCTURAL DESIGN

Raymond G. Kvaternik and John H. Cline
Configuration Aeroelasticity Branch
Extension 2661

RTOP 505-61-51

Research Objective - Helicopters are prone to vibrations which can seriously degrade both service life and ride quality. With only a few exceptions vibrations problems have not been identified and attacked until the flight test and operational stages. There is now a recognized need to account for vibrations during the analytical phases of design. The advent of modern methods of computer analysis has provided the opportunity to achieve such a capability. The objective is to emplace in the United States a superior capability for design analysis of helicopter vibrations (figure 44(b)).

Approach/Status/Plans - Two meetings of the company participants have been held during which representatives from each company reported on the research tasks that they have underway. With the exception of completing the editing of the final reports the companies have finished the following tasks: preparation of data describing AH-1G helicopter (Bell); development of AH-64 finite-element model and calculation of AH-1G flight vibrations (McDonnell-Douglas); and development of UH-60 finite-element model and calculation of AH-1G flight vibrations (Sikorsky).

The following additional tasks are underway and are expected to be completed and reported on this year: development of ACAP finite-element model and correlation of analytical vibration characteristics with experimental ground test results (Bell); development of Model 360 finite-element model and conducting ground vibration tests of Model 360, calculating AH-1G flight vibrations (Boeing Vertol); conducting ground vibration tests of AH-64 (McDonnell-Douglas); and conducting ground vibration tests of UH-60 (Sikorsky).

Figure 44(a).

DESIGN ANALYSIS METHODS FOR VIBRATIONS (DAMVIBS) PROGRAM

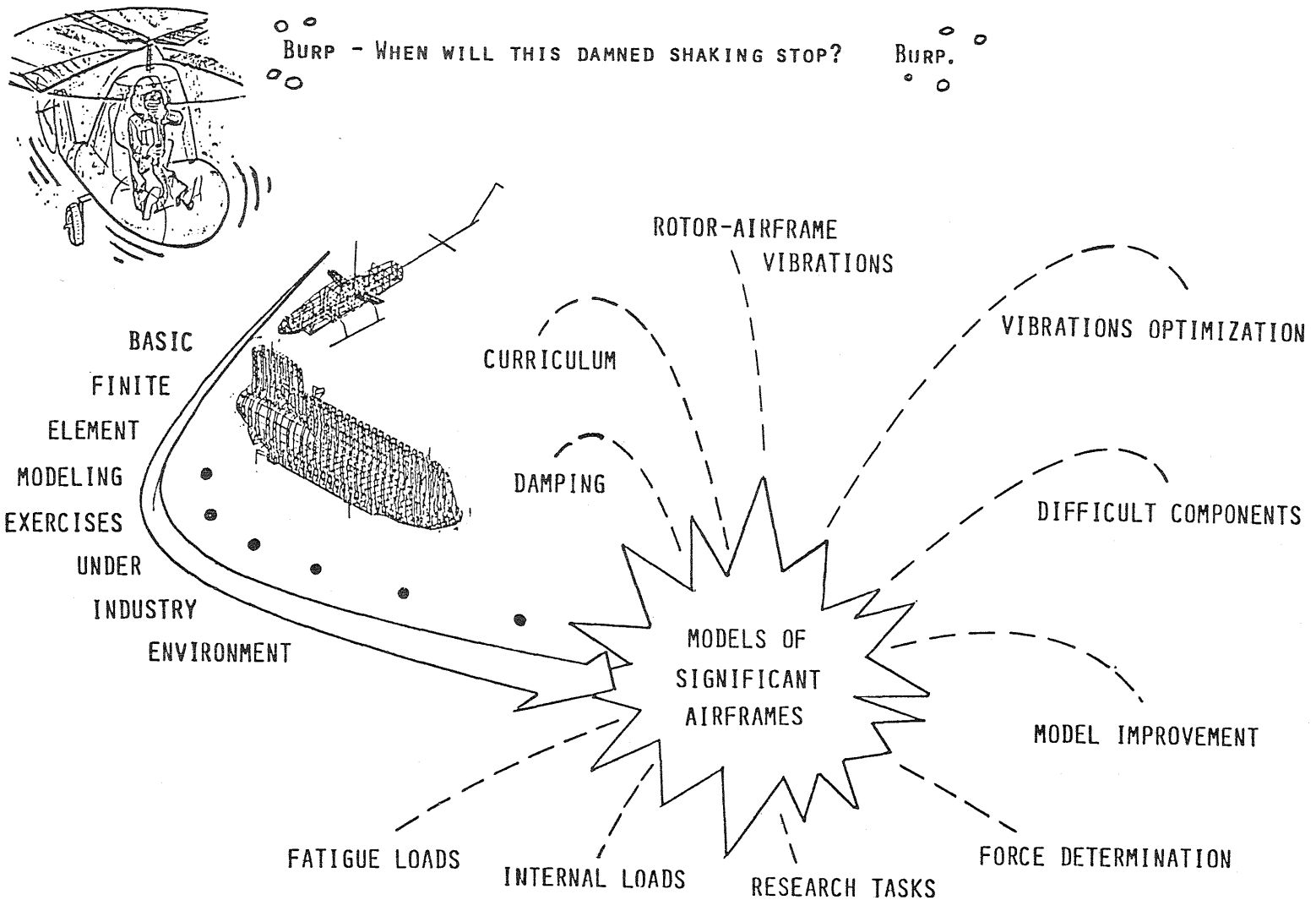

Figure 44(b).

UNSTEADY AERODYNAMICS

FY 86 PLANS

- COLLOCATION OF COMPUTATIONAL GROUPS NEAR CONTROL COMPUTER
- XTRAN3S APPLICATIONS AND MODIFICATIONS
  - ESTABLISH "COMMON" CODE
  - CONTINUE COMPARISON WITH DATA SETS
  - CONTINUE AUGMENTATION OF CODE
- ALTERNATIVE 3-D SOLUTION ALGORITHMS FOR IMPROVED STABILITY
- EFFECT OF LEADING-EDGE VORTICES ON AEROELASTIC STABILITY
- 3-D UNSTEADY BOUNDARY LAYER CODE CONTRACT
- FULL POTENTIAL AEROELASTIC CODE CONTRACT
- EXPERIMENTS
  - FABRICATION FOR CLIPPED DELTA WING/CANARD TEST
  - DESIGN BENCHMARK AEROELASTIC MODEL

Figure 45.

AEROSERVOELASTICITY

FY-86 PLANS

- DEVELOP COMPUTATIONAL PROCEDURE FOR SIMULTANEOUSLY ITERATING FLEXIBLE STRUCTURE AND NONLINEAR STEADY AERO CODE (FLO22) ON VPS32
- SYNTHESIZE OPTIMAL CONTROL LAWS FOR AFW WIND-TUNNEL MODEL
- INCLUDE OPTIMUM SENSITIVITY TECHNIQUE IN CONTROL LAW OPTIMIZATION METHODOLOGY
- COMPARE ARW-2 WIND-TUNNEL PRESSURE DATA WITH PREDICTED LINEAR STEADY AND UNSTEADY AERO
- DEVELOP A NONLINEAR SIMULATION CAPABILITY FOR FLEXIBLE VEHICLES INCLUDING UNSTEADY AERO AND ACTIVE CONTROLS
- CONVERT ISAC TO RUN ON VAX HARDWARE
- DEMONSTRATE ACTIVE CONTROL OF "SHOCK-INDUCED" INSTABILITY DURING ARW-2 WIND-TUNNEL TEST
- PERFORM X-WING ASE ANALYSES USING COMPLETE VEHICLE NASTRAN MODEL
- BEGIN ASE ANALYSES ON A "HYPERSONIC-TYPE" CONFIGURATION

Figure 46.

DEMONSTRATE ACTIVE CONTROL OF "SHOCK-INDUCED" INSTABILITY DURING ARW-2 WIND-TUNNEL TEST

Clinton V. Eckstrom
Aeroservoelasticity Branch
Ext. 3834

William M. Adams, Jr.
Analytical Methods Branch
Ext. 4681

RTOP 505-63-21

Research Objective - During a previous wind tunnel test of the ARW-2 right semispan, an unusual instability, at a frequency of the wing first bending mode, was encountered (Reference AIAA Paper No. 85-0598-CP). The instability was unusual in that the boundary followed essentially a constant Mach number over a wide range of dynamic pressures (figure 47(b)). The boundary was traced as a function of Mach number and dynamic pressure from 50 psf up to the tunnel limit of 300 psf. The boundary was near M = 0.90 except for a region near q = 100 psf where the boundary moved to about M = 0.95. The objective of this research is to determine if this instability can be controlled using a feedback control system using one or more wing mounted vertical accelerometers as sensors and the outboard control surface as the controller by applying design methods similar to those used for control of conventional wing flutter modes.

Approach - Accelerometer recordings from two wing tip locations obtained during the previous wind tunnel test have been used to develop a control law that will be implemented on an analog computer and used as the initial control law to be evaluated. However, during the initial portion of this wind tunnel test, when the instability boundary will be further explored, signals from four additional accelerometers will also be measured and recorded during control surface sweeps. Transfer functions will be derived using an HP5451C analyzer. This may result in refinement of the basic control law (gain and phase) and/or additional control laws which can also be implemented for evaluation during the active control demonstration and evaluation phase of the wind tunnel test series.

Status/Plans - The ARW-2 instrumentation system has been checked out and the wing is ready for transfer to Bldg. 648 for final checkout. The ARW-2 is currently scheduled for installation in the TDT test section during the two week holiday period from December 23, 1985 to January 3, 1986 with test time scheduled from January 6th through January 24th. Programming of the available control law on the analog computer has started. Training in the use of the HP5451C Analyzer is also underway.

Figure 47(a).

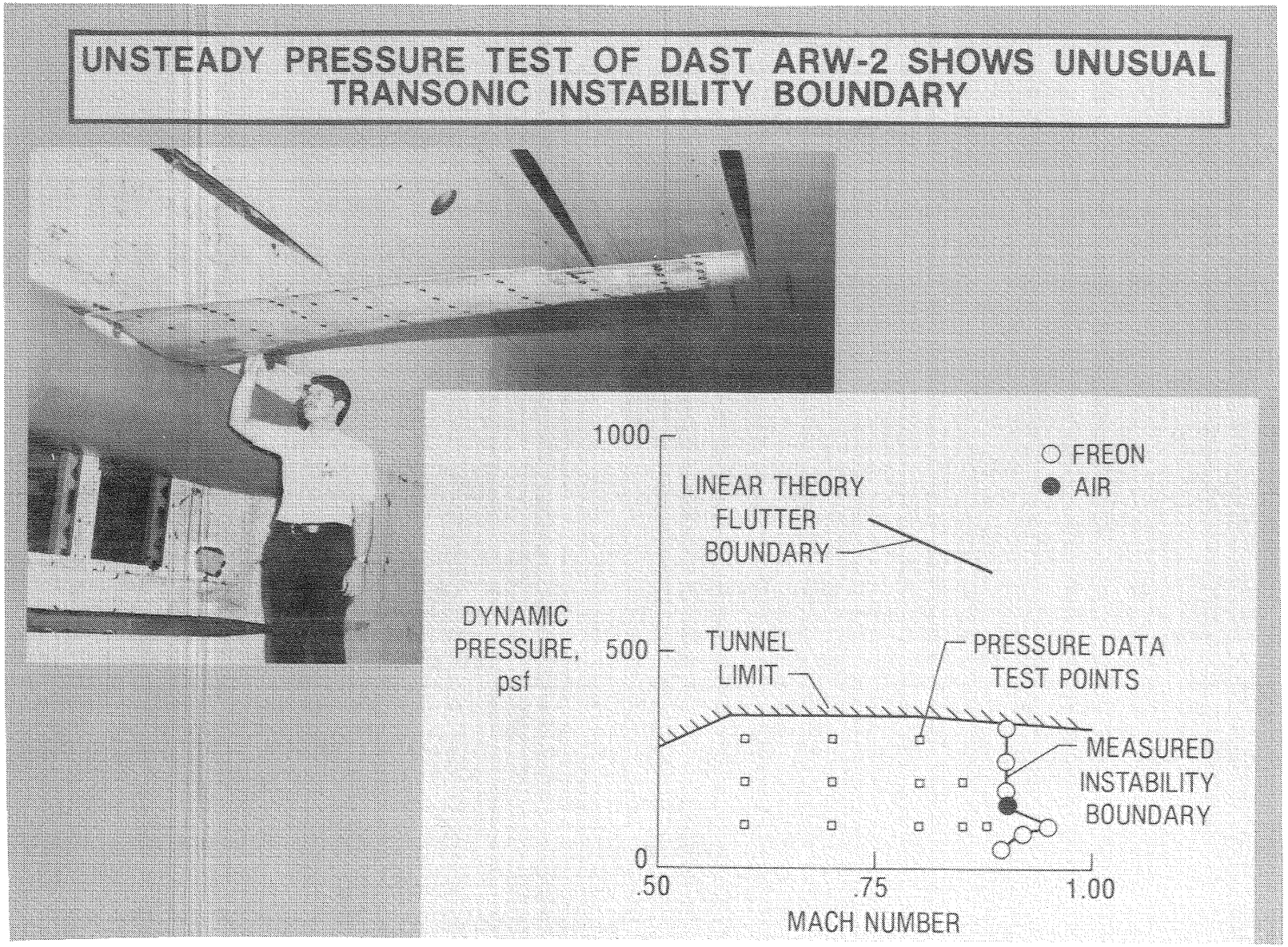
UNSTEADY PRESSURE TEST OF DAST ARW-2 SHOWS UNUSUAL TRANSONIC INSTABILITY BOUNDARY
1000
500
0
DYNAMIC PRESSURE, psf
FREON
AIR
LINEAR THEORY FLUTTER BOUNDARY
TUNNEL LIMIT
PRESSURE DATA TEST POINTS
MEASURED INSTABILITY BOUNDARY
.50
.75
1.00
MACH NUMBER

Figure 47(b).

COMPARISON OF ARW-2 WIND-TUNNEL DATA WITH LINEAR STEADY AND UNSTEADY AERODYNAMIC PREDICTIONS

William E. McCain
Aeroservoelasticity Branch
Extension 4490

RTOP 505-63-21

Research Objective - Control law synthesis and analysis methods continue to rely on linear steady and unsteady aerodynamic predictions. Although considerable progress has been made with nonlinear transonic aerodynamic codes, these methods are yet to be practical enough for production-type analysis, due to time and cost constraints of available vector computers. The objective of this research is to provide theoretical predictions, using the linear lifting-surface aerodynamics of the doublet lattice method, for detailed comparisons with available wind-tunnel data of the ARW-2. This information will help both the developers of the nonlinear aerodynamic codes and the users of the linear aerodynamic codes, to assess the extent of nonlinear effects associated with the aeroelastic response of a flexible wing at critical Mach number and dynamic pressure conditions.

Approach - The first series of ARW-2 tests in the TDT obtained unsteady pressure distributions on the cantilevered flexible semispan wing panel by oscillating the outboard control surface. To provide a qualitative analysis for comparison to the experimental results, the ARW-2 wind-tunnel configuration has to be modeled accurately. The analytical model of ARW-2 has to not only include a rigid pitch degree of freedom, but also measured or predicted mode shapes due to structural flexibilty, control-surface deflection, and camber. For this particular study, the camber shape was included to account for the significant trailing-edge loads generated by the supercritical airfoil design. The primary analytical tool for this research is the computer program system known as ISAC (Interaction of Structures, Aerodynamics, and Controls). The equations of motion (EOM) for the forced dynamic response of the aeroelastic system (figure 48(b)) are solved to obtain the values for the generalized coordinate vector (Q) of the aeroelastic system. The generalized coordinate vector is then used to solve for such parameters as pressure distributions and tip deflections.

Status/Plans - ISAC has been used to generate the generalized aerodynamic forces (GAF) at Mach number and frequency values corresponding to the wind-tunnel data. A processor has been programmed to solve the equations of motion for the generalized coordinate vectors, check for modal convergence, and calculate chordwise pressure distributions. Preliminary results have been obtained at zero frequency for a steady pressure distribution due to control-surface deflection (see figure). Modal convergence was checked for this one case, but further checks will be made. Detailed calculations will soon be made for comparison to the measured steady and unsteady pressures at appropriate (M, q, α, δ, k) conditions.

Figure 48(a).

THE EQUATIONS OF MOTION FOR THE DYNAMIC RESPONSE OF AN AEROELASTIC SYSTEM

$$(-\omega^2[M_J] + I\omega\,[2\zeta_J M_J \omega_J] + [M_J \omega_J^2] + \frac{1}{2}\rho V^2\,[Q_{QQ}])\{Q\} = [Q_{\alpha Q}]\{\alpha\} + [Q_{CQ}]\{C\} + [Q_{\delta Q}]\{\delta\}$$

$$\Delta C_P = \sum_J \Delta C_{P_I}\, Q_J$$

WHERE Q_J IS THE GENERALIZED COORDINATE VECTOR CORRESPONDING TO THE JTH MODE

IN GENERAL

$$Z_N = \sum_J \phi_N Q_J$$

WHERE ϕ_N IS A KNOWN MODE SHAPE

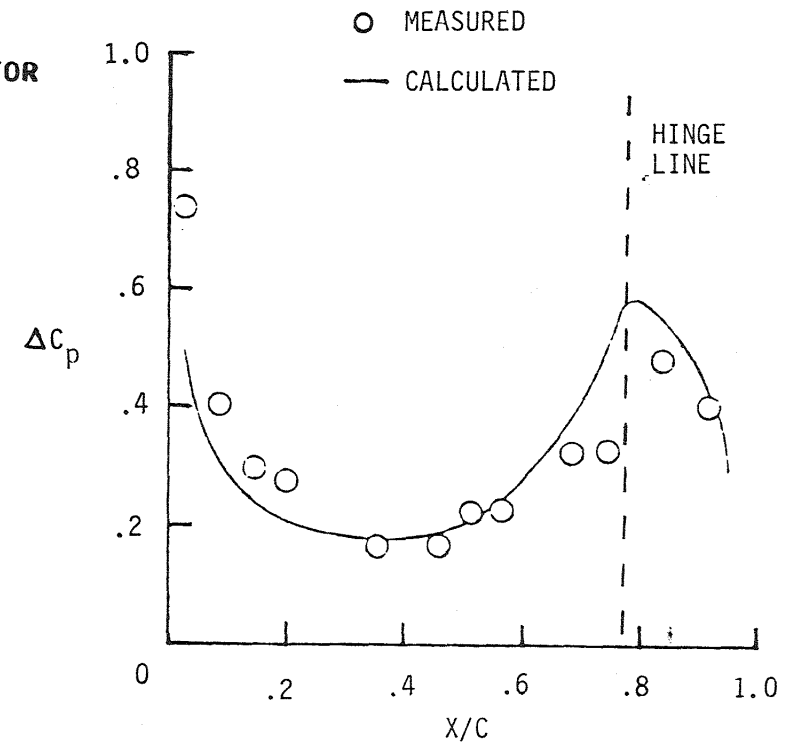

η=0.87, M=0.60, $\bar{q}$=100 PSF

α=0.0, δ=1.0°, k=0.0

Figure 48(b).

This Page Intentionally Left Blank

AEROTHERMAL LOADS

FY 86 PLANS

- COMPLETE AEROTHERMAL LOADS TESTS FOR SHOCK/SHOCK INTERACTION ON A BLOUNT LEADING EDGE IN 8' HTT
- COMPLETE TESTS OF CHINE GAP HEATING MODEL IN 8' HTT
- COMPLETE NUMERICAL ANALYSIS OF THE GAS-JET-NOSE-TIP CONFIGURATION
- COMPLETE NUMERICAL ANALYSIS OF THE SIMULATED SPACE SHUTTLE WING-ELEVON COVE
- DOCUMENT SPHERICAL PROTUBERANCE, SPLIT ELEVON, SIMULATED THERMALLY BOWED METALLIC TPS, AND GAS-JET-NOSE-TIP AEROTHERMAL LOADS TEST RESULTS
- COMPLETE INSTRUMENTATION EVALUATION FOR 8' HTT
- CONTINUE DEVELOPMENT AND VALIDATION OF VISCOUS FLOW FINITE ELEMENT ANALYSIS CAPABILITIES
- CONTINUE DEVELOPMENT OF THE INTEGRATED FLUID-THERMAL-STRUCTURAL FINITE ELEMENT ANALYSIS CAPABILITY
- INITIATE CONSTRUCTION PHASE OF OXYGEN ENRICHMENT AND ALTERNATE MACH NUMBER MODIFICATION OF THE 8' HIGH TEMPERATURE TUNNEL

Figure 49.

NUMERICAL ANALYSIS OF A GAS-JET-NOSE-TIP

Michele G. Macaraeg
Aerothermal Loads Branch
Ext. 2325

RTOP 506-43-31 and 506-40-21

Research Objective - Determine the aerothermal environment in gas-jet-nose-tip, GJNT, configuration with a Navier-Stokes numerical analysis and compare with experimental results. Provide computational results to enhance understanding of the phenomena involved.

Approach - Initially a two dimensional finite difference code utilizing a Beam and Warming ADI solution algorithm and a Jameson adaptive dissipation scheme was applied to the gas-jet-nose tip configuration. Later the code was modified to general curvilinear coordinates and reapplied to the GJNT configuration as an axisymmetric body. The GJNT configuration tested in the LaRC 8' HTT, upper left of figure, is a 12.5° cone with an opening in the tip for injection of a gas jet into the flow field in the upstream direction to reduce aerothermal heating on the cone. Several injection rates were investigated.

Status/Plans - Initial results from the two dimensional analysis of the GJNT by the flow field temperature distributions for the no-injection, low-injection and high-injection cases are shown at the lower left of figure 50(b). The temperature distributions show the shock stand-off distance increases and the heating rate decreases as the injection rate increases. Later results from the axisymmetric analysis of the GJNT are illustrated by the flow field density contours which show the same shock formations and flow patterns as the schlieren photograph from the experiment, upper right of figure. Comparison of the heating rate for the no-injection case with experimental data for a blunt cone, which began about ten inches downstream of the tip, show good correlation up to the point where the experimental data begins to transition to turbulent flow, lower right of figure. Continuing work will include complete quantitative comparisons of the analytical data with the experimental results. The code will be used as a tool for further parametric studies to enhance the experimental data and improve understanding of the phenomena involved.

Figure 50(a).

NUMERICAL ANALYSIS OF A GAS-JET-NOSE-TIP

EXPERIMENTAL MODEL

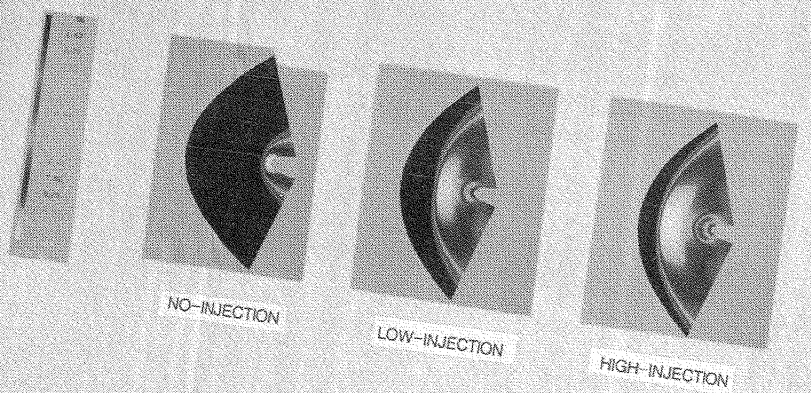

FLOW FIELD TEMPERATURE DISTRIBUTIONS

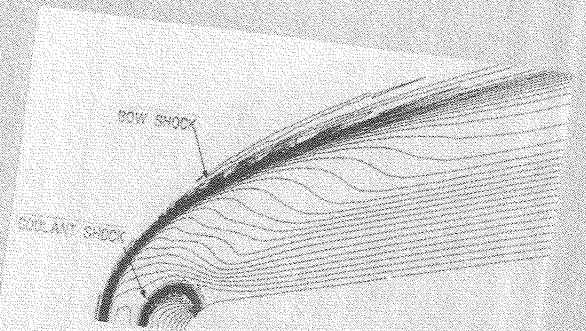

ANALYTICAL DENSITY CONTOURS

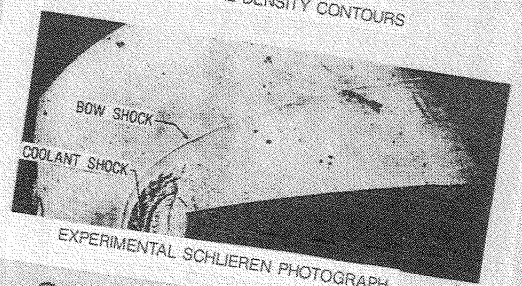

EXPERIMENTAL SCHLIEREN PHOTOGRAPH

SHOCK STRUCTURE

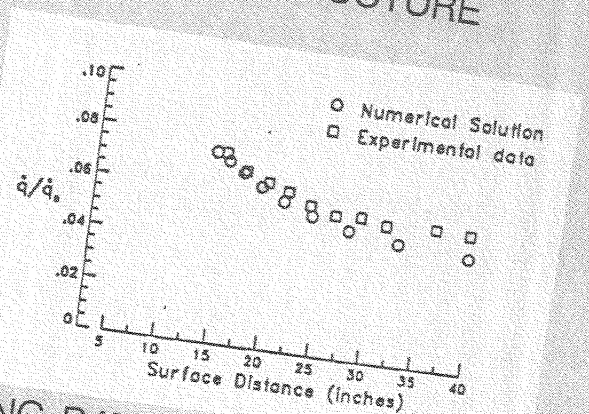

HEATING RATES WITH NO-INJECTION

Figure 50(b).

NUMERICAL ANALYSIS OF THE AEROTHERMAL ENVIRONMENT IN A SIMULATED SPACE SHUTTLE WING-ELEVON COVE

Michele G. Macaraeg
Aerothermal Loads Branch
Ext. 2325

RTOP 506-43-31 and 506-40-21

Research Objective - Determine the aerothermal environment in a simulated space shuttle wing-elevon cove with a two dimensional Navier-Stokes numerical analysis and compare with experimentally measured heating rate and pressure distributions.

Approach - A two dimensional finite difference code utilizing a robust Beam and Warming ADI algorithm was applied to the wing-elevon cove configuration, upper left of figure 51(b), as tested in the LaRC 8' HTT. The computational grid for the complex geometrical configuration, upper right of figure, was generated with a sophisticated grid generation method under development in the Computational Methods Branch (G. Erlebacher).

Status Plans - Initial results on a course grid capture the qualitative features of the flow as illustrated by the density contour plot, lower left of figure, and the velocity direction vector plot at the mouth of the cove, lower right of figure. The upstream shear layer bridges the gap at the mouth of the cove and impinges on the deflected elevon forming a shock wave. Viscous forces dominate flow in the mouth of the cove forming vortices and the lower pressure outside of the leaking seal at the end of the cove draws some of the hot gas from the external boundary layer through the cove. Continuing applications will obtain higher resolution results with a finer grid to make quantitative comparisons with experimentally measured wall pressures and heating rates. Once validated with the experimental data, the code will be used as a tool for parametric studies to enhance the experimental investigations.

Figure 51(a).

NUMERICAL ANALYSIS OF SIMULATED SPACE SHUTTLE WING-ELEVON COVE

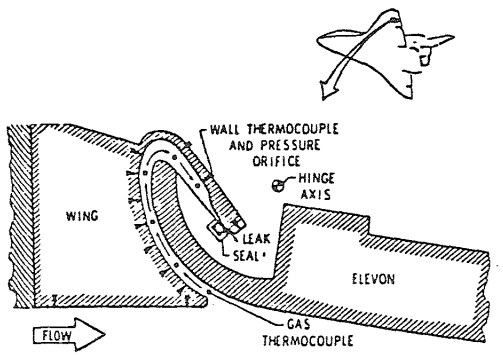

EXPERIMENTAL MODEL

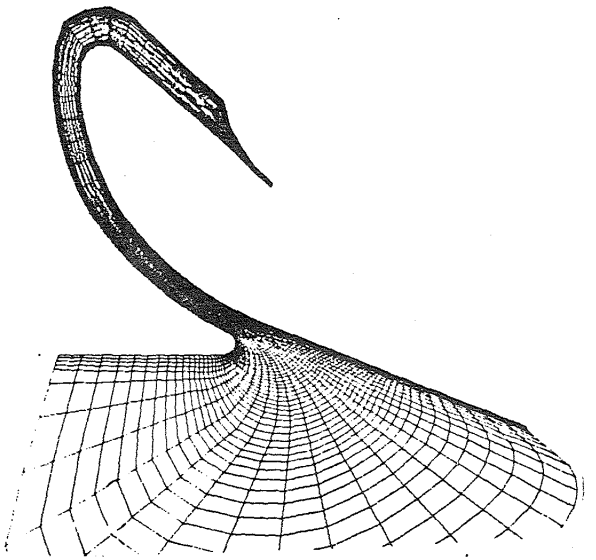

COMPUTATIONAL GRID

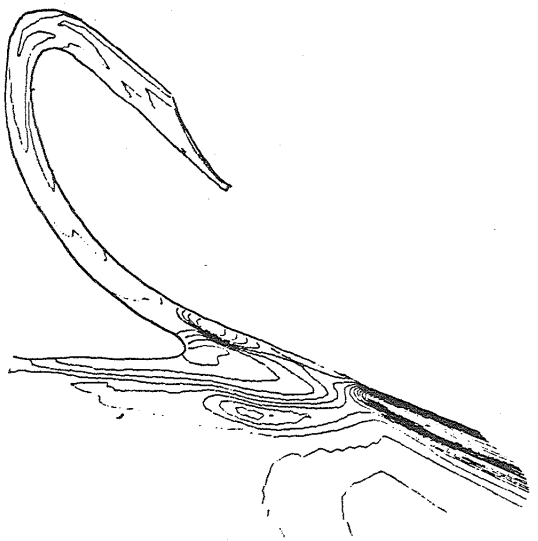

DENSITY CONTOURS

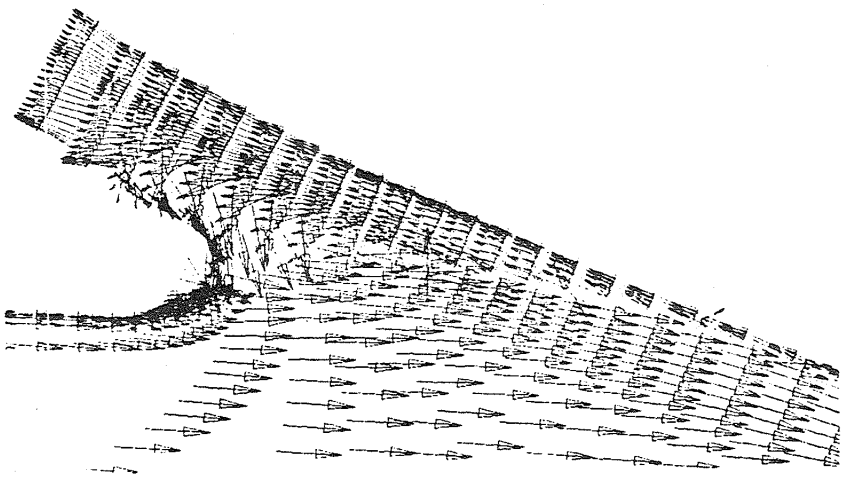

VELOCITY VECTORS AT MOUTH OF COVE

Figure 51(b).

INTEGRATED FLOW-THERMAL-STRUCTURAL FINITE ELEMENT ANALYSIS

Allan R. Wieting
Aerothermal Loads Branch
Ext. 3423

RTOP 506-43-31 and 506-40-21

Research Objective - The long range objective of this research is to develop a fully integrated fluid-thermal-structural analysis capability. A capability that would utilize a single model and a single algorithm for all three disciplines to simultaneously compute the coupled response of the structure when it is exposed to the aerothermal loading of super/hypersonic flows. This capability will help to reduce design margins and reduce the time required to do a load cycle on future vehicles.

Approach - Evaluation of the options available led to the selection of finite element theory as the targeted methodology to accomplish this integrated analysis capability. Finite element theory was firmly entrenched as the method of choice in thermal and structural analysis but would require a major effort to develop its use in high-speed computational fluid dynamics. Application of finite element theory to CFD problems, though somewhat more complex than the classical approaches, offers the advantage of unstructured gridding to enhance adaptive gridding strategies, it offers the possibility of additional adaptive refinement thru local modification of the interpolation functions and it permits accurate estimation of local errors. A team of world class investigators was assembled on grant and contracts to aid in the development of the integrated capability. The early emphasis was on fluid dynamics but now, as the CFD capability begins to mature, the integration of the disciplines is being addressed. An efficient vectorized algorithm that can be applied to all three disciplines has been developed and demonstrated.

Status/Plans - Continued development of the fully integrated flow-thermal-structural including efficient interfacing of the disciplines, inclusion of nonlinear structural effects like elastic-plastic models and improved computational efficiency thru coupling strategies. In parallel, development of the finite element CFD methodology will continue including algorithms, adaptive refinement, local error estimates, improved accuracy and improved efficiency.

Figure 52(a).

INTEGRATED FLOW-THERMAL-STRUCTURAL FINITE ELEMENT ANALYSIS

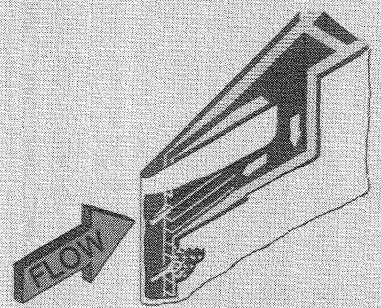

AEROTHERMALLY LOADED - ACTIVELY COOLED STRUCTURE (SCRAM JET STRUT)

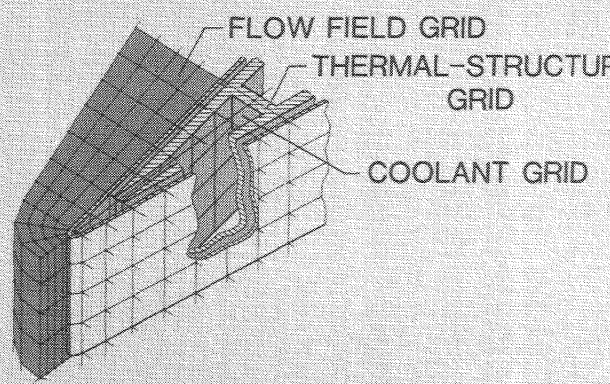

FINITE ELEMENT DISCRETIZATION

ANALYSIS PROCESS

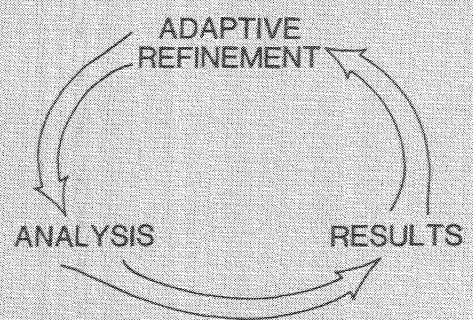

ANALYSIS FEATURES

- GENERAL AUTOMATED UNSTRUCTURED GRIDDING
- SINGLE F.E. ALGORITHM FOR ALL DISCIPLINES
- EFFICIENT TRANSIENT VECTORIZED ANALYSIS
- NONLINEAR
- SIMULTANEOUS SOLUTION FOR ENVIRONMENT, LOADS AND RESPONSE
- ADAPTIVE REFINEMENT
- COLOR GRAPHICS

Figure 52(b).

This Page Intentionally Left Blank

OXYGEN ENRICHMENT AND ALTERNATE MACH NUMBER MODIFICATION TO THE 8' HIGH TEMPERATURE TUNNEL

H. Neale Kelly
Aerothermal Loads Branch
Ext. 3423

Research Objective - The 8' HTT is to be modified to provide a unique national facility for a hypersonic air-breathing propulsion system. The modified facility, which can accommodate free standing engines, will complement existing lower speed Air Force facilities by providing true flight simulation for Mach numbers from 4 to 7 over a wide range of altitudes. These expansions in capability are shown in figure 53(b).

Approach/Accomplishments - An oxygen enrichment system will be added which will maintain the correct oxygen concentration for propulsion testing in the methane-air combustion-heated test stream. A cryogenic hydrogen supply system will be installed to provide fuel for the propulsion system. Supplemental nozzles will be provided for testing at Mach numbers of 4 and 5. These nozzles will be coupled with a mixer which will reduce the temperature of the test stream and increase the mass flow to provide the correct flow conditions for the lower mach numbers. In addition, various existing tunnel components will be refurbished and updated to increase facility productivity. One of these modifications will be the replacement of the present water cooled contraction section and the film cooled throat of the Mach 7 nozzle with air transpiration cooled components which should improve the performance and increase the life of the nozzle.

Status/Plans - The schedule for completion of the modifications is shown in figure 53(c). The final design and mixer development have been completed and the oxygen enrichment development will be completed by February 86. The contract for the construction phase is in preparation. Construction is expected to be complete by the spring of 1989 and the facility ready for propulsion testing by the spring of 1990.

Figure 53(a).

OPERATIONAL ENVELOPES FOR PROPULSION FACILITIES

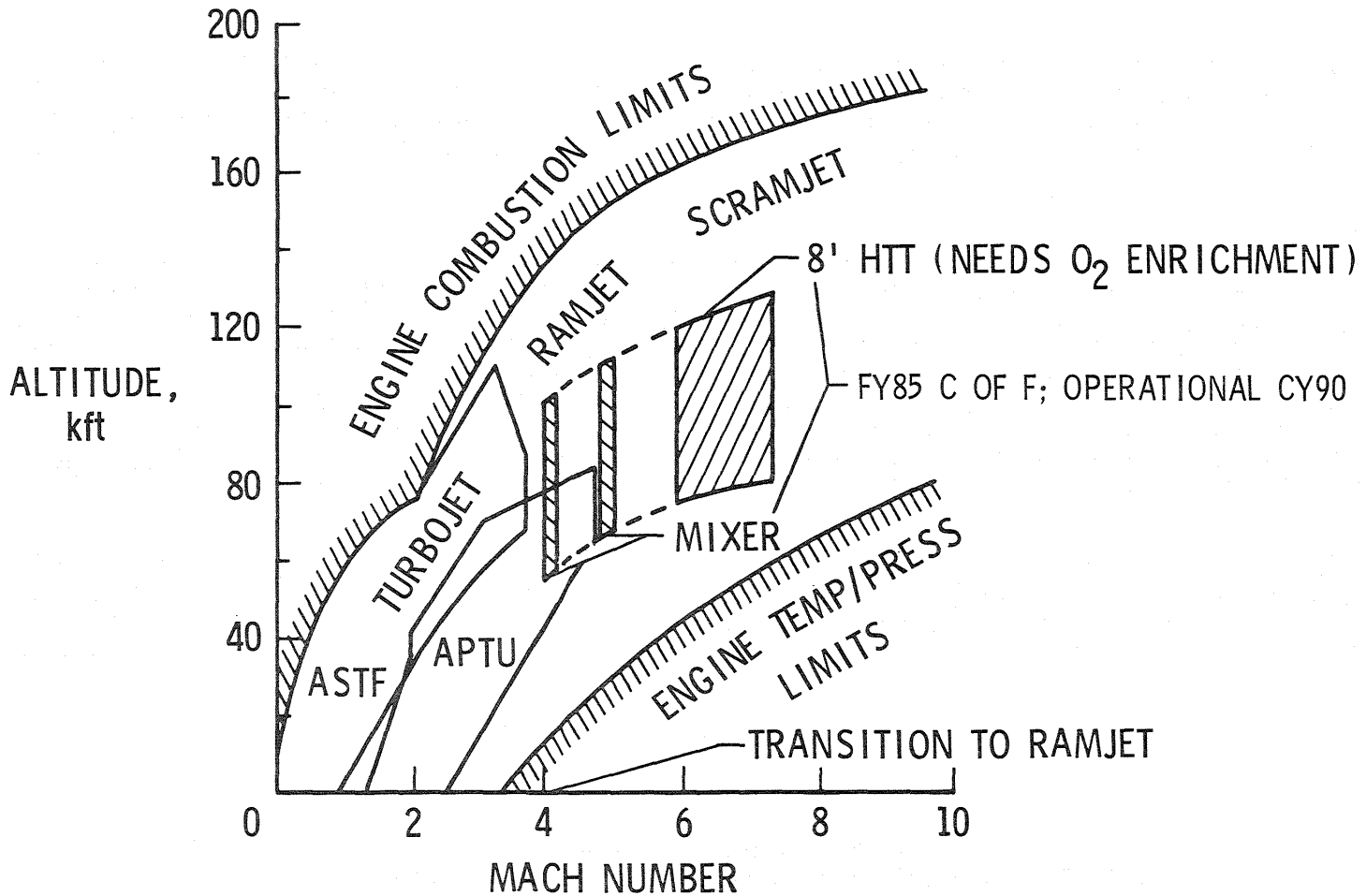

Figure 53(b).

SCHEDULE FOR 8-FOOT HTT MODIFICATION

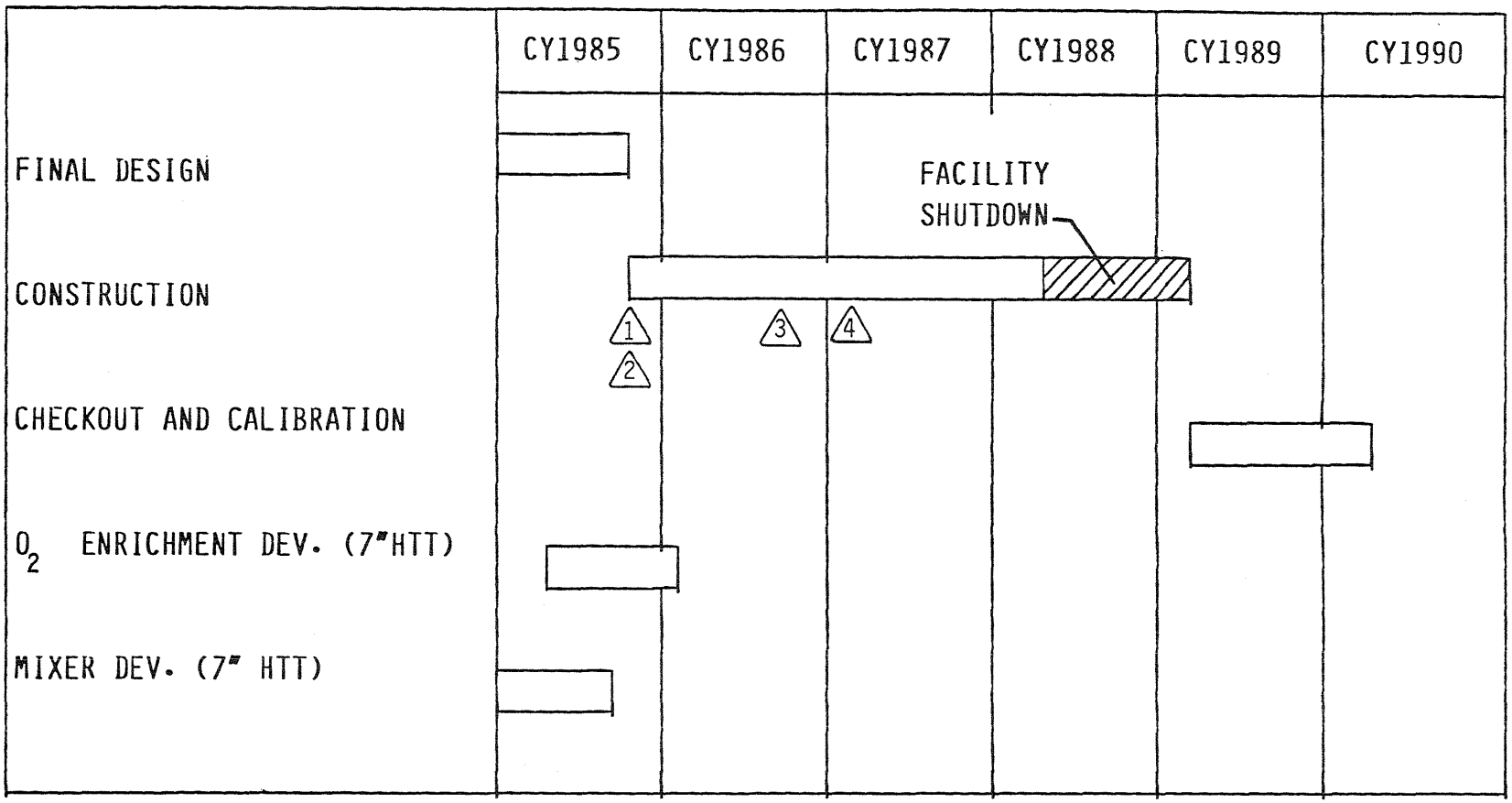

1 CONTRACT AWARD FOR TRANSPIRATION COOLED NOZZLE
2 INITIATE TWO PHASE CONSTRUCTION CONTRACT
3 CONTRACT AWARD
4 PHASE II OPTION

Figure 53(c).

This Page Intentionally Left Blank

THERMAL STRUCTURES

FY 86 PLANS

- PROPULSION STRUCTURAL CONCEPTS VERIFICATION
  - RECEIVE AND INITIATE TEST PROGRAM FOR SCRAMJET STRUT
  - CONTINUE RAMJET INDIRECT COOLING SYSTEM STUDY AT UTRC
  - CONTINUE MISSILE/SCRAMJET ENGINE STRUCTURE PROGRAM
- AIRFRAME STRUCTURAL CONCEPT VERIFICATIONS
  - DESIGN AND FAB TRUSS CORE PANELS
  - DESIGN AND FAB C/C STIFFENED PANELS
- TPS CONCEPT VERIFICATION
  - RE-TEST CURVED SUPERALLOY PANELS
  - COMPLETE TEST AND ANALYSIS OF C/C PANEL JOINT
  - LEADING EDGE HEAT PIPE STUDY
- ANALYTICAL METHODS AND APPLICATIONS
  - ENHANCE CAPABILITY OF SPAR THERMAL ANALYZER
  - DOCUMENT CONCEPTUAL; DESIGN ANALYSIS PROGRAMS
  - CONTINUE USE OF PANDA AND PASCO FOR STRUCTURAL OPTIMIZATIONS
- CONTINUE STRUCTURAL SYSTEM STUDIES
  - HYPERSONIC AEROSPACE VEHICLES (TAV)
  - ENTRY RESEARCH VEHICLE (ERV)
  - AEROASSISTED ORBITAL TRANSFER VEHICLE (AOTV)

Figure 54.

1. Report No.	2. Government Accession No.	3. Recipient's Catalog No.
NASA TM-87676		

4. Title and Subtitle	5. Report Date
LOADS AND AEROELASTICITY DIVISION RESEARCH AND TECHNOLOGY ACCOMPLISHMENTS FOR FY 1985 AND PLANS FOR FY 1986	January 1986
	6. Performing Organization Code: 505-63-21-02
7. Author(s): JAMES E. GARDNER AND S. C. DIXON	8. Performing Organization Report No.
9. Performing Organization Name and Address: LANGLEY RESEARCH CENTER, HAMPTON, VIRGINIA 23665-5225	10. Work Unit No.
	11. Contract or Grant No.
12. Sponsoring Agency Name and Address: NATIONAL AERONAUTICS AND SPACE ADMINISTRATION, WASHINGTON, DC 20546	13. Type of Report and Period Covered: TECHNICAL MEMORANDUM
	14. Sponsoring Agency Code

15. Supplementary Notes

16. Abstract

The purpose of this paper is to present the Loads and Aeroelasticity Division's research accomplishments for FY 85 and research plans for FY 86. The work under each branch (technical area) will be described in terms of highlights of accomplishments during the past year and highlights of plans for the current year as they relate to five year plans for each technical area. This information will be useful in program coordination with other government organizations and industry in areas of mutual interest.

17. Key Words (Suggested by Authors(s))	18. Distribution Statement
Accomplishments, research plans, Loads and Aeroelasticity	Unclassified - Unlimited Subject Category - 02

19. Security Classif.(of this report)	20. Security Classif.(of this page)	21. No. of Pages	22. Price
Unclassified	Unclassified	124	A06

For sale by the National Technical Information Service, Springfield, Virginia 22161

NASA-Langley, 1986

End of Document